



# Power System Design Trades for a Pressurized Lunar/Mars Rover

*Steven Oleson  
Glenn Research Center, Cleveland, Ohio*

*Jim Fittje  
Science Application International Corporation, Brunswick, Ohio*

*Paul Schmitz  
Power Computing Solutions Inc., Avon, Ohio*

*Lucia Tian, Brandon Klefman, Steven Korn, and Max Chaiken  
Glenn Research Center, Cleveland, Ohio*

*Mike Smith  
Oak Ridge National Laboratory, Oak Ridge, Tennessee*

*Tom Packard, Tony Colozza, and John Gyekenyesi  
HX5, LLC, Brookpark, Ohio*

*Elizabeth Turnbull and Tom Parkey  
Glenn Research Center, Cleveland, Ohio*

*Taylor Phillips-Hungerford  
KBR Wyle Services, LLC, Houston, Texas*

## NASA STI Program . . . in Profile

Since its founding, NASA has been dedicated to the advancement of aeronautics and space science. The NASA Scientific and Technical Information (STI) Program plays a key part in helping NASA maintain this important role.

The NASA STI Program operates under the auspices of the Agency Chief Information Officer. It collects, organizes, provides for archiving, and disseminates NASA's STI. The NASA STI Program provides access to the NASA Technical Report Server—Registered (NTRS Reg) and NASA Technical Report Server—Public (NTRS) thus providing one of the largest collections of aeronautical and space science STI in the world. Results are published in both non-NASA channels and by NASA in the NASA STI Report Series, which includes the following report types:

- TECHNICAL PUBLICATION. Reports of completed research or a major significant phase of research that present the results of NASA programs and include extensive data or theoretical analysis. Includes compilations of significant scientific and technical data and information deemed to be of continuing reference value. NASA counter-part of peer-reviewed formal professional papers, but has less stringent limitations on manuscript length and extent of graphic presentations.
- TECHNICAL MEMORANDUM. Scientific and technical findings that are preliminary or of specialized interest, e.g., “quick-release” reports, working papers, and bibliographies that contain minimal annotation. Does not contain extensive analysis.
- CONTRACTOR REPORT. Scientific and technical findings by NASA-sponsored contractors and grantees.
- CONFERENCE PUBLICATION. Collected papers from scientific and technical conferences, symposia, seminars, or other meetings sponsored or co-sponsored by NASA.
- SPECIAL PUBLICATION. Scientific, technical, or historical information from NASA programs, projects, and missions, often concerned with subjects having substantial public interest.
- TECHNICAL TRANSLATION. English-language translations of foreign scientific and technical material pertinent to NASA's mission.

For more information about the NASA STI program, see the following:

- Access the NASA STI program home page at <http://www.sti.nasa.gov>
- E-mail your question to [help@sti.nasa.gov](mailto:help@sti.nasa.gov)
- Fax your question to the NASA STI Information Desk at 757-864-6500
- Telephone the NASA STI Information Desk at 757-864-9658
- Write to:  
NASA STI Program  
Mail Stop 148  
NASA Langley Research Center  
Hampton, VA 23681-2199



# Power System Design Trades for a Pressurized Lunar/Mars Rover

*Steven Oleson  
Glenn Research Center, Cleveland, Ohio*

*Jim Fittje  
Science Application International Corporation, Brunswick, Ohio*

*Paul Schmitz  
Power Computing Solutions Inc., Avon, Ohio*

*Lucia Tian, Brandon Klefman, Steven Korn, and Max Chaiken  
Glenn Research Center, Cleveland, Ohio*

*Mike Smith  
Oak Ridge National Laboratory, Oak Ridge, Tennessee*

*Tom Packard, Tony Colozza, and John Gyekenyesi  
HX5, LLC, Brookpark, Ohio*

*Elizabeth Turnbull and Tom Parkey  
Glenn Research Center, Cleveland, Ohio*

*Taylor Phillips-Hungerford  
KBR Wyle Services, LLC, Houston, Texas*

National Aeronautics and  
Space Administration

Glenn Research Center  
Cleveland, Ohio 44135

## Acknowledgments

This work was funded by the Radioisotope Power Systems (RPS) Program. The team wishes to thank June Zakrasjek, Michelle Rucker, Bret Drake, and Jeff George for their guidance. Additionally, the team thanks Jim Fincannon, and Susan Jansen for their technical reviews and probing questions.

This report contains preliminary findings,  
subject to revision as analysis proceeds.

Trade names and trademarks are used in this report for identification  
only. Their usage does not constitute an official endorsement,  
either expressed or implied, by the National Aeronautics and  
Space Administration.

*Level of Review:* This material has been technically reviewed by technical management.

# Contents

1.0	Introduction.....	1
2.0	Study Background and Assumptions .....	2
2.1	Assumptions and Approach .....	2
2.1.1	Baseline Rover Performance .....	2
2.1.2	Figures of Merit .....	3
2.1.3	Redundancy Assumptions .....	3
2.2	Radiation Considerations and Analysis.....	3
2.2.1	Radioisotope Power System (RPS) Radiation.....	3
2.2.2	Space Radiation .....	4
2.2.3	Federal Regulatory Limits and Guidance for Radiation Exposures .....	5
2.2.4	Rover Concept’s Radioactive Fuel Payload Considerations .....	5
2.2.5	Radiation Analysis for RPS .....	7
2.2.6	Radiation Analysis Conclusions .....	10
2.3	Mass Growth, Contingency, and Margin Policy .....	10
2.3.1	Terms and Definitions .....	10
2.3.2	Mass Growth.....	13
2.3.3	Power Growth.....	15
3.0	Baseline Design.....	15
3.1	Top-Level Design Details .....	16
3.1.1	Baseline Design Master Equipment List (MEL) .....	16
3.1.2	Spacecraft Total Mass Summary .....	16
3.1.3	Power Equipment List (PEL).....	17
3.2	Concept Drawing and Description .....	17
3.3	Architecture Trades.....	21
3.3.1	Case 2: Rechargeable Fuel Cell.....	22
3.3.2	Case 3: Self-Contained Fuel Cell .....	23
3.3.3	Mass Comparison of Rover Design Trades .....	23
4.0	Subsystem Breakdown.....	25
4.1	Electrical Power System (EPS).....	25
4.1.1	System Requirements .....	25
4.1.2	System Assumptions.....	26
4.1.3	System Designs and Trades .....	26
4.1.4	Summary.....	33
4.1.5	Master Equipment List .....	33
4.2	Thermal System .....	35
4.2.1	System Requirements .....	35
4.2.2	System Assumptions.....	35
4.2.3	System Design .....	35
4.2.4	Analytical Methods.....	39
4.2.5	System Lunar Operation.....	52
4.2.6	Master Equipment List .....	53
4.3	Fuel Cell Reactant Storage.....	56
4.3.1	System Requirements .....	56
4.3.2	System Assumptions.....	57

4.3.3	System Trades.....	57
4.3.4	Fuel Cell Reactant Storage Design .....	57
4.3.5	Fuel Cell Reactants Storage Analytical Methods .....	60
4.3.6	Fuel Cell Reactants Storage Risk Inputs.....	60
4.3.7	Fuel Cell Reactant Storage Recommendations.....	61
4.3.8	Fuel Cell Reactant Storage System MEL .....	61
4.4	Structures and Mechanisms.....	63
4.4.1	System Requirements .....	63
4.4.2	System Assumptions.....	63
4.4.3	System Trades.....	63
4.4.4	Analytical Methods.....	63
4.4.5	Risk Inputs .....	63
4.4.6	System Design .....	63
4.4.7	Recommendation(s).....	67
4.4.8	Master Equipment List .....	68
5.0	Cost.....	69
5.1	Ground Rules and Assumptions.....	69
5.2	Estimating Methodology.....	69
5.3	Cost Estimates.....	70
Appendix A.—Acronyms and Abbreviations .....		73
Appendix B.—Study Participants .....		75
Appendix C.—Radiation Contributions to Total Mission Dose .....		77
References.....		79

# Power System Design Trades for a Pressurized Lunar/Mars Rover

Steven Oleson  
National Aeronautics and Space Administration  
Glenn Research Center  
Cleveland, Ohio 44135

Jim Fittje  
Science Application International Corporation  
Brunswick, Ohio 44212

Paul Schmitz  
Power Computing Solutions Inc.  
Avon, Ohio 44011

Lucia Tian, Brandon Klefman, Steven Korn, and Max Chaiken  
National Aeronautics and Space Administration  
Glenn Research Center  
Cleveland, Ohio 44135

Mike Smith  
Oak Ridge National Laboratory  
Oak Ridge, Tennessee 37830

Tom Packard, Tony Colozza, and John Gyekenyesi  
HX5, LLC  
Brookpark, Ohio 44142

Elizabeth Turnbull and Tom Parkey  
National Aeronautics and Space Administration  
Glenn Research Center  
Cleveland, Ohio 44135

Taylor Phillips-Hungerford  
KBR Wyle Services, LLC  
Houston, Texas 77002

## 1.0 Introduction

To enable future human exploration missions, the lunar surface will serve as a crucial training ground and technology demonstration test site where NASA will prepare for future human missions to Mars and other destinations. Key enablers in this exploration are rover systems intended to operate in both the lunar and Mars surface environments. This study focused primarily on the Mars surface environment because, compared to the near-continuous illumination near the lunar poles, the day/night cycles and the reduced solar illumination on Mars make it much more difficult to use solar power. However, solar power is not the only power generation technology available.

Top-level energy studies have shown that a radioisotope power system (RPS) has promise for supplying both power and thermal energy for crewed rovers on both the Moon and Mars. This design study investigates how a RPS could potentially meet the power and thermal needs of a pressurized rover with applications for both destinations. The design focus is on what service a RPS can provide and how it

would be integrated into a rover (power and thermal interfaces, placement, radiation shielding, fairing installation on the pad, etc.). Section 3.3 of this report compares the RPS-based design to other potential rover power solutions, including solar and fuel cells.

## 2.0 Study Background and Assumptions

### 2.1 Assumptions and Approach

The current rover approach assumes a small pressurized rover (SPR) with an unpressurized rover (UPR) “bolted” to it for stability, mobility, and crew access. Figure 2.1 shows this configuration. It is envisioned that the UPR could be detached (one extravehicular activity (EVA)) and driven back to base solo. The Compass Team deemed the UPR appropriate for carrying a multiday power system, with three options to be evaluated: solar panels, RPS, and gaseous hydrogen (GH<sub>2</sub>)/gaseous oxygen (GO<sub>2</sub>) fuel cells. The design approach worked to maintain both suit-port and passthrough access for the crew through the UPR, with the power being carried on the UPR and assumed to be cabled to the SPR.

Radiation mitigation for the RPS design is accomplished by placing the plutonium 238 (<sup>238</sup>Pu) at the rear of the aft rover with a small shield. The addition of approximately 10 kg of water at the aft of the SPR is assumed to keep the radiation exposure levels of the crew to near that of the Mars surface background. See also Section 2.2.5.

#### 2.1.1 Baseline Rover Performance

The assumed mission for this study is a 2035 opportunity for two crew. Maximum excursion time is 21 Earth days with a maximum travel distance from the ascent vehicle of 10 km. A second UPR is assumed to follow as a chase vehicle to provide a backup for return to the ascent vehicle. The rover is assumed capable of traversing 2 km per day while requiring a nominal 1.8 kWe for hotel loads, 250 We for science, and 10.0 kWe for mobility. Due to the high power demands of the mobility system, the Compass Team assumed that lithium- (Li-) ion batteries would be used primarily for that power mode. The team assumed a 5-year life and an estimated baseline mass of approximately 6,000 kg for the rover system.



Figure 2.1.—Combined SPR and UPR quads.



### 2.1.2 Figures of Merit

The Compass Team used largely qualitative parameters to define figures of merit (FOMs) that guided the subsystems' design and implementation. The FOM for this design focused more on usability and impacts to rover system performance than on current technology readiness level (TRL) or cost. For this design study, the Compass Team assumed the following FOMs:

- System reusability
- Number of Space Launch Systems (SLSs)
- Number of Crew Launch Vehicles (CLVs)
- Feasibility and TRL
- Mass impacts to landers
- Cost
- Range
- Rover maneuverability impacts
- Applicability to both lunar and martian environments
- Usability of rover system by the crew
- Crew radiation dose
- Simplicity of implementation
- Mission cadence

### 2.1.3 Redundancy Assumptions

This system is required to be nominally human rated and is thus required to be single-fault tolerant in the design of the subsystems wherever possible and/or feasible. Exceptions to this include subsystems that have zero fault tolerance, although designed to accommodate some performance degradation (i.e., the electric power system, reactant tanks, lines, and radiators).

## 2.2 Radiation Considerations and Analysis

The rover concept proposes a radioisotope power system (RPS) for the primary source of electrical power, which presents a nontrivial source of radiation. In addition, operations in spaceflight scenarios involve exposing personnel to naturally occurring, ambient space radiation. This section describes the concepts, analyses, and modeling efforts to predict the radiological implications of various rover designs, general mission architectures, and notional concept-of-operations from the combined effects of RPS and natural radiation sources.

### 2.2.1 Radioisotope Power System (RPS) Radiation

Radioactive isotopes—radioisotopes—are unstable atoms that emit particles as a method to move toward a more stable atomic configuration. Plutonium oxide ( $\text{PuO}_2$ ) is the radioisotope fuel used by NASA's RPS program and is, therefore, the fuel proposed for this power system. While  $\text{PuO}_2$  fuel comprises multiple radioisotopes (e.g.,  $^{236}\text{Pu}$ ,  $^{238}\text{Pu}$ ,  $^{239}\text{Pu}$ ,  $^{240}\text{Pu}$ ,  $^{241}\text{Pu}$ , and  $^{242}\text{Pu}$ ), which all have various decay chains and radiation characteristics (Ref. 1), this discussion will relegate the overall radiation effects and emissions of the fuel to a bulk level and discuss  $\text{PuO}_2$  as a whole. The primary interest in  $\text{PuO}_2$  for an RPS fuel is that it emits hundreds of billions of alpha particles (i.e., helium nuclei) per second, per gram of  $\text{PuO}_2$ . Each of these particles are relatively large, charged particles, that once emitted, are completely attenuated in the fuel, converting all their kinetic energy into thermal energy, generating on the order of  $\sim 0.40$  Wth/g- $\text{PuO}_2$  at the beginning of life (BOL) (Ref. 2). However, ancillary emissions of smaller, neutral particles/waves (i.e., neutrons and photons) also occur during the  $\text{PuO}_2$  decay process that do not attenuate in the fuel, do not contribute significantly to heat generation, and do escape to pose a radiation concern for personnel, materials, and equipment in the environment around a given RPS (see Table 2.1).

TABLE 2.1.—GENERAL CHARACTERISTICS OF PuO<sub>2</sub> PARTICLE EMISSIONS

Particle type	Charge state of particle	Mass of particle, ~kg	PuO <sub>2</sub> typical specific activity, #/s/g-PuO <sub>2</sub>	Contributes significantly to radioisotope power system (RPS) heat	Escapes RPS to interact with environment, fraction of total activity
Alpha (α)	+2	6.64×10 <sup>-27</sup>	~5.00×10 <sup>11a</sup>	Yes	~0.00×10 <sup>0</sup>
Neutron (η)	+0	1.67×10 <sup>-27</sup>	~8.00×10 <sup>3ab†</sup>	No	~1.00×10 <sup>0</sup>
Photon (γ)	+0	0.00×10 <sup>0</sup>	~7.00×10 <sup>10a</sup>	No	~1.00×10 <sup>-6</sup>

<sup>a</sup>Approximate activities at BOL (Ref. 1).

<sup>b</sup>Activity levels are referenced from flight-qualified compositions with reduced neutron emission rates (Ref. 3).

### 2.2.2 Space Radiation

Space radiation is a generic term to describe radiation from multiple naturally occurring cosmogenic sources like galactic cosmic rays (GCRs), solar particle events (SPEs), and trapped radiation belts. When trying to determine an ambient background radiation baseline for various lunar and martian mission architectures, one can assume an average dose rate from the unavoidable presence of GCRs while neglecting effects from more sporadic and unpredictable SPEs along with trapped radiation belts not present in operations for lunar and martian environments. Therefore, GCRs will be the primary source of naturally occurring space radiation considered in this analysis.

The magnetic field intensity of the Sun (heliosphere) ebbs and flows on an ~11-year cycle. This cycle directly affects the intensity of the incident GCR spectrum by deflecting more particles during periods of high magnetic intensity and deflecting less particles during periods of low magnetic intensity (Figure 2.2 and Figure 2.3).

The fluctuating ambient GCR particle flux inside the heliosphere is the direct cause of background dose rates in deep space, and thus, the ambient dose rate is not a constant value either. However, averages based on historic trends can be used for baseline estimates of dose rates for mission architectures that have unknown launch dates and span timeframes where the dose rate would be expected to change significantly, which is expected of a Martian mission architecture. The team assumed an average background dose rate of ~0.17 for deep space exposure based on an average modulation value of 675 MV. The modulation value was calculated using parametric models of fluctuating deep space dose rates based on the most recent high-resolution measurements of GCR that were conducted during the Earth-Mars transit of Mars Science Laboratory (MSL) (Ref. 4). GCR radiation is an isotropic source of radiation, so in deep space environments, it is impinging on a ship, astronaut, or system from all solid angles—4π steradians (sr). However, when on an airless planetary surface with no magnetosphere, such as the Moon, one can assume the background dose rates to be half that of deep space because of the planetary surface blocking nearly half of the viewing angle of the sky—2π sr. While Mars has a negligible magnetosphere, slight atmospheric shielding benefits approximately 20 to 30 percent are additionally awarded by being on the surface of Mars compared to the Moon (Ref. 5). Table 2.2 presents the assumptions for background radiation used in this analysis.

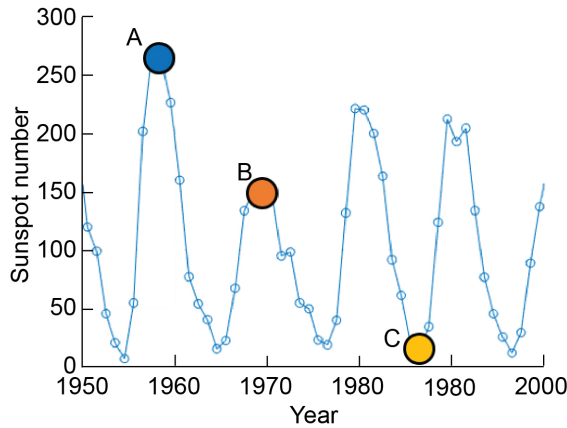


Figure 2.2.—Cyclical solar intensity.

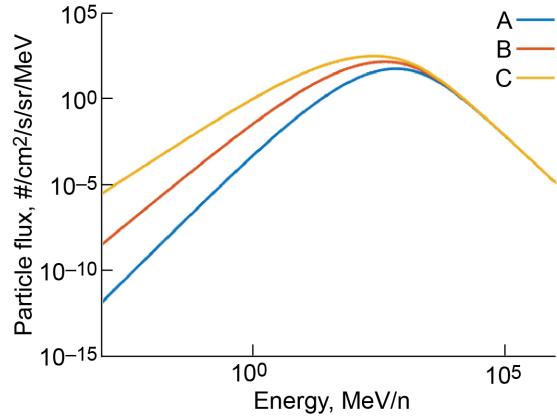


Figure 2.3.—Effects of solar intensity on GCR.

TABLE 2.2.—AMBIENT SPACE RADIATION ASSUMPTIONS FOR ANALYSIS

Scenario	GCR dose rate, rem/day	Assumed duration, days	Total time-integrated dose, rem
Round-trip lunar transit	0.170	10	1.70
Lunar surface	0.092	30	2.76
Combined transit and surface GCR dose for lunar mission	-----	-----	4.46
Round-trip martian transit	0.170	730	124.10
Martian surface	0.064	30	1.92
Combined transit and surface GCR dose for martian mission	-----	-----	126.02

TABLE 2.3.—RELEVANT FEDERAL DOSE LIMITS AND DEFINITIONS

Agency	Short title	Reference	Rem/h	Rem/month	Rem/year	Rem/career
NRC	Radiation area	6	0.005	----	----	-----
NRC	High-radiation area	6	0.100	----	----	-----
NASA	Astronaut limits	7	----	25 <sup>a</sup>	50 <sup>a</sup>	100 to 400 <sup>b</sup>

<sup>a</sup>The monthly and annual values are related to deterministic effects for blood forming organs (Ref. 7).

<sup>b</sup>NASA career limits are age- and sex-dependent values covering this entire range. These values are related to risk of cancer (Ref. 7).

### 2.2.3 Federal Regulatory Limits and Guidance for Radiation Exposures

Working in radiation environments is a common occurrence in many fields, and as such, guidelines, regulations, and limits have been issued for various radiation worker scenarios. While each nation, agency, or company may have specific guidance for their radiation workers, a general philosophy, as low as reasonably achievable (ALARA), is typically exercised when designing radiological workflows to minimize personnel exposures to radiation. For context, some high-level guidelines, vocabulary, and limits for the Nuclear Regulatory Commission (NRC) and NASA are presented in Table 2.3.

### 2.2.4 Rover Concept’s Radioactive Fuel Payload Considerations

The power system for the rover concept uses a traditional fuel form factor of PuO<sub>2</sub> common to modern NASA spaceflight RPS. PuO<sub>2</sub> powder is pressed and encased in an iridium cladding, which contains ~151 g PuO<sub>2</sub> per pellet. Four of these claddings are housed inside a single accident-tolerant aeroshell known as the general-purpose heat source (GPHS) (Ref. 8), which are designed to be stacked atop one another and allow modularity of RPS designs without changing the fundamental fuel form.

These GPHS stacks are then placed in a heat-source management apparatus and used as the primary thermal supply for an energy conversion system (i.e., thermoelectric, Stirling, etc.).

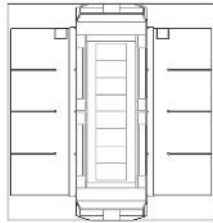
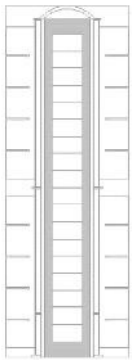
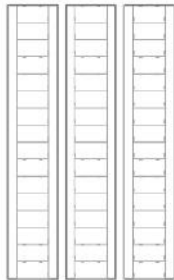
As discussed in Section 2.2.1, the radiation emitted from RPS fuels can impose an occupational hazard on personnel in close physical proximity. The radiation hazard scales with the amount of fuel present in the system and with the time-spent exposed to the radiation field. The power system for the rover concept requires three heat source assemblies, each with 16 GPHS, totaling 48 GPHS on the rover. For perspective, two NASA RPS of historic significance are used here for comparison; the multi-mission radioisotope thermoelectric generator (MMRTG) (Ref. 9) requires eight GPHS and the general-purpose heat source radioisotope thermoelectric generator (GPHS-RTG) (Ref. 9) requires 18 GPHS, as shown in Table 2.4.

Both systems (MMRTG and GPHS-RTG) have been used in spaceflight missions and both introduce radiation hazards that must be considered and managed when implementing and designing occupational workflows involving fueling, shipping, handling, and spacecraft integration procedures. Similarly, the RPS proposed for the rover concept will impose a radiation hazard on the crew but with three distinct differences from traditional radiation exposures from RPS:

1. Crew habitat with relation to RPS will decrease the distance that personnel can maintain from the radiation source.
2. Crew habitat with relation to RPS will increase the time that personnel will be exposed to the radiation source.
3. The amount of fuel is ~6 times more than a single MMRTG, thus imposing a higher intensity from the radiation source.

For these reasons, the RPS proposed for the rover concept required special attention and analysis to demonstrate the feasibility of using such large amounts of PuO<sub>2</sub>, in close proximity, and for long durations in a manned spaceflight scenario.

TABLE 2.4.—COMPARING FUEL AND DOSE IMPLICATIONS OF VARIOUS RPS DESIGNS

Power system	MMRTG	GPHS-RTG	Rover Concept Power System
Render of GPHS orientation			
Number of GPHS	8	18	48
Total PuO <sub>2</sub> mass, kg	~5	~11	~29
Radial dose at 1 m, rem/h	~0.03 <sup>a</sup>	~0.08 <sup>a</sup>	~0.25 <sup>b</sup>

<sup>a</sup>Based on averages of multiple measured dose rates at or near BOL.

<sup>b</sup>Based on calculations from this analysis.

### 2.2.5 Radiation Analysis for RPS

The RPS radiation analysis for this effort was performed using the SCALE nuclear software suite developed at Oak Ridge National Laboratory (Ref. 10), while the assumptions for space radiation were based on empirical models derived from measurements of the Radiation Assessment Detector (RAD) onboard the MSL spacecraft (Ref. 4).

The RPS radiation analysis was performed by making dimensional and material analogs of the rover concept computer-aided design (CAD) models into SCALE particle transport geometries, both of which are shown in Figure 2.4.

The RPS-fueled regions were populated with PuO<sub>2</sub> aged to ~10-years-old to account for the time-dependent radiation characteristics of PuO<sub>2</sub>, and for the notional production time of ~30 kg of fuel. This portion of the calculation is what provides the simulation with the appropriately weighted isotopic composition of fuel, which is what drives the specifics of the time-dependent neutron and gamma spectra. Some distinct differences between isotopic compositions and radiation emissions from fresh fuel versus 10-year-old fuel are shown in Figure 2.5.

The aged-source terms are simulated from inside the PuO<sub>2</sub> where each particle is transported isotopically out from the fuel and allowed to travel throughout the virtual environment, interacting with the materials in the geometry. As the simulation runs, three-dimensional pixels—voxels—are used to tally the particle fluxes and human response functions are used to determine what the dose to humans would be throughout the entire geometry. This technique is used to assess the spatial, radiological impact of various RPS layouts with respect to the SPR along with shielding strategies discussed here. While known limits and recommendations for radiation exposure are issued by various federal agencies (Table 2.3), this analysis additionally self-imposed a desire to bring the dose contribution from the RPS to the SPR (crew quarters) down to background space radiation levels for an added layer of conservatism.

Initial studies were performed with the RPS shielded and unshielded and inside the SPR, to use the decay heat as an auxiliary source of environmental heating inside the habitat. However, resulting dose rates inside the SPR were found to be on the order of ~0.05 to 0.18 rem/h (~36 to 130 rem/month), which would qualify the living quarters of the crew at or above what is traditionally considered a high-radiation area by the NRC (i.e., >0.1 rem/h) (Ref. 6). This would also exceed NASA’s monthly occupational dose limits (i.e., >25 rem/month) (Ref. 7). For these reasons, the internal RPS location concept was abandoned, and the decision to move the RPS to the unpressurized portion of the rover was analyzed.

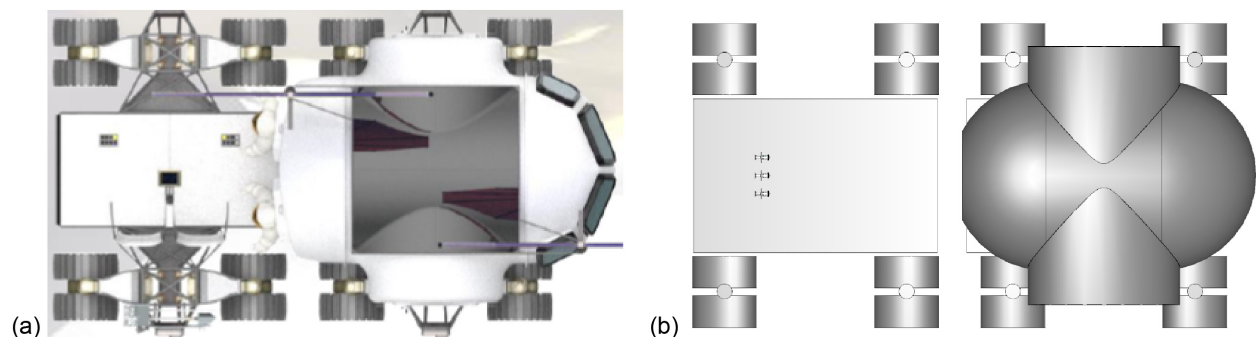


Figure 2.4.—Comparing (a) rover concept CAD and (b) SCALE (Oak Ridge National Laboratory) geometry models.

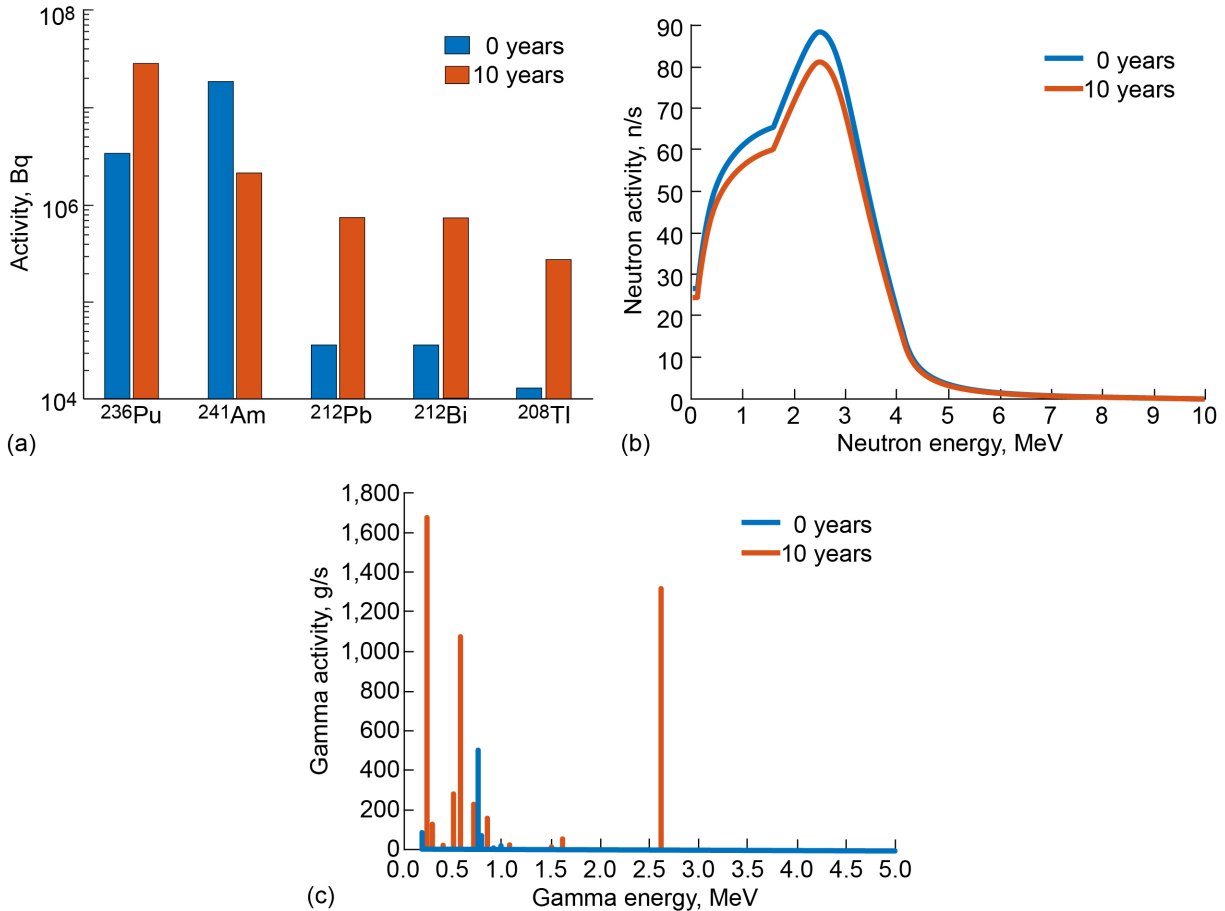


Figure 2.5.—Isotopic composition of PuO<sub>2</sub>. (a) Time-dependence. (b) Neutron spectrum. (c) Gamma spectrum.

Simulations were performed for this new arrangement for both the unshielded and shielded configurations. Dose profiles were assessed along an axis representative of the approximate height of an astronaut’s torso above the chassis, as shown in Figure 2.6.

The corresponding horizontal dose profile lines for unshielded (solid black) and shielded (dotted black) configurations as a function of distance from center of rover are also shown. Note that the center of the SPR is at  $x = 0$  cm, and the center of the RPS is at  $x = 500$  cm.

The center of the SPR is assumed to be the mean location of a given astronaut throughout the month-long surface operations (at  $x = 0$  cm). Radiation intensity follows the inverse square law— $1/r^2$ —and by moving the RPS to the aft portion of the rover concept, significant benefits in mean dose rates to the habitat are realized with no use of additional shielding. However, while the proximity adjustment of the RPS alone brought the mean dose rate of the SPR below deep space background levels, the self-imposed constraint of providing dose rates below surface background for lunar and martian conditions drove further investigation into additional shielding strategies.

A cursory shielding scenario was simulated, placing an assumed 126 kg of onboard water (i.e., drinking water and wastewater) in the aft-most portion of the SPR, along with an additional ~33 kg of water in the chassis around the RPS fuel on the UPR. This preliminary investigation provided ample shielding to bring the SPR’s mean dose rates (from the RPS radiation source alone) down to ~0.0018 rem/h, which is below lunar and martian ambient background radiation levels. Furthermore, EVA will

require personnel to periodically pass by elevated areas of radiation that would normally be defined as high-radiation areas (i.e., above the chassis of the UPR). However, the high-radiation areas presented by the rover concept's stowage of the RPS in the UPR chassis will not present radiological concerns that are significantly more than traditional radiation worker scenarios if ALARA principles are upheld during operations. Tabulated estimations of RPS and space radiation contributions can be found in Appendix B.

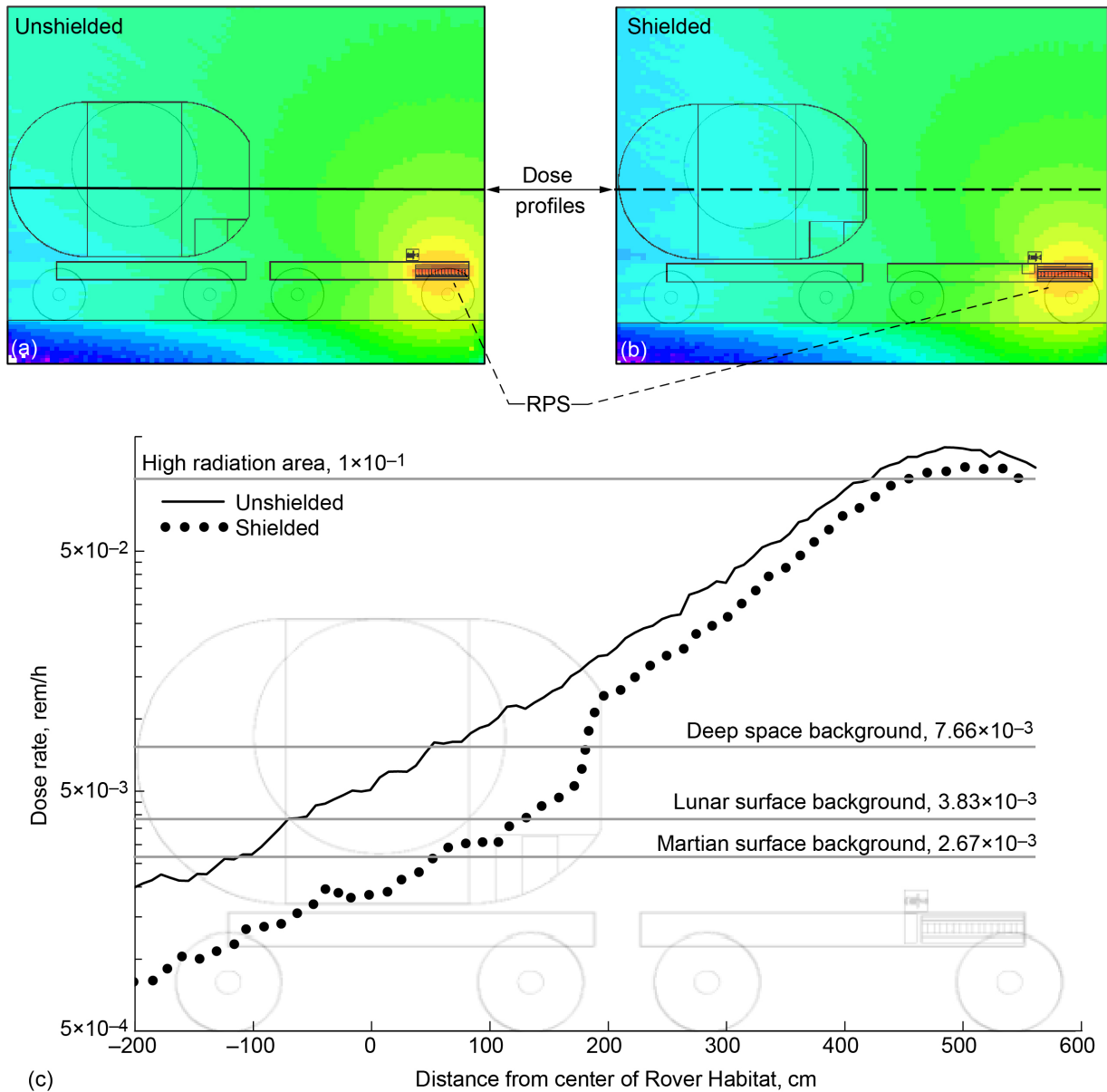


Figure 2.6.—Radioisotope power system (RPS) (a) unshielded and (b) shielded. (c) Calculated dose fields.

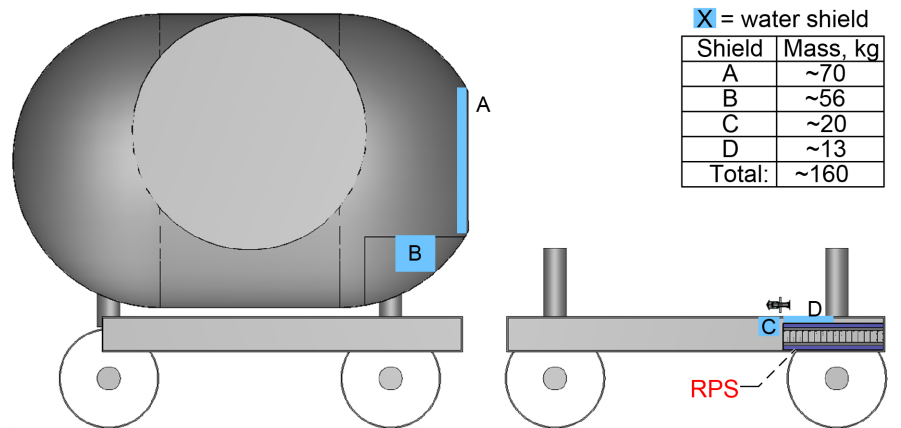


Figure 2.7.—Preliminary simulated water shielding layout.

## 2.2.6 Radiation Analysis Conclusions

This analysis concludes that while the amount of RPS fuel required for the rover concept is significant compared to traditional RPS fuel inventories, some simple implementations demonstrated that it is a viable option. Limiting time, maximizing distance, and adding shielding are sufficient to provide a reasonable occupational working environment for astronauts living inside the SPR and during EVA with limited time spent in high-radiation areas. With adequate consideration for the ALARA principle when designing the concept of operations, the RPS radiation field can pose less of a threat to the total mission dose than natural background radiation, especially for martian mission architectures. See Appendix B for further representations of the respective radiation contributions to total mission dose.

## 2.3 Mass Growth, Contingency, and Margin Policy

The mass growth, contingency, and mass margin policy used by the Compass Team is congruent with the standards described in American Institute of Aeronautics and Astronautics (AIAA) Standard S-120A-2015 (2019), Mass Properties Control for Space Systems (Ref. 11). This methodology starts with the basic mass of the components, to which the mass growth allowance (MGA) is added. This subtotal is defined as the predicted mass. Mass margin is then added to the predicted mass to calculate the allowable mass. Many in the aerospace community also refer to the mass margin as system-level growth.

### 2.3.1 Terms and Definitions

#### Mass

The measure of the quantity of matter in a body.

#### Basic mass

Mass data based on the most recent baseline design. This is the bottoms-up estimate of component mass, as determined by the subsystem leads. It is also known as current best estimate (CBE) mass.

Note 1: This design assessment includes the estimated, calculated, or measured (actual) mass, and includes an estimate for undefined design details like cables, multilayer insulation (MLI), and adhesives.

Note 2: The MGA and uncertainties are not included in the basic mass.

Note 3: Compass has referred to this as CBE in past mission designs.

Note 4: During the course of the design study, the Compass Team carries the propellant as line items in the propulsion system in the master equipment list (MEL). Therefore, propellant is carried in the



	basic mass listing, but MGA is not applied to the propellant. Margins on propellant are handled differently than they are on dry masses.
<b>CBE mass</b>	See basic mass.
<b>Dry mass</b>	The total mass of the system or spacecraft (S/C) when no propellant or pressurants are added.
<b>Wet mass</b>	Is the total mass of the system, including the dry mass and all the pressurants and propellants (used, predicted boiloff, residuals, reserves, etc.). It should be noted that in human S/C designs the wet masses would include more than propellant. In these cases, instead of propellant, the design uses consumables and will include the liquids necessary for human life support.
<b>Inert mass</b>	Is the sum of the dry mass, along with any nonused, and therefore trapped, wet materials, such as residuals and pressurants. In simplest terms, the inert mass is what the trajectory analyst plugs into the rocket equation to size the amount of propellant necessary to perform the mission delta-velocities ( $\Delta V$ ). When the propellant being modeled has a time variation along the trajectory, such as is the case with a boiloff rate, the inert mass can be a variable function with respect to time.
<b>Basic dry mass</b>	Basic mass (a.k.a. CBE mass) minus the propellant, or wet portion of the S/C mass. Mass data is based on the most recent baseline design. This is the bottoms-up estimate of component mass, as determined by the subsystem leads. This does not include the wet mass (e.g., propellant, pressurant, cryofluids boiloff, etc.).
<b>CBE dry mass</b>	See basic dry mass.
<b>Mass growth allowance (MGA)</b>	Defined as the predicted change to the basic mass of an item based on an assessment of its design maturity, fabrication status, and any in-scope design changes that may still occur.
<b>Predicted mass</b>	Basic mass plus the MGA for each line item, as defined by the subsystem engineers.  Note: When creating the MEL, the Compass Team uses predicted mass as a column header and includes the propellant mass as a line item of this section. Again, propellant is carried in the basic mass listing, but MGA is not applied to the propellant. Margins on propellant are handled differently than they are handled on dry masses. Therefore, the predicted mass as listed in the MEL is a wet mass, with no growth applied on the propellant line items.
<b>Predicted dry mass</b>	Predicted mass minus the propellant or wet portion of the mass. The predicted mass is the basic dry mass plus the MGA as the subsystem engineers apply it to each line item. This does not include the wet mass (e.g., propellant, pressurant, cryofluids boiloff, etc.).
<b>Mass reserve (a.k.a. margin)</b>	Difference between the allowable mass for the space system and its total mass. Compass does not set a mass reserve; it is arrived at by subtracting the total mass of the design from the design requirement established at the start of the design study, such as an allowable mass.

The goal is to have a mass reserve greater than or equal to zero to arrive at a feasible design case. A negative mass reserve would indicate that the design has not yet been closed and cannot be considered feasible. More work would need to be completed.

**Mass margin**

Extra allowance carried at the system level needed to reach the AIAA recommended “green” mass risk assessment level, which is currently set at >15 percent for the authorization to proceed program milestone. This value is defined as the difference between allowable mass and predicted mass, with the percentage being with respect to basic mass:

$$\% \text{ mass margin} = (\text{allowable mass} - \text{predicted mass}) / \text{basic mass} * 100$$

For the current Compass design process, a mass margin of 15 percent is applied with respect to the basic mass and added to the predicted mass. The resulting total mass is compared to the allowable mass as the design progresses. If the total mass is less than the allowable mass, then the mass margin is >15 percent and the design closes while maintaining a “green” mass risk assessment level.

If total mass  $\geq$  allowable mass, then the design does not close with the required 15 percent mass margin, and either the total mass needs to be reduced, or the mass risk posture reevaluated, and the mass margin reduced. However, depending on the numerical difference, the design may not close even if the mass margin is set to 0 percent.

**System-level growth**

see mass margin.

**Total mass**

The summation of basic mass, applied MGA, and the mass margin (a.k.a. system-level growth).

**Allowable mass**

The limits against which margins are calculated.

Note: Derived from or given as a requirement early in the design, the allowable mass is intended to remain constant for its duration.

Table 2.5 expands on the definitions for the MEL column titles to provide information on the way masses are tracked through the MEL and used in the Compass design sessions. These definitions are consistent with those in Figure 2.8 in their terms and definitions. This table is an alternate way to present the same information to provide more clarity.

TABLE 2.5.—DEFINITION OF MASSES TRACKED IN MEL

Item	Definition
Basic mass	Mass data based on the most recent baseline design (includes propellants and pressurants)
	Basic dry mass + propellants + pressurants + residuals
MGA growth	Predicted change to the basic dry mass of an item phrased as a percentage of basic dry mass
	MGA% $\times$ basic dry mass = growth
Predicted mass	The basic mass plus the MGA
	Basic dry mass + propellant + growth
Total mass	Predicted mass plus the mass margin (a.k.a., system-level growth)
	Basic dry mass + propellant + growth + mass margin

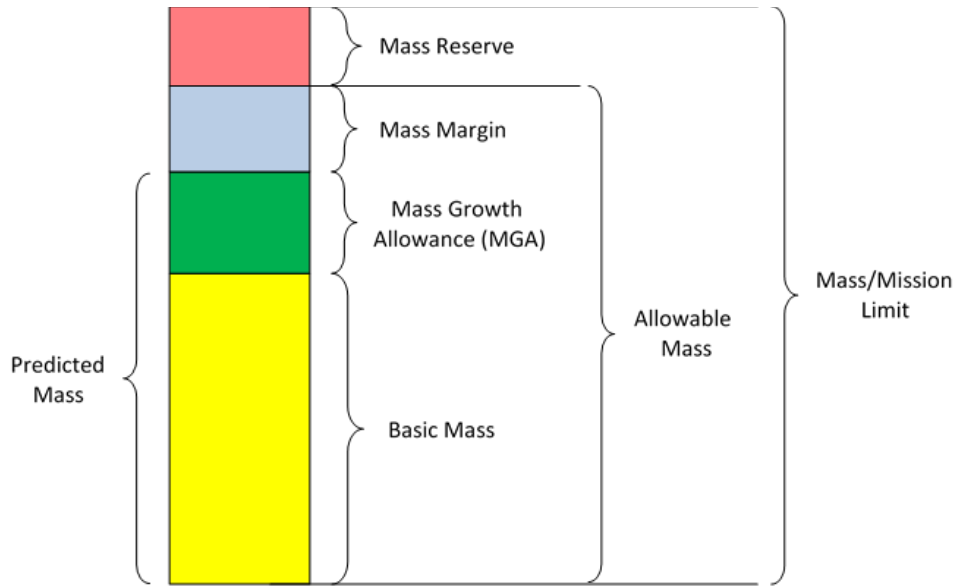


Figure 2.8.—General mass definitions.

TABLE 2.6.—MASS RISK ASSESSMENT

Program milestone	Recommended MGA, percent	Recommended mass margin, percent	MGA + mass margin, percent	Grade
Authorization to proceed	>15	>15	>30	Green
	$9 < \text{MGA} \leq 15$	$10 < \text{mass margin} \leq 15$	$19 < \text{MGA} + \text{mass margin} \leq 30$	Yellow
	$\leq 9$	$\leq 10$	$\leq 19$	Red

For the conceptual level studies conducted by the Compass Team, a mass margin of 15 percent based on basic dry mass is used, which is recommended in AIAA Standard S-120A-2015 (2019) (Ref. 11), for a grade of “green” at the authorization to proceed milestone, as is shown in Table 2.6. The aggregate masses and margins for each design variant are discussed in Section 3.3.

### 2.3.2 Mass Growth

The Compass Team normally uses the AIAA Standard (Ref. 11) as the guideline for its mass growth calculations. Table 2.7 on the next page shows the percent mass growth of a piece of equipment based on both its level of design maturity and its functional subsystem.

TABLE 2.7.—AIAA MGA GUIDELINES FROM AIAA STANDARD S-120A-2015 (2019)

[The MGA percentage ranges in table are applied to basic mass to arrive at predicted mass. Environmental Control and Life Support System (ECLSS) (Ref. 11).]

Maturity code	Design maturity (basis for mass determination)	Percentage MGA														
		Electrical/electronic components			Primary structure	Secondary structure	Mechanisms	Propulsion, fluid systems hardware	Batteries	Wire harnesses	Solar array	ECLSS, crew systems	Thermal control	Instrumentation		
		0 to 5 kg	5 to 15 kg	>15 kg												
E	1	Estimated	20 to 35	15 to 25	10 to 20	18 to 25	20 to 35	18 to 25	15 to 25	20 to 25	50 to 100	20 to 35	20 to 30	30 to 50	25 to 75	
	2	Layout	15 to 30	10 to 20	5 to 15	10 to 20	10 to 25	10 to 20	10 to 20	10 to 20	15 to 45	10 to 20	10 to 20	15 to 30	20 to 30	
C	3	Preliminary design	5 to 20	3 to 15	3 to 12	4 to 15	8 to 15	5 to 15	5 to 15	5 to 15	10 to 25	5 to 15	5 to 15	8 to 15	10 to 25	
	4	Released design	5 to 10	2 to 10	2 to 10	2 to 6	3 to 8	3 to 4	2 to 7	3 to 7	3 to 10	3 to 5	3 to 8	3 to 8	3 to 5	
A	5	Existing hardware	1 to 5	1 to 3	1 to 3	1 to 3	1 to 5	1 to 3	1 to 3	1 to 3	1 to 5	1 to 3	1 to 4	1 to 3	1 to 3	
	6	Actual mass	Measured mass of specific flight hardware; no MGA; use appropriate measurement uncertainty.													
S	7	CFE or specification value	Typically, an NTE value is provided, and no MGA is applied.													
Expanded definitions of maturity categories																
E1	Estimated	a. An approximation based on rough sketches, parametric analysis, or incomplete requirements														
		b. A guess based on experience														
		c. A value with unknown basis or pedigree														
E2	Layout	a. A calculation or approximation based on conceptual designs (layout drawings or models) prior to initial sizing														
		b. Major modifications to existing hardware														
C3	Preliminary design	a. Calculations based on new design after initial sizing but prior to final structural, thermal, or manufacturing analysis														
		b. Minor modification of existing hardware														
C4	Released design	a. Calculations based on a design after final signoff and release for procurement or production														
		b. Minor modification of existing hardware														
A5	Existing hardware	a. Measured mass from another program, assuming that hardware will satisfy program requirements with no changes.														
		b. Values substituted based on empirical production variation of same or similar hardware or qualification hardware.														
		c. Catalog values.														

### 2.3.3 Power Growth

The Compass Team typically uses a 30-percent growth on the bottoms-up power requirements of the various subsystems when modeling the amount of required electrical power. The exception, however, is for the propulsion subsystem. For this design, only 5-percent growth is applied to the electric motor power requirements. No additional margin is carried on top of this power growth.

## 3.0 Baseline Design

The baseline design is an RPS-powered rover system consisting of an UPR and SPR connected together. The RPS is located at the aft of the UPR behind a radiation shield and consists of three GPHS stacks. The UPR also contains the Stirling convertors, radiators, power management and distribution (PMAD), and other power system support equipment. The rear of the SPR contains a water tank to act as a shadow shield to help protect the crew from radiation. Figure 3.1 is a system-level block diagram that captures the major elements of the rover system.

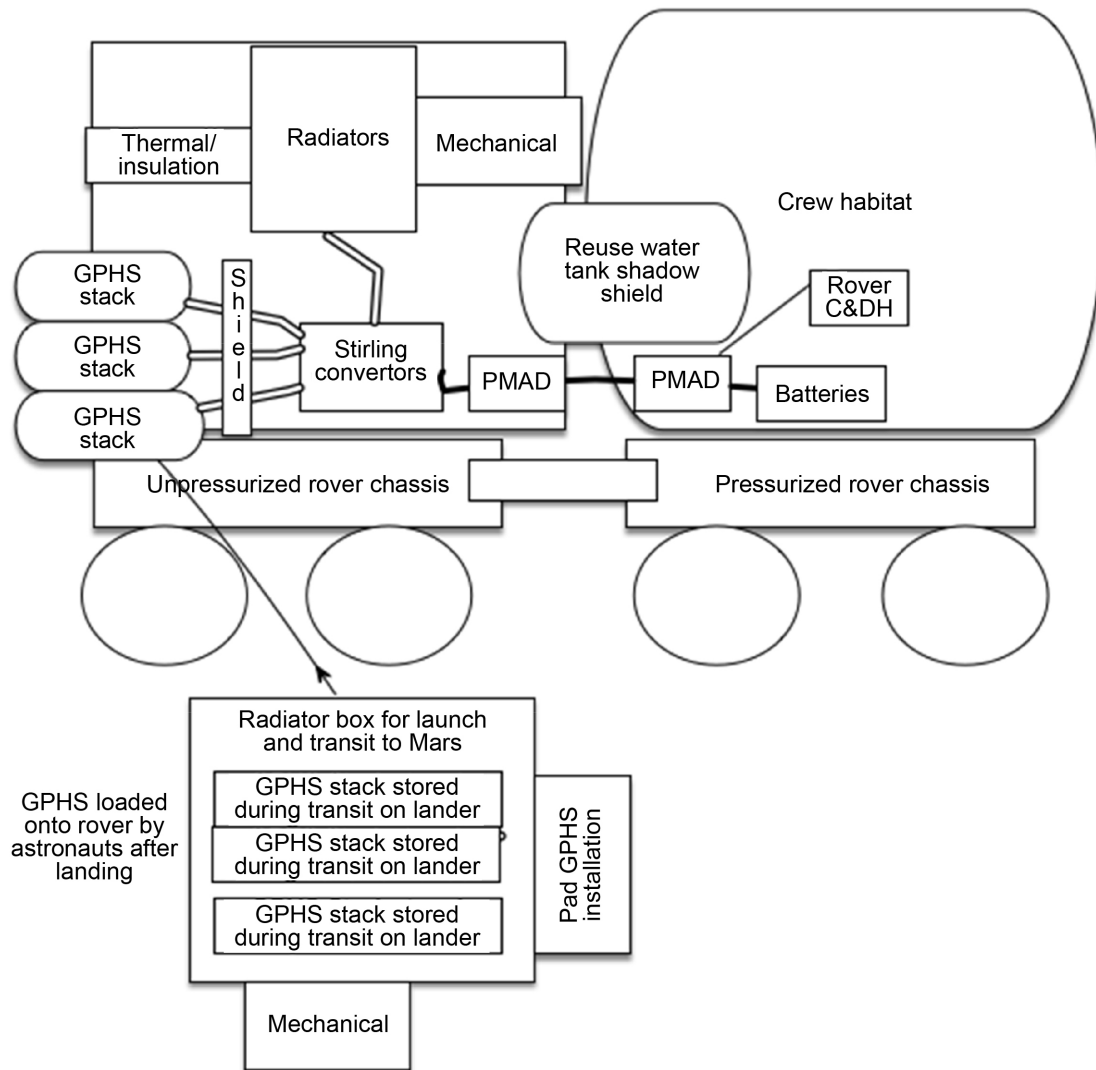


Figure 3.1.—Baseline RPS rover schematic.

### 3.1 Top-Level Design Details

#### 3.1.1 Baseline Design Master Equipment List (MEL)

The MEL for the baseline RPS rover includes the subsystem-level basic mass, the aggregate subsystem MGA in both percentage and mass terms, and then total (or predicted) mass. Table 3.1 shows this for all three major elements; the UPR, SPR, and GPHS launch and transit box. In MEL tables, Destination Agnostic Pressurized System (DAPS) may be used to denote the overarching system.

#### 3.1.2 Spacecraft Total Mass Summary

Table 3.2 shows a summary of the system-level basic masses, predicted masses, and mass margins applied to the three elements of the baseline RPS rover. These three terms are added to determine the allowable mass for all three major elements, and then combined to yield the total allowable mass for the system. The aggregate MGA and system-level growth for the baseline system are 25.8 and 15 percent, respectively, for a combined total of 40.8 percent. This is greater than the 30 percent, which is recommended in the AIAA standard for a grade of “green” at the authorization to proceed milestone, which was discussed previously.

TABLE 3.1.—BASELINE RPS ROVER MEL

Description	Unit Mass	Basic Mass	Growth	Growth	Total Mass
Case 1 DAPS CD 2019-172	(kg)	(kg)	(%)	(kg)	(kg)
<b>DAPS</b>		<b>987</b>	<b>26%</b>	<b>255</b>	<b>1243</b>
<b>Unpressurized Rover</b>		<b>580</b>	<b>20%</b>	<b>117</b>	<b>697</b>
<b>Electrical Power Subsystem</b>		<b>352.7</b>	<b>21%</b>	<b>73.3</b>	<b>426.0</b>
<b>Thermal Control (Non-Propellant)</b>		<b>188.5</b>	<b>18%</b>	<b>33.9</b>	<b>222.4</b>
Structures and Mechanisms		38.9	25%	9.7	48.7
<b>Pressurized Rover</b>		<b>406</b>	<b>34%</b>	<b>138</b>	<b>544</b>
<b>Habitat and Rover Subsystem</b>		<b>0.0</b>	<b>0%</b>	<b>0.0</b>	<b>0.0</b>
<b>Electrical Power Subsystem</b>		<b>406.2</b>	<b>34%</b>	<b>138.1</b>	<b>544.3</b>
<b>Propulsion (EP Hardware)</b>		<b>0.0</b>	<b>0%</b>	<b>0.0</b>	<b>0.0</b>
<b>GPHS Launch and Transit Box</b>		<b>1</b>	<b>18%</b>	<b>0</b>	<b>1</b>
Structures and Mechanisms		1.0	18%	0.2	1.2

TABLE 3.2.—SYSTEM-LEVEL MASS SUMMARY FOR BASELINE RPS ROVER

MEL Summary: Case 1 DAPS CD 2019-172	Unpressurized Rover	Pressurized Rover	GPHS Launch and Transit Box	TOTAL
Main Subsystems	Basic Mass (kg)	Basic Mass (kg)	Basic Mass (kg)	Total Basic Mass(kg)
Electrical Power Subsystem	352.7	406.2	0.0	758.9
Thermal Control (Non-Propellant)	188.5	0.0	0.0	188.5
Structures and Mechanisms	38.9	0.0	1.0	40.0
<b>Element Total</b>	<b>580.2</b>	<b>406.2</b>	<b>1.0</b>	<b>987.4</b>
<b>Element Dry Mass (no prop,consum)</b>	<b>580.2</b>	<b>406.2</b>	<b>1.0</b>	<b>987.4</b>
<b>Element Mass Growth Allowance (Aggregate)</b>	<b>116.9</b>	<b>138.1</b>	<b>0.2</b>	<b>255.2</b>
<b>Predicted Mass (Basic + MGA)</b>	<b>697.1</b>	<b>544.3</b>	<b>1.2</b>	<b>1242.6</b>
<b>Recommended Mass Margin (Additional System Level Growth) 15%</b>	<b>87.0</b>	<b>60.9</b>	<b>0.2</b>	<b>148.1</b>
<b>Element Dry Mass (Basic+MGA+Margin)</b>	<b>784.1</b>	<b>605.2</b>	<b>1.4</b>	<b>1390.8</b>
<b>Element Inert Mass (Basic+MGA+Margin)</b>	<b>784.1</b>	<b>605.2</b>	<b>1.4</b>	<b>1390.8</b>
<b>Total Wet Mass (Allowable Mass)</b>	<b>784.1</b>	<b>605.2</b>	<b>1.4</b>	<b>1390.8</b>

### 3.1.3 Power Equipment List (PEL)

Table 3.3 shows a summary of the PEL for the baseline RPS-powered rover design. For this design, there are six power modes encompassing all anticipated major operational modes from commissioning to resupply. A margin of 30 percent is applied to all power loads, except for propulsion. Since the exact terrain and soil composition are unknown, 10 kWe is allocated for drive power with a 5-percent margin. The exact distance trekked during the 1-h daily driving window will vary based on terrain, but the budgeted power will remain the same for each day.

### 3.2 Concept Drawing and Description

For this lunar/Mars rover study, the Compass Team was to take a crewed lunar rover concept and integrate a power system that would allow for use on the martian surface. NASA Johnson Space Center provided the lunar rover concept (Figure 3.2) (Ref. 12). This rover comprises two main elements, a SPR and an UPR, with both utilizing identical mobility platforms. Both elements are bolted together for stability, mobility, and to allow crew access between the pressurized cabin and the martian atmosphere, with the UPR element trailing the SPR. The crew will enter the EVA suits from inside the rear of pressurized cabin and access the martian surface from the back end of the UPR.

While selecting a power system to integrate with the rover, mass was a key driver along with packaging, functionality on the martian surface, roving durations (desired 21 days continuous), and crew access to the lunar surface from the SPR. The Compass Team examined three power systems: solar power, fuel cells, and a RPS, with the RPS selected as the baseline design and the primary focus of this section.

TABLE 3.3.—BASELINE RPS ROVER PEL

Description	Power Mode 1	Power Mode 2	Power Mode 3	Power Mode 4	Power Mode 5	Power Mode 6
Case 1 DAPS CD 2019-172	Commissioning	Parked/Science (Day)	Parked/Science (Night)	Driving (Day)	Driving/Recharging (Night)	Resupply
	7 Days	9 hours	14 hours	1 hours	14 hours	24 hours
	(W)	(W)	(W)	(W)	(W)	(W)
<b>DAPS</b>	<b>2078.8</b>	<b>2328.8</b>	<b>2328.8</b>	<b>12258.8</b>	<b>2328.8</b>	<b>2078.8</b>
<b>Unpressurized Rover</b>	<b>152.8</b>	<b>152.8</b>	<b>152.8</b>	<b>152.8</b>	<b>152.8</b>	<b>152.8</b>
<b>Electrical Power Subsystem</b>	<b>36.0</b>	<b>36.0</b>	<b>36.0</b>	<b>36.0</b>	<b>36.0</b>	<b>36.0</b>
<b>Thermal Control (Non-Propellant)</b>	<b>116.8</b>	<b>116.8</b>	<b>116.8</b>	<b>116.8</b>	<b>116.8</b>	<b>116.8</b>
Structures and Mechanisms	0.0	0.0	0.0	0.0	0.0	0.0
<b>Pressurized Rover</b>	<b>1926.0</b>	<b>2176.0</b>	<b>2176.0</b>	<b>12106.0</b>	<b>2176.0</b>	<b>1926.0</b>
<b>Habitat and Rover Subsystem</b>	<b>1850.0</b>	<b>2100.0</b>	<b>2100.0</b>	<b>1850.0</b>	<b>2100.0</b>	<b>1850.0</b>
<b>Electrical Power Subsystem</b>	<b>76.0</b>	<b>76.0</b>	<b>76.0</b>	<b>256.0</b>	<b>76.0</b>	<b>76.0</b>
<b>Propulsion (EP Hardware)</b>	<b>0.0</b>	<b>0.0</b>	<b>0.0</b>	<b>10000.0</b>	<b>0.0</b>	<b>0.0</b>
<b>GPFS Launch and Transit Box</b>	<b>0.0</b>	<b>0.0</b>	<b>0.0</b>	<b>0.0</b>	<b>0.0</b>	<b>0.0</b>
Structures and Mechanisms	0.0	0.0	0.0	0.0	0.0	0.0
<b>Bus Power, System Total</b>	2079	2329	2329	2259	2329	2079
<b>30% growth</b>	624	699	699	678	699	624
<b>Total Bus Power Requirement</b>	2702	3027	3027	2936	3027	2702
<b>EP System power, System total</b>	0	0	0	10000	0	0
<b>5% growth</b>	0	0	0	500	0	0
<b>EP System total Requirement</b>	0	0	0	10500	0	0

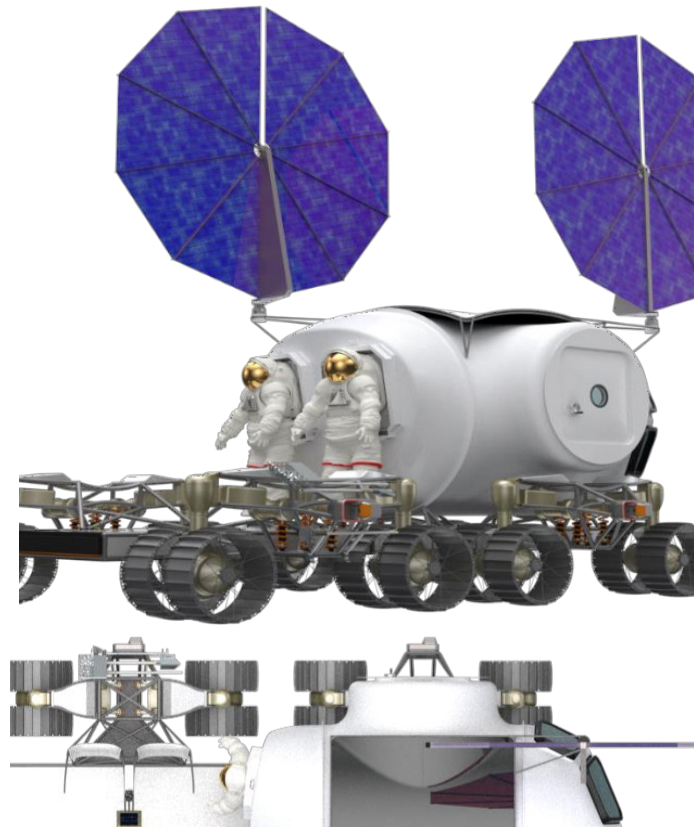


Figure 3.2.—Lunar rover concept.

Utilizing solar power on the martian surface would require two UltraFlex<sup>®</sup> (Ultraflex Technologies Group) arrays, each at an 8.3-m diameter, or a single 9.6-m-diameter array. Tracking the Sun with two arrays that large proved to be difficult, as they would shadow each other most of the time. Packaging of both arrays for launch, transit, and landing would be difficult as well. The Compass Team deemed a single 9.6-m-diameter array too large because it might present a risk to the rover and crew in a high-wind situation. Packaging of an array that large would also be difficult.

Fuel cells would require large reactant tanks for the desired 21-day continuous use. The reactant tanks would need to be located on the mobile platform of the UPR and would not allow the crew access to the surface. In addition, after the 21-day trip, it is assumed the rover would be parked while water was electrolyzed using 500 W from a lander power source over a 6-month period.

Based on the quick trades and assessments, the RPS was selected as the baseline to integrate with the rover, as it packaged easiest, allowed the crew access to the surface, and was lower in mass with comparable radiator sizes when compared to the fuel cell option. The RPS integration with the rover concept can be seen in Figure 3.3. Please note that the lunar rover (shown as transparent in Figure 3.3) is a simplified version of the rover that maintains the same dimensions and deck (or envelope space) as the rover concept shown in Figure 3.2. This was used to allow for quicker modeling as the rover concept in Figure 3.1 was very detailed and severely slowed down the process of integrating the RPS within the CAD software due to the size of the file.



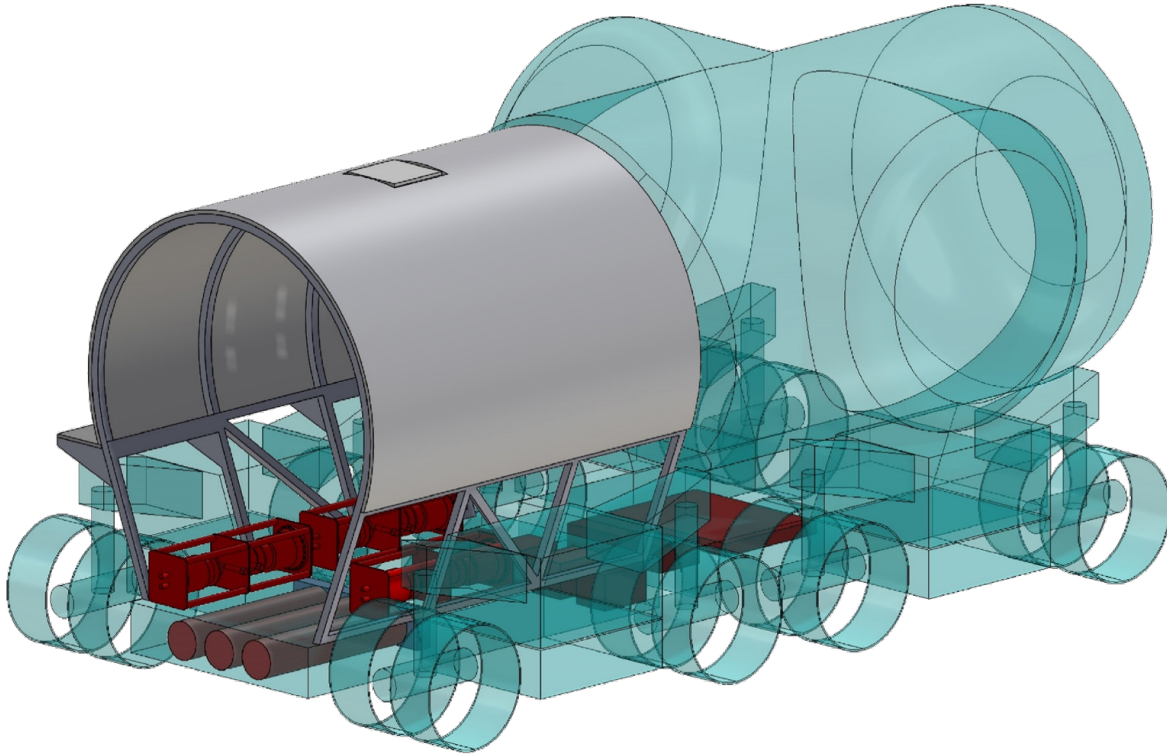


Figure 3.3.—Lunar rover concept with integrated RPS to be used on Mars.

Those components that make up the power system integrated with the lander include various radiators, power generation equipment, and electrical components. There are three radiators (power, parasitic loads, and electronics) and radiator support structures. There are three Stirling convertor units with individual controllers with each string powered by a GPHS stack and heat source assembly. Water is used for shielding, and there is a Li-ion battery for energy storage. Finally, there are two 120-V PMAD boxes, one for the battery and one for the RPS.

Some of the components are located within the mobility deck of both the UPR and SPR because the deck comprises a space frame structure with external closeout panels, thus providing sufficient volume for these components. Figure 3.4 shows all these components contained within the deck structure.

The three GPHS stacks and heat source assemblies are located within the UPR deck near the aft end (furthest from the SPR). They are to be installed robotically after delivery to the martian surface through the back end of the deck. A 10-cm-thick water shield is located directly in front of the GPHS stacks to reduce the radiation to acceptable levels for both the electronics and crew. The closest electronics to the water shield are the three Stirling controllers and the 120-V PMAD box associated with the RPS. These four boxes are located within the deck of the UPR and are at least 124.8 cm away from the forward end of the water shield. The Li-ion battery and 120-V PMAD box associated with it are located inside the deck on the SPR. The exact location of the battery and PMAD box are not optimized, but there is enough volume within the deck to locate them where needed to minimize harness mass, reduce radiation exposure, and allow for an optimal center of gravity location on the rover.

Figure 3.5 shows all the components to be integrated to the outside of the mobility platform deck. These components are all located on the top of the UPR deck.

The largest of the three radiators is the power system radiator. It is shaped to form a “canopy” over the deck of the UPR, thus allowing the crew to exit the SPR and access the surface from the back end of the UPR deck. Located inside a small cutout on top of the power system radiator is the parasitic load

radiator, the smallest of the three radiators. This location is due to the high rejection temperature of this radiator, requiring an unobstructed view upwards, away from the martian surface. Finally, the electronics radiator is located along one side at the base of the power system radiator. This radiator is oriented horizontally to obtain an upward view away from the martian surface. All three radiators are mounted to the same structural frame, which in turn is mounted to the top of the UPR deck at the edge of the long sides, allowing the maximum width on the deck for the crew to access the surface.

Finally, the three dual Stirling convertors are mounted to the top of the UPR deck. Two are located along one side of the deck, while the third is on the opposite side. They are pushed as far out to the edges as possible (right up to the radiator structure) and leave approximately 71 cm between them to allow room for single-file crew access to the martian surface from the back end of the UPR deck. While the Stirling convertors only provide a narrow path for the crew and are not located behind the water shield, they are too large to fit within the deck structure and are not sensitive to the radiation given off by the GPHS stacks.

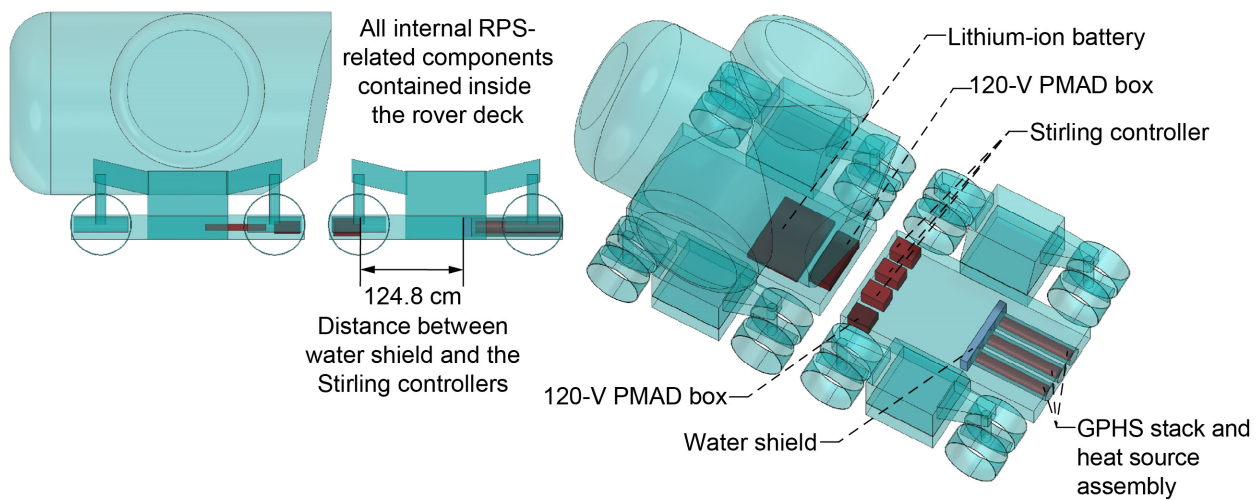


Figure 3.4.—Components contained inside rover mobility platform decks.

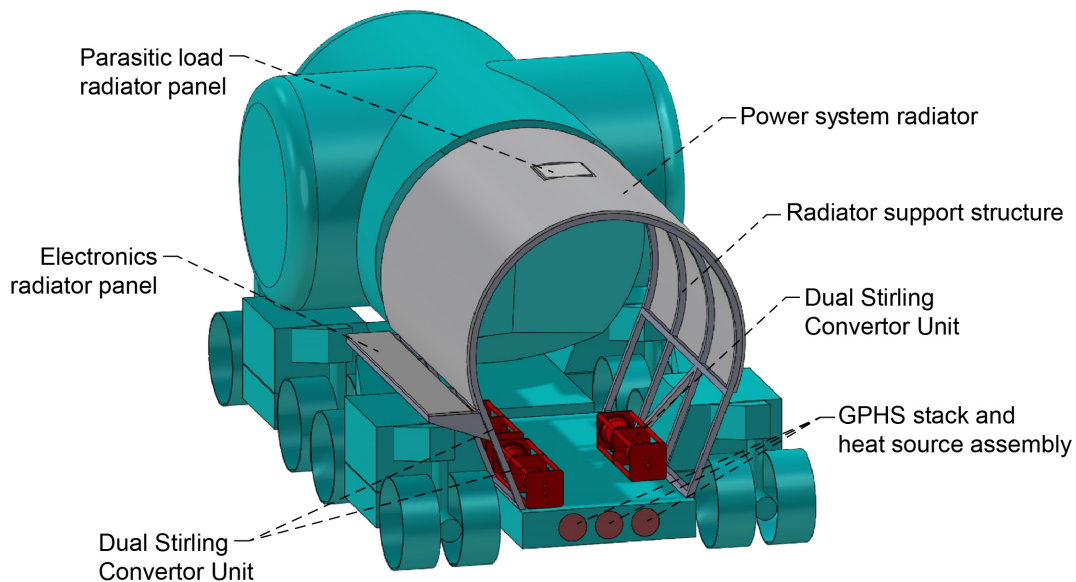


Figure 3.5.—Components located on top of UPR mobility platform deck.

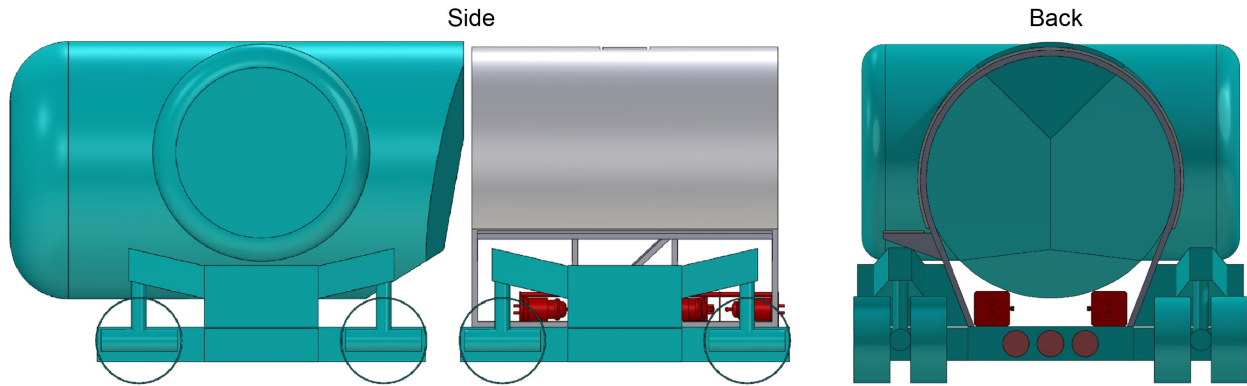


Figure 3.6.—Side and back view of RPS-powered crewed Mars rover concept.

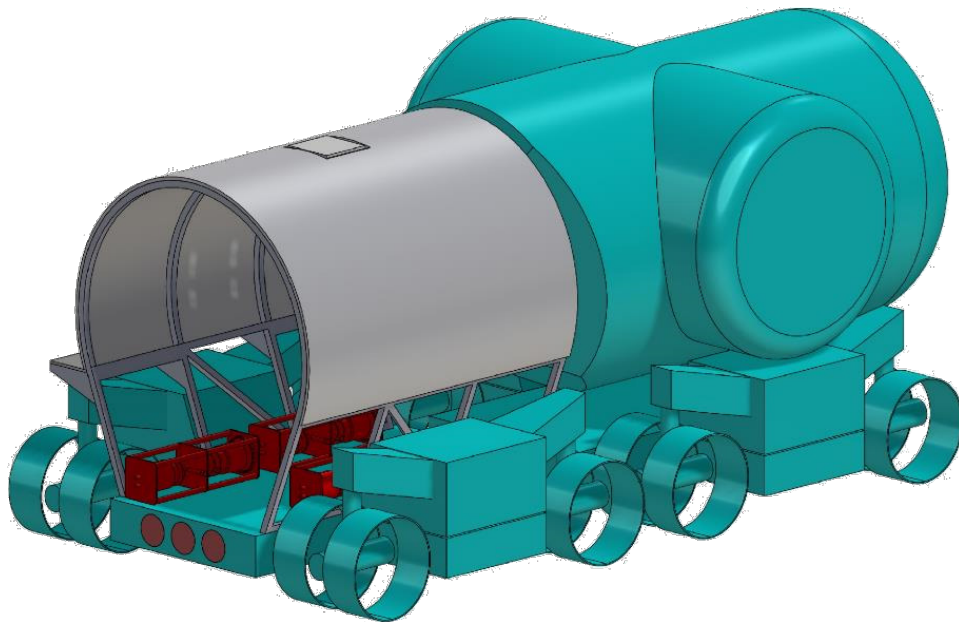


Figure 3.7.—Isometric view of RPS-powered crewed Mars rover.

Figure 3.6 shows a side and back view of the rover, while Figure 3.7 shows an additional isometric view. Section 4.0 provides additional information on all the components in their respective subsystem sections.

### 3.3 Architecture Trades

For this design study, the Compass Team traded both  $\text{GH}_2/\text{GO}_2$  fuel cells and solar panels against the RPS baseline case (case 1). The solar panel case turned out to be infeasible from the start, as it required dual 8.3-m-diameter solar arrays. This left the two fuel cell trades. Case 2 is a fuel-cell-based design with a 6-day excursion limit and rechargeable fuel cells. For this case, the recharging is done at the lander, which provides both the electrolysis of the water byproduct and recompression of the hydrogen and oxygen gases for transfer back to the rover for the next mission. Case 3 is a similar fuel cell design, except there is no processing of reactants at the lander. Instead, 21 days' worth of reactants is carried on the UPR. Lastly, case 4 is an evaluation of the baseline RPS design (case 1) operating at the lunar south pole to simulate pre-Mars mission testing. The Compass Team did not generate a CAD layout or MEL for this case; instead, the team evaluated the preliminary impacts to the design, and the RPS in particular.

### 3.3.1 Case 2: Rechargeable Fuel Cell

The design for case 2 utilized a  $\text{GH}_2/\text{GO}_2$ -based fuel cell for power. The fuel cell reactant storage system is designed for a 6-day excursion, with the pressurized reactants being recharged via an electrolysis and pressurization system located on the rover. Table 3.4 shows a summary of the system-level basic masses, predicted masses, and mass margins applied to the three elements of this design. Table 3.5 shows the power requirements for case 2.

TABLE 3.4.—SYSTEM-LEVEL MASS SUMMARY FOR CASE 2

MEL Summary: Case 2 DAPS CD 2019-172	Unpressurized Rover	Pressurized Rover	Additional Lander Hardware	TOTAL
Main Subsystems	Basic Mass (kg)	Basic Mass (kg)	Basic Mass (kg)	Total Basic Mass(kg)
Electrical Power Subsystem	300.5	33.1	30.0	363.6
Thermal Control (Non-Propellant)	169.1	0.0	0.0	169.1
Fuel Cell Reactant Hardware	355.0	0.0	471.2	826.2
Fuel Cell Reactants (Chemical)	220.6	0.0	220.6	441.3
Structures and Mechanisms	108.5	1.3	35.6	145.3
<b>Element Total</b>	<b>1153.7</b>	<b>34.4</b>	<b>757.4</b>	<b>1945.5</b>
<b>Element Dry Mass (no prop,consum)</b>	<b>933.0</b>	<b>34.4</b>	<b>536.8</b>	<b>1504.2</b>
<b>Element Propellant</b>	<b>220.6</b>	<b>0.0</b>	<b>220.6</b>	<b>441.3</b>
<b>Element Mass Growth Allowance (Aggregate)</b>	<b>197.4</b>	<b>11.5</b>	<b>87.3</b>	<b>296.2</b>
<b>Predicted Mass (Basic + MGA)</b>	<b>1130.4</b>	<b>45.9</b>	<b>624.1</b>	<b>1800.4</b>
<b>Recommended Mass Margin (Additional System Level Growth) 15%</b>	<b>140.0</b>	<b>5.2</b>	<b>80.5</b>	<b>225.6</b>
<b>Element Dry Mass (Basic+MGA+Margin)</b>	<b>1270.4</b>	<b>51.1</b>	<b>704.6</b>	<b>2026.1</b>
<b>Element Inert Mass (Basic+MGA+Margin)</b>	<b>1285.0</b>	<b>51.1</b>	<b>719.2</b>	<b>2055.3</b>
<b>Total Wet Mass (Allowable Mass)</b>	<b>1491.0</b>	<b>51.1</b>	<b>925.2</b>	<b>2467.3</b>

TABLE 3.5.—CASE 2 RECHARGEABLE FUEL CELL ROVER PEL

Description	Power Mode 1	Power Mode 2	Power Mode 3	Power Mode 4	Power Mode 5	Power Mode 6
Case 2 DAPS CD 2019-172	Commissioning	Parked/Science (Day)	Parked/Science (Night)	Driving (Day)	Driving/Recharging (Night)	Resupply
	7 Days	9 hours	14 hours	1 hours	14 hours	24 hours
	(W)	(W)	(W)	(W)	(W)	(W)
<b>Unpressurized Rover</b>	<b>164.8</b>	<b>164.8</b>	<b>164.8</b>	<b>200.8</b>	<b>164.8</b>	<b>164.8</b>
<b>Electrical Power Subsystem</b>	<b>36.0</b>	<b>36.0</b>	<b>36.0</b>	<b>72.0</b>	<b>36.0</b>	<b>36.0</b>
<b>Thermal Control (Non-Propellant)</b>	<b>116.8</b>	<b>116.8</b>	<b>116.8</b>	<b>116.8</b>	<b>116.8</b>	<b>116.8</b>
<b>Fuel Cell Reactant Hardware</b>	<b>12.0</b>	<b>12.0</b>	<b>12.0</b>	<b>12.0</b>	<b>12.0</b>	<b>12.0</b>
<b>Pressurized Rover</b>	<b>1886.0</b>	<b>2136.0</b>	<b>2136.0</b>	<b>11922.0</b>	<b>2136.0</b>	<b>1886.0</b>
<b>Habitat and Rover Subsystem</b>	<b>1850.0</b>	<b>2100.0</b>	<b>2100.0</b>	<b>1850.0</b>	<b>2100.0</b>	<b>1850.0</b>
<b>Electrical Power Subsystem</b>	<b>36.0</b>	<b>36.0</b>	<b>36.0</b>	<b>72.0</b>	<b>36.0</b>	<b>36.0</b>
<b>Propulsion (EP Hardware)</b>	<b>0.0</b>	<b>0.0</b>	<b>0.0</b>	<b>10000.0</b>	<b>0.0</b>	<b>0.0</b>
<b>Additional Lander Hardware</b>	<b>0.0</b>	<b>0.0</b>	<b>0.0</b>	<b>0.0</b>	<b>0.0</b>	<b>0.0</b>
<b>Bus Power, System Total</b>	2051	2301	2301	2123	2301	2051
<b>30% growth</b>	615	690	690	637	690	615
<b>Total Bus Power Requirement</b>	2666	2991	2991	2760	2991	2666
<b>EP System power, System total</b>	0	0	0	10000	0	0
<b>5% growth</b>	0	0	0	500	0	0
<b>EP System total Requirement</b>	0	0	0	10500	0	0
<b>Total System power with growth</b>	<b>2666</b>	<b>2991</b>	<b>2991</b>	<b>13260</b>	<b>2991</b>	<b>2666</b>

### 3.3.2 Case 3: Self-Contained Fuel Cell

The design for case 3 also utilized a  $\text{GH}_2/\text{GO}_2$ -based fuel cell for power. The fuel cell reactant storage system for case 3, however, is designed to store adequate reactants for a full 21-day mission with no recharging. Table 3.6 shows a summary of the system-level basic masses, predicted masses, and mass margins applied to the three elements of the rechargeable fuel-cell-based rover design. Table 3.7 shows the power requirements for case 3.

### 3.3.3 Mass Comparison of Rover Design Trades

Table 3.8 shows a mass comparison of the three rover designs. This table shows the major subsystem masses, MGAs, mass margins, and total wet mass for all three elements of all three Compass Team rover designs.

TABLE 3.6.—SYSTEM-LEVEL MASS SUMMARY FOR CASE 3

MEL Summary: Case 3 DAPS CD 2019-172	Unpressurized Rover	Pressurized Rover	Additional Lander Hardware	TOTAL
Main Subsystems	Basic Mass (kg)	Basic Mass (kg)	Basic Mass (kg)	Total Basic Mass(kg)
Electrical Power Subsystem	330.5	33.1	0.0	363.6
Thermal Control (Non-Propellant)	169.1	0.0	0.0	169.1
Fuel Cell Reactant Hardware	1179.4	0.0	0.0	1179.4
Fuel Cell Reactants (Chemical)	859.9	0.0	0.0	859.9
Structures and Mechanisms	134.7	1.3	0.0	136.0
<b>Element Total</b>	<b>2673.6</b>	<b>34.4</b>	<b>0.0</b>	<b>2708.1</b>
<b>Element Dry Mass (no prop,consum)</b>	1813.7	34.4	0.0	1848.1
<b>Element Propellant</b>	859.9	0.0	0.0	859.9
<b>Element Mass Growth Allowance (Aggregate)</b>	334.8	11.5	0.0	346.3
<b>Predicted Mass (Basic + MGA)</b>	2148.5	45.9	0.0	2194.4
<b>Recommended Mass Margin (Additional System Level Growth) 15%</b>	272.1	5.2	0.0	277.2
<b>Element Dry Mass (Basic+MGA+Margin)</b>	2420.6	51.1	0.0	2471.6
<b>Element Inert Mass (Basic+MGA+Margin)</b>	2477.6	51.1	0.0	2528.7
<b>Total Wet Mass (Allowable Mass)</b>	<b>3280.5</b>	<b>51.1</b>	<b>0.0</b>	<b>3331.6</b>

TABLE 3.7.—CASE 3 SELF-CONTAINED FUEL CELL ROVER PEL

Description	Power Mode 1	Power Mode 2	Power Mode 3	Power Mode 4	Power Mode 5	Power Mode 6
Case 3 DAPS CD 2019-172	Commissioning	Parked/Science (Day)	Parked/Science (Night)	Driving (Day)	Driving/Recharging (Night)	Resupply
	7 Days	9 hours	14 hours	1 hours	14 hours	24 hours
	(W)	(W)	(W)	(W)	(W)	(W)
<b>DAPS</b>	<b>2050.8</b>	<b>2300.8</b>	<b>2300.8</b>	<b>12122.8</b>	<b>2300.8</b>	<b>2050.8</b>
<b>Unpressurized Rover</b>	<b>164.8</b>	<b>164.8</b>	<b>164.8</b>	<b>200.8</b>	<b>164.8</b>	<b>164.8</b>
<b>Electrical Power Subsystem</b>	<b>36.0</b>	<b>36.0</b>	<b>36.0</b>	<b>72.0</b>	<b>36.0</b>	<b>36.0</b>
<b>Thermal Control (Non-Propellant)</b>	<b>116.8</b>	<b>116.8</b>	<b>116.8</b>	<b>116.8</b>	<b>116.8</b>	<b>116.8</b>
<b>Fuel Cell Reactant Hardware</b>	<b>12.0</b>	<b>12.0</b>	<b>12.0</b>	<b>12.0</b>	<b>12.0</b>	<b>12.0</b>
<b>Pressurized Rover</b>	<b>1886.0</b>	<b>2136.0</b>	<b>2136.0</b>	<b>11922.0</b>	<b>2136.0</b>	<b>1886.0</b>
<b>Habitat and Rover Subsystem</b>	<b>1850.0</b>	<b>2100.0</b>	<b>2100.0</b>	<b>1850.0</b>	<b>2100.0</b>	<b>1850.0</b>
<b>Electrical Power Subsystem</b>	<b>36.0</b>	<b>36.0</b>	<b>36.0</b>	<b>72.0</b>	<b>36.0</b>	<b>36.0</b>
<b>Propulsion (EP Hardware)</b>	<b>0.0</b>	<b>0.0</b>	<b>0.0</b>	<b>10000.0</b>	<b>0.0</b>	<b>0.0</b>
<b>Additional Lander Hardware</b>	<b>0.0</b>	<b>0.0</b>	<b>0.0</b>	<b>0.0</b>	<b>0.0</b>	<b>0.0</b>
<b>Bus Power, System Total</b>	2051	2301	2301	2123	2301	2051
<b>30% growth</b>	615	690	690	637	690	615
<b>Total Bus Power Requirement</b>	2666	2991	2991	2760	2991	2666
<b>EP System power, System total</b>	0	0	0	10000	0	0
<b>5% growth</b>	0	0	0	500	0	0
<b>EP System total Requirement</b>	0	0	0	10500	0	0
<b>Total System power with growth</b>	<b>2666</b>	<b>2991</b>	<b>2991</b>	<b>13260</b>	<b>2991</b>	<b>2666</b>

TABLE 3.8.—ROVER DESIGN MASS COMPARISON

MEL Comparison: DAPS CD 2019-172	Case 1: GHPS				Case 2: Fuel Cells (Six Days w/ Lander Reprocessing)				Case 3: Fuel Cells (21 Days, All Reactants on Rover)			
	Unpressurized Rover	Pressurized Rover	GPHS Launch and Transit Box	Total	Unpressurized Rover	Pressurized Rover	Additional Lander Hardware	Total	Unpressurized Rover	Pressurized Rover	Additional Lander Hardware	Total
<b>Main Subsystems</b>	<b>Basic Mass (kg)</b>	<b>Basic Mass (kg)</b>	<b>Basic Mass (kg)</b>	<b>Total Basic Mass(kg)</b>	<b>Basic Mass (kg)</b>	<b>Basic Mass (kg)</b>	<b>Basic Mass (kg)</b>	<b>Total Basic Mass(kg)</b>	<b>Basic Mass (kg)</b>	<b>Basic Mass (kg)</b>	<b>Basic Mass (kg)</b>	<b>Total Basic Mass(kg)</b>
Electrical Power Subsystem	352.7	406.2	0.0	758.9	300.5	33.1	30.0	363.6	330.5	33.1	0.0	363.6
Thermal Control (Non-Propellant)	188.5	0.0	0.0	188.5	169.1	0.0	0.0	169.1	169.1	0.0	0.0	169.1
Fuel Cell Reactant Hardware	0.0	0.0	0.0	0.0	355.0	0.0	471.2	826.2	1179.4	0.0	0.0	1179.4
Fuel Cell Reactants (Chemical)	0.0	0.0	0.0	0.0	220.6	0.0	220.6	441.3	859.9	0.0	0.0	859.9
Structures and Mechanisms	38.9	0.0	1.0	40.0	108.5	1.3	35.6	145.3	134.7	1.3	0.0	136.0
<b>Element Total</b>	<b>580.2</b>	<b>406.2</b>	<b>1.0</b>	<b>987.4</b>	<b>1153.7</b>	<b>34.4</b>	<b>757.4</b>	<b>1945.5</b>	<b>2673.6</b>	<b>34.4</b>	<b>0.0</b>	<b>2708.1</b>
<b>Element Dry Mass (no prop, consum)</b>	580.2	406.2	1.0	987.4	933.0	34.4	536.8	1504.2	1813.7	34.4	0.0	1848.1
<b>Element Propellant</b>	0.0	0.0	0.0	0.0	220.6	0.0	220.6	441.3	859.9	0.0	0.0	859.9
<b>Element Mass Growth Allowance (Aggregate)</b>	116.9	138.1	0.2	255.2	197.4	11.5	87.3	296.2	334.8	11.5	0.0	346.3
<b>Predicted Mass (Basic + MGA)</b>	697.1	544.3	1.2	1242.6	1130.4	45.9	624.1	1800.4	2148.5	45.9	0.0	2194.4
<b>Recommended Mass Margin (Additional System Level Growth) 15%</b>	87.0	60.9	0.2	148.1	140.0	5.2	80.5	225.6	272.1	5.2	0.0	277.2
<b>Element Dry Mass (Basic+MGA+Margin)</b>	784.1	605.2	1.4	1390.8	1270.4	51.1	704.6	2026.1	2420.6	51.1	0.0	2471.6
<b>Element Inert Mass (Basic+MGA+Margin)</b>	784.1	605.2	1.4	1390.8	1285.0	51.1	719.2	2055.3	2477.6	51.1	0.0	2528.7
<b>Total Wet Mass (Allowable Mass)</b>	<b>784.1</b>	<b>605.2</b>	<b>1.4</b>	<b>1390.8</b>	<b>1491.0</b>	<b>51.1</b>	<b>925.2</b>	<b>2467.3</b>	<b>3280.5</b>	<b>51.1</b>	<b>0.0</b>	<b>3331.6</b>

## 4.0 Subsystem Breakdown

This section provides a detailed description of each major rover subsystem. In addition to the descriptions and diagrams, each subsection includes a subsystem MEL, which rolls up into the overall system-level MEL and mass summary for each case.

### 4.1 Electrical Power System (EPS)

The EPS provides electrical power to the loads on the lunar/Mars rover for the duration of the exploration mission. Though this rover is intended to operate in both the lunar and Mars surface environments, this study focused primarily on the Mars surface environment, and examined the use of both a dynamic RPS and solar power for power generation on the rover. The Compass Team also studied utilizing a proton-exchange membrane (PEM) fuel cell to provide electrical power to the rover.

The team separated these various power trades into different cases for this study. Case 1 utilizes the RPS for power generation, supplemented by a rechargeable Li-ion battery to meet the high power demand of the rover motors. Since the RPS provides power generation, the rover is assumed to be away from base for the full 21 days. Case 2 utilizes a PEM fuel cell to provide electrical power to the rover loads, and the total mission duration was reduced to 6 days instead of 21 days. On the last day, the rover returns to the base and exchanges the product water from the fuel cell with fresh reactants (O<sub>2</sub> and H<sub>2</sub>) from the lander. While the rover is away from the base, the lander utilizes its power supply to electrolyze the product water back into reactants for the next rover mission. The lander’s electrolyzer system is not included as part of the rover EPS for case 2. Case 3 also utilizes a PEM fuel cell for power, but with the full mission length of 21 days to provide a proper comparison to the case 1 EPS design. Early into the study, solar power was deemed unsuitable for the Mars surface application. While no full case study was performed, this study did evaluate the approximate mass and size of a solar array for power generation on the Mars surface.

#### 4.1.1 System Requirements

To encompass the various operational modes of the rover and the associated load demand in each phase, Table 4.1 illustrates the rover’s power modes, durations, and electrical load demand for the three cases in this study. The electrical load demands shown in the table include a 30-percent growth margin for all estimated loads except the driving motor power, which only has a 5-percent growth margin. All EPS losses and parasitic power required for the EPS components are included in these power levels.

TABLE 4.1.—CASES 1 TO 3 POWER MODES AND TOTAL ELECTRICAL LOAD DEMANDS

Power modes	Commissioning and resupply	Parked and science operations (day)	Parked and science operations (night)	Driving (day)
Duration	7 days Resupply: ≥1 day	At lander: 10 h/day On mission: 9 h/day	14 h/day	1.0 h/day
Case 1 load demand	2,702 W	3,027 W	3,027 W	13,436 W
Cases 2 and 3 load demand	2,666 W	2,991 W	2,991 W	13,260 W

## 4.1.2 System Assumptions

There are many assumptions made in the design of the EPS that the Compass Team applied where applicable. These assumptions are grouped into three major categories: environmental, operational, and design. The environmental assumptions are primarily for the worst case (Mars), and include:

- The martian day consists of 10 h of daylight and 14 h of darkness.
- The martian wind produces negligible structural loading.
- Mars atmospheric light spectrum has a constant optical depth of  $1 \tau$ .

Next are the operational assumptions, which were made regarding the operational characteristics of the EPS design. These assumptions include:

- The solar arrays have continuous and perfect Sun-tracking sans shadowing.
- The EPS supports a constant hotel load for all power modes.
- The rover drives without interruption for a maximum of 1 h/day while away from base.
- The EPS supports science loads whenever it is parked (23 h minimum per day).
- The lander can provide effectively unlimited power and energy for recharging and resupply.

Finally, there are design assumptions regarding various aspects of the hardware. These assumptions for the EPS include:

- The nominal EPS bus voltage is 120 VDC.
- The energy storage components are sized to provide 120 VDC nominally to the bus while having a maximum depth of discharge (DOD) of 80 percent.
- Batteries are assumed to include two spare strings for redundancy, while fuel cells are assumed to include one spare stack and one spare set of ancillaries for redundancy.
- PMAD boxes include a cold spare for each card type in use, making them single fault tolerant.

## 4.1.3 System Designs and Trades

### 4.1.3.1 Case 1—Radioisotope Power System (RPS)

Case 1 utilizes a dynamic RPS consisting of 48 GPHS bricks that convert thermal power into electrical power using Stirling convertors. Each set of 16 GPHS bricks is paired with dual opposed Stirling convertors to create one power conversion module that generates 1.16 kWe. The RPS on the rover uses three power conversion modules in total to produce a maximum of 3.39 kWe, which exceeds the parked/science electrical load demand of the rover (power positive). Any excess RPS power produced is used to recharge the Li-ion battery during the nondriving phases of the mission. The RPS has a 16.22-m<sup>2</sup> radiator area, a specific mass of 9.62 W/kg, and a mass of 352.92 kg, and can be considered at technology readiness level (TRL) 3 through 4. Figure 4.1 illustrates the RPS configuration onboard the UPR section.

The GPHS has been the core element of modern RPS and is used for many deep space missions when there is a lack of adequate solar illumination to power solar cells. It is a Department of Energy (DOE) standardized thermal source that produces approximately 250 Wth at the BOL. Table 4.2 shows the dimensions of a GPHS module.



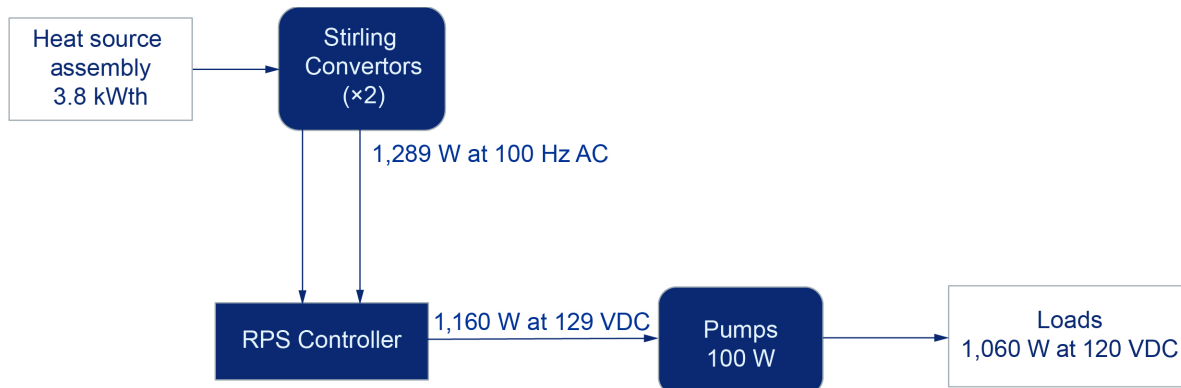


Figure 4.1.—Case 1 RPS. Alternating current (AC).

TABLE 4.2.—STEP 2 GPHS DIMENSIONS

Height, cm.....	5.82
Width, cm.....	9.32
Length, cm .....	9.96

The fuel for the GPHS is PuO<sub>2</sub>, the ceramic form of <sup>238</sup>Pu. PuO<sub>2</sub> is placed in four iridium capsules and surrounded by a graphite shell to form each GPHS module. Most of <sup>238</sup>Pu radioactive decay energy comes from an alpha emission and it has a long half-life (87.7 years). Relatively low amounts of neutron emission come from both spontaneous fission and (α, n) reactions, which result from the interactions of the high-energy alpha particles with materials of low atomic mass. Specifically, the iridium capsule prevents the alpha particles from leaving the fuel pellet (and interacting with the surrounding graphite), but interactions with both O<sub>17</sub> and O<sub>18</sub> in the PuO<sub>2</sub> mixture produces some neutron flux. Production of <sup>238</sup>Pu is commonly done by neutron irradiation of <sup>237</sup>Np in a high-flux reactor. The product of this irradiation is <sup>238</sup>Np that decays (2.117-day half-life) via beta emission into <sup>238</sup>Pu.

#### 4.1.3.1.1 Design Overview

The concept builds on the GPHS-RTG layout and couples this to a pair of Stirling convertors. Modifications to the heat source assembly would include removing the MLI, thermoelectric convertors, and radiator fins while adding solid insulation (for use on the Mars surface) and a sodium-potassium (NaK) liquid metal flow loop surrounding the GPHS modules. The GPHS-RTG contains 16 GPHS modules (producing about 4,000 W of heat BOL) and has an overall diameter of 0.422 m and a length of 1 m. The outer shell would be made of an aluminum alloy. The housing needs to be larger in diameter due to the poorer performance of the solid insulation (versus MLI) and the fluid tubes wrapped around the GPHS modules.

Figure 4.2 shows a sketch of the heat source conceptual layout. Fixing each heat source assembly to 16 GPHS modules and then estimating losses and component efficiencies produces a total estimated direct current (DC) power output to the bus of slightly more than 1 kWe.

Heat loss through the insulation, structure, and piping is sized to be 5 percent of the total heat generated, with a fixed 1.5-percent heat loss assumed through the piping and structure. Heat is taken from the heat source assembly via a flowing NaK loop, split into two channels and moved to the pair of Stirling convertors.

The NaK is pumped around the hot side of the system with two series annular linear induction electromagnetic pumps (ALIPs). The series configuration shown in Figure 4.3 is possible because the ALIPs are open channel pumps with external coils that provide a magnetic field. The ALIPs have an assumed efficiency of 15 percent.

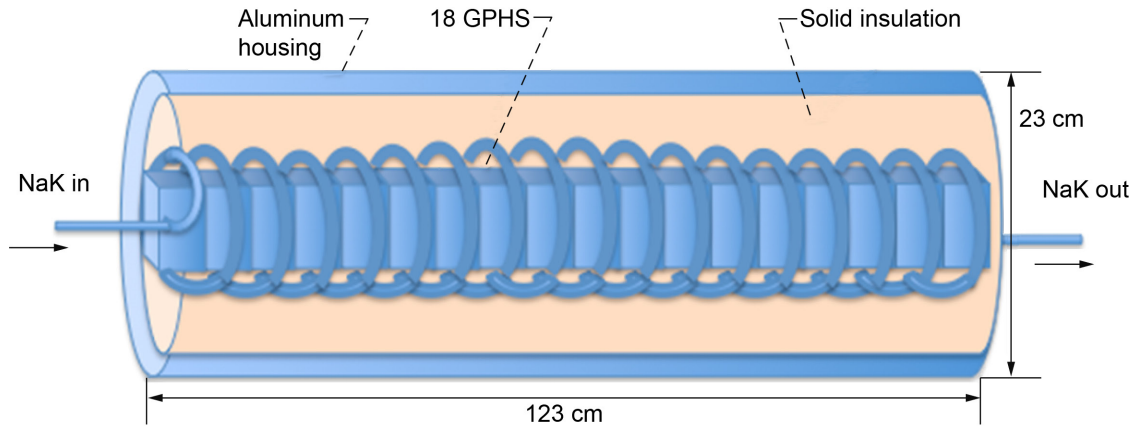


Figure 4.2.—Conceptual layout of isotope heat source.

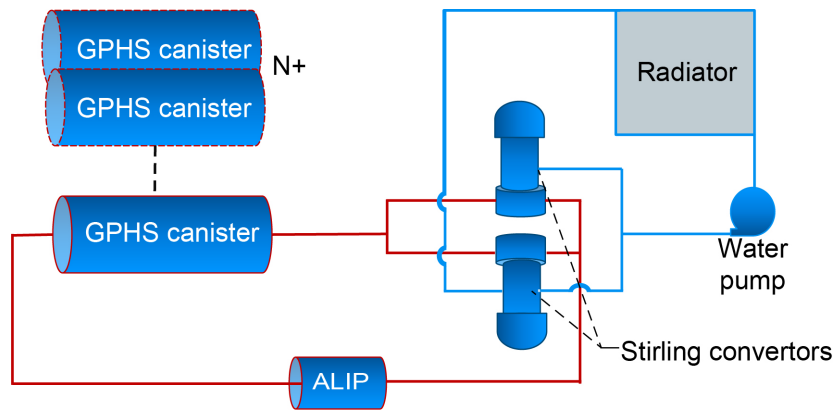


Figure 4.3.—Stirling isotope power system layout.

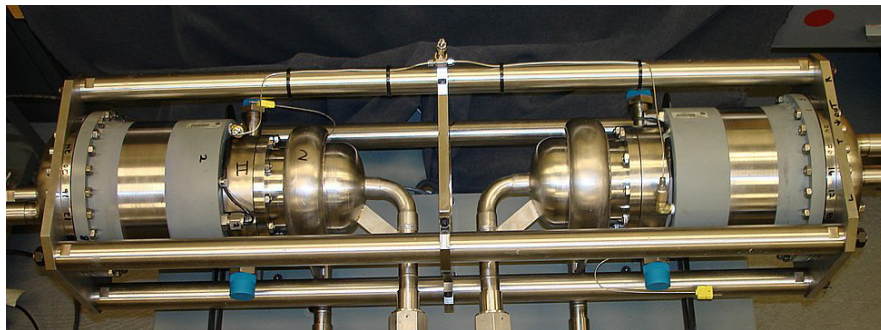


Figure 4.4.—Sunpower's 2-kWe dual-opposed converter with integrated NaK loop.

For this study we used a well-defined 1-kWe Sunpower, Inc. converter as a reference point. This specific converter is of a very robust design developed initially for residential micro cogeneration applications and modified for space operation. All the fundamental converter technologies employed (e.g., the linear alternator design, piston/displacer assembly, gas bearing system, etc.) are the same as those that would be employed in a high-power, space-based design and are currently used in the Advanced Stirling Radioisotope Generator (ASRG) converter. This 1-kWe converter has been modified to incorporate a pumped NaK hot-end heat exchanger as shown in Figure 4.4, operating at the NaK pumped loop test facility located at NASA Marshall Space Flight Center. The only change to the basic

converter is the additional inlet/outlet manifold that directs the NaK over the existing converter heater head. The Stirling converters performed identically to their gas burner heater heads.

Building on this 2-kWe overall layout, we then applied the higher hot-end material capabilities demonstrated in the current Dynamic Radioisotope Power Systems (DRPS) contracts in development at Glenn. The most direct method of removing the waste heat from the Stirling convertor is to have a conductive coupling between the cooler section of the Stirling and a heat rejection surface. This method is used in the ASRG and consists of a cylindrical ring with the inner portion contacting the Stirling cooler and the outer surface of the ring in contact with the ASRG housing/radiator. The advantage of this configuration is its simplicity. As the amount of heat rejected increases the trade between material thicknesses (and thus mass), an allowable temperature drop eventually favors other heat transport augmentation methods. For this system, a pumped loop heat transport system is used for heat rejection. Water is passed over the Stirling cold end, transported out to the radiator panels and through the pumps, and returned to the Stirling convertor.

Stirling convertors operate best when the inlet-to-exit coolant temperature difference is kept to a minimum. In general, the temperature rise of a fluid used to remove the waste heat should be about 25 K or less (inlet to outlet of the Stirling) to ensure minimal Stirling cycle performance penalty. Figure 4.5 shows the radiator panel design consists of water heat pipes sandwiched between two outer face sheets. Panel mass was approximately 3.5 kg/m<sup>2</sup> for the cases shown for the two-sided radiator. This areal mass does not include the fluid ducts, fluid, or pumps, which are accounted for separately. The pump design selected is scaled from other space pumps and is scaled in both efficiency and mass to meet the pressure drop and flow rate requirements of the system.

#### 4.1.3.1.2 Energy Storage

Since the maximum RPS power generation is 3.4 kWe, energy storage is required to supplement the power system during driving. Of the 13.4 kW peak power needed for driving, 10 kW is provided by a Li-ion battery. This rechargeable Li-ion battery is designed using commercial off-the-shelf (COTS) LG 18650 MJ1 battery cells. The battery contains 34 cells per string to provide a nominal 120 VDC and a total of 132 strings in parallel to meet the total rover energy needs. To minimize mass, the battery starts at 100 percent state of charge (SOC) but is not recharged back to 100 percent each day. Instead, it is recharged to 96.2 percent (for a loss of 3.8 percent) SOC every day. At the end of the drive back on the 21st day, the rover battery has only 20 percent of its full charge, or 80 percent DOD, as limited by the system assumptions. This results in a battery sized for 52.7 kWh with a maximum discharge rate of 10 kW for 1 h of mobility each day, a total capacity of 448.8 Ah, and a mass of 285.9 kg. This particular battery is not available off-the-shelf, but instead is custom-designed using COTS battery cells, so the battery is considered at TRL 6.

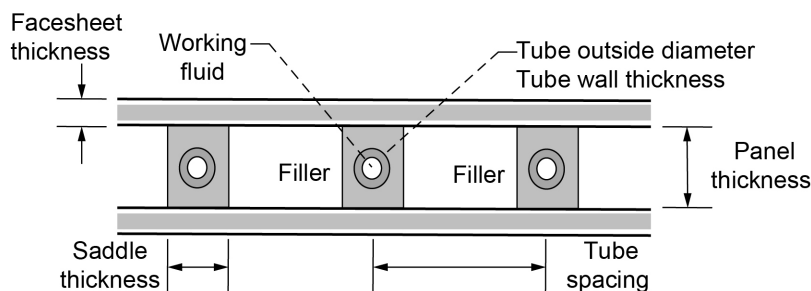


Figure 4.5.—Radiator panel layout.

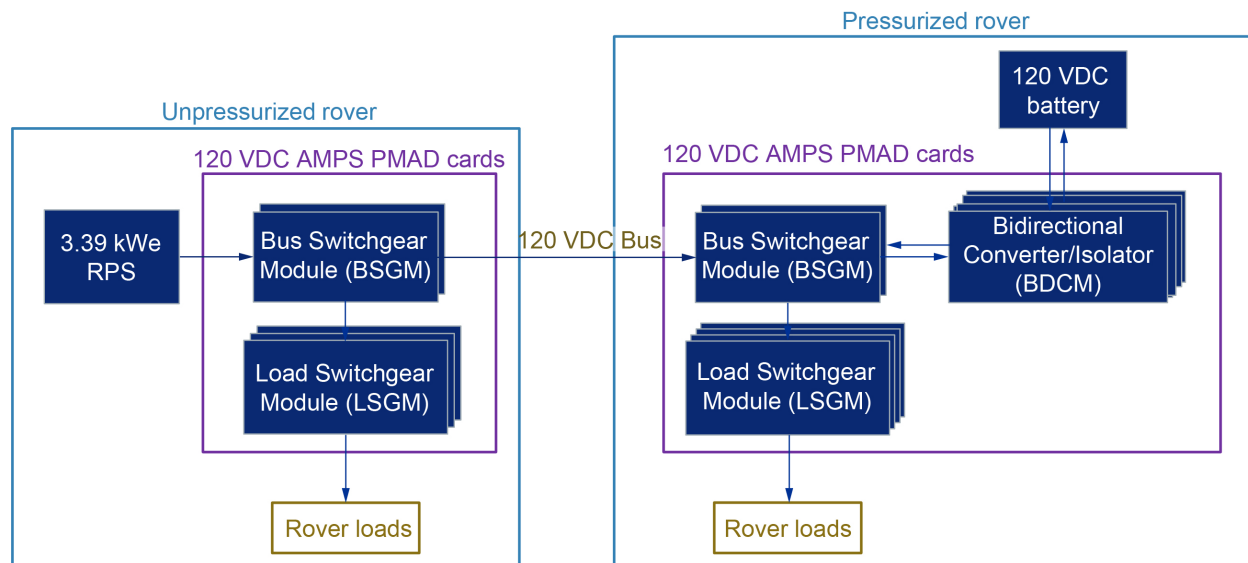


Figure 4.6.—Case 1 PMAD schematic.

Case 1 assumes that a third, unattached rover (not sized) will provide the necessary power to return to base in case of an RPS failure, thus eliminating the need for extra battery reserves onboard the rover.

#### 4.1.3.1.3 Power Management and Distribution (PMAD)

The PMAD for each part of the system is sized with Advanced Exploration Systems (AES) Modular Power System (AMPS) card components, which provide specific functions in parallel and are all distributed within a single 120-VDC PMAD box. The SPR and UPR each have an AMPS PMAD box that contains housekeeping, control, and power distribution unit (PDU) electronics. In addition, the SPR also contains bidirectional converter cards that provide battery charge and discharge regulation. Figure 4.6 shows the system configuration and PMAD. The total mass of the 120-VDC PMAD box is 15.5 kg for the UPR and 39.1 kg for the SPR. A detailed EPS wire-harnessing layout was not completed due to the short turnaround of this study. Instead, the wire harnessing to connect the various EPS components together was approximated as 25 percent of the EPS base mass—3.9 kg for the UPR and 81.2 kg for the SPR. The PMAD boxes are considered TRL 5, while the wire harnessing is TRL 6.

Including both the RPS and subsystem MGA, the total mass of the EPS amounts to 970.3 kg.

#### 4.1.3.2 Case 2—Fuel Cell

Case 2 investigates a 6-day PEM fuel cell mission using two sets of supercritically stored O<sub>2</sub> and H<sub>2</sub> reactants. One set of reactants is onboard the rover along with two fuel cell stacks and the necessary ancillaries; as the mission progresses, the water product is stored in a water tank onboard the rover. The other set of reactants and a 5-kW electrolyzer remain with the lander. Upon completion of the mission, the rover returns to the lander and exchanges its water product for the lander's reactants. The rover is then ready for another 6-day mission with fresh reactants, and the lander spends the duration of the mission electrolyzing the old product back into reactants.

The case 2 mission requires a power demand of 2.99 kW when parked and 13.2 kW when mobile, amounting to a total energy requirement of 343.9 kWh while parked and 79.6 kWh while driving. The fuel cell is sized for 527.1 kWh over 6-days at a maximum discharge of 13.2 kW for 1 h of mobility each sol. Table 4.3 shows a mass and volume breakdown of the fuel cell system. The reactant masses in this table

include usable, margin, and residual components. The fuel cell reactant storage subsystem, detailed in Section 4.4, describes the two sets of reactant hardware (reactant/product tanks and feed systems), but they are also listed in the table below for convenience. Not including this reactant hardware, the total mass of the listed fuel cell components is 738.6 kg, and their total volume is 0.368 m<sup>3</sup>. With the reactant hardware included, the total mass of the fuel cell system sums to 1,564.8 kg. The PEM fuel cells are TRL 6.

#### 4.1.3.2.1 Power Management and Distribution (PMAD)

The SPR and UPR each have an AMPS PMAD box that contains housekeeping, control, and PDU electronics, with the total mass of each PMAD box being 26.5 kg. Figure 4.7 shows the system configuration and PMAD. The wire harnessing to connect the various EPS components together is approximated as 25 percent of the EPS PMAD mass only—6.6 kg for each of the rovers. The PMAD boxes are considered TRL 5, while the wire harnessing is TRL 6.

Without the fuel cell tanks and feed systems, the case 2 EPS mass amounts to 916.6 kg with growth. Including all fuel cell reactant hardware, the case 2 EPS total mass amounts to 1,868.0 kg with growth.

#### 4.1.3.3 Case 3—Fuel Cell

Case 3 investigates a 21-day PEM fuel cell mission using one set of supercritically stored O<sub>2</sub> and H<sub>2</sub> reactants. The reactants and a 5-kW electrolyzer are carried onboard the rover, as well as the resulting water product. Upon completion of the mission, the rover returns to the lander and slowly electrolyzes its

TABLE 4.3.—CASE 2 COMPONENT BREAKDOWN

Section 4.4	Quantity	Base mass/unit, kg	Volume/unit, m <sup>3</sup>	Location
O <sub>2</sub>	2	196.0	-----	Rover, lander
H <sub>2</sub>	2	24.6	-----	Rover, lander
Stack	2	68.5	0.131	Rover
Ancillaries	2	65.2	0.053	Rover
Electrolyzer	1	30.0	-----	Lander
Tanks + feed systems	1	355.0	See storage system	Rover
Tanks + feed systems	1	471.2	See storage system	Lander

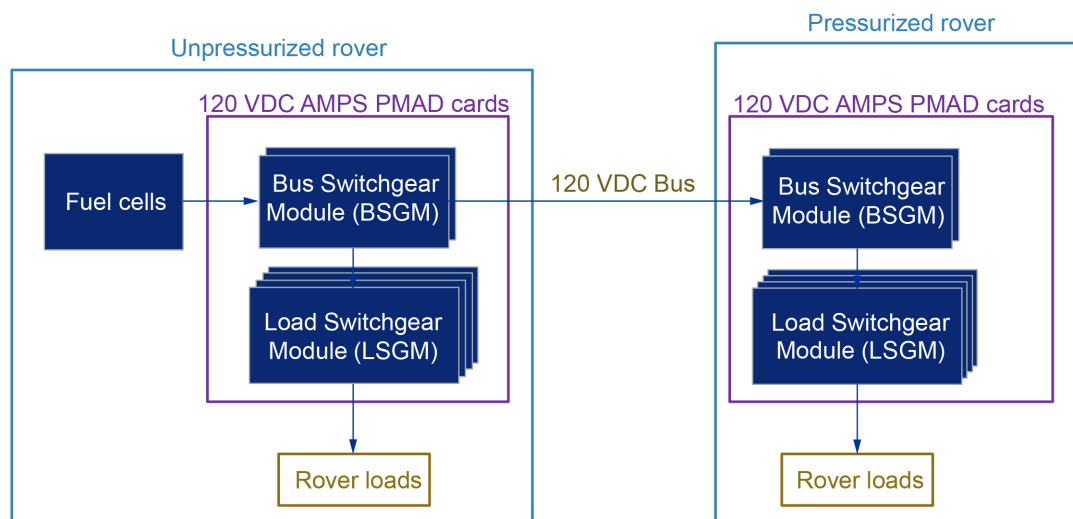


Figure 4.7.—Case 2 PMAD schematic.

product back into reactants using any excess electrical power from the lander, in preparation for a new mission.

The mission requires a power demand of 2.99 kW when parked and 13.2 kW when mobile, amounting to a total energy requirement of 1,375.4 kWh while parked and 278.5 kWh while driving. The fuel cell is sized for 2,059.0 kWh over 21 days at a maximum discharge of 13.2 kW for 1 h of mobility each day. Table 4.4 shows a mass and volume breakdown of the fuel cell system. Here, the reactant masses include usable, margin, and residual components. The fuel cell reactant storage subsystem, discussed in Section 4.4, further describes the single set of reactant hardware (reactant/product tanks and feed systems), but it is also listed in Table 4.4 for convenience. Not including this hardware, the total mass of the listed fuel cell components is 1,157.3 kg, and their total volume is 0.368 m<sup>3</sup>. With the reactant hardware included, the total mass of the fuel cell system sums to 2,336.7 kg. The PEM fuel cells are TRL 6.

#### 4.1.3.3.1 Power Management and Distribution (PMAD)

The SPR and UPR each have an AMPS PMAD box that contains housekeeping, control, and PDU electronics, with the total mass of each PMAD box being 26.5 kg. Figure 4.8 shows the system configuration and PMAD. As in case 2, the wire harnessing to connect the various EPS components together is approximated as 25 percent of the PMAD mass only—6.6 kg for each of the rovers. The PMAD boxes are considered TRL 5, while the wire harnessing is TRL 6.

Without the fuel cell tanks and feed systems, the case 3 EPS mass amounts to 1,335.3 kg with growth. Including all fuel cell reactant hardware, the case 3 EPS total mass amounts to 2,691.7 kg with growth.

TABLE 4.4.—CASE 3 COMPONENT BREAKDOWN

Component	Quantity	Base mass/unit, kg	Volume/unit, m <sup>3</sup>	Location
O <sup>2</sup>	1	763.6	-----	Rover
H <sup>2</sup>	1	96.3	-----	Rover
Stack	2	68.5	0.131	Rover
Ancillaries	2	65.2	0.053	Rover
Electrolyzer	1	30.0	-----	Rover
Tanks + feed systems	1	1,179.4	See storage system	Rover

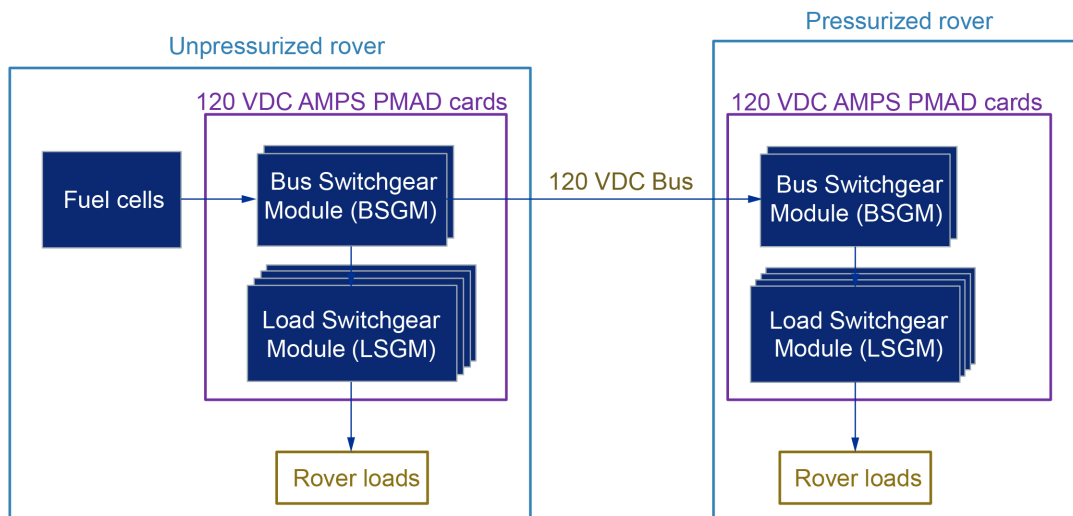


Figure 4.8.—Case 3 PMAD schematic.

#### 4.1.3.4 Solar Power System Option

This study examined the use of a solar array and rechargeable battery option to power the rover. Batteries are fully recharged each day by the onboard solar array. It is assumed that the solar array is stowed during mobility, and therefore, there is no power generation while driving. This assumption eliminates the need for more massive structural support of the solar array. A constant optical depth of  $1 \tau$  was used.

The mission has an energy demand of 13.5 kWh when driving, 27.1 kWh when parked during the daytime, and 42.2 kWh during nighttime. The martian night is the most constraining mission phase. To meet the power demand of the mission and recharge the batteries, the solar array must generate 82.8 kWh during the parked portion of the martian day. Accounting for losses, the solar array should be able to output at least 9.4 kW.

The solar array uses an UltraFlex<sup>®</sup> design that attaches to a boom and gimbal to extend above the UPR. Only one solar panel was used to reduce the possibility of array shadowing. The array requires 62 m<sup>2</sup> of cell area, which amounts to a total solar array area of 73 m<sup>2</sup>, an array diameter of 9.6 m, and a wing mass of 140 kg. The solar cells are state-of-the-art inverted metamorphic n-on-p (IMM- $\alpha$ ) solar cells with a BOL efficiency of 33 percent. Bus regulation is maintained at 120 V. UltraFlex<sup>®</sup> has flown many times, including on multiple Mars surface missions with Phoenix and InSight, so these solar arrays are considered TRL 8.

The rechargeable Li-ion battery is designed from COTS LG 18650 MJ1 cells. The battery is designed to contain 72.7 kWh, enough to power the driving and nighttime loads and remain above the 80 percent DOD operational limit with the spare strings. It can also support the maximum power discharge of 13.5 kW during the 1 h of mobility each day. The battery thus has 173 strings at 34 cells per string for a total capacity of 588 Ah and a mass of 375 kg. Because it is custom designed using COTS cells, the battery can be considered TRL 6.

This option also uses a TRL 5 AMPS PMAD box that contains housekeeping, control, PDU, and battery charge-discharge unit electronics, for a total mass of 77.0 kg.

Even though the solar array option has lower system mass and no need for nuclear materials, the large size of the solar array makes this design unfavorable. Mission trades could favor the solar array option by either adjusting the mission location on Mars or the date of the mission. The current mission date occurs near the middle of winter in the martian northern hemisphere. If the mission were to occur in the southern hemisphere for the same dates, there would be 14 h of daylight and 10 h of night. This would reduce the solar array surface area requirement by about 20 percent and the battery mass requirement by about 30 percent. If the mission were to occur during summer in the Mars northern hemisphere, there would be more hours of daylight as well, but Mars would be further from the Sun. The lower intensity of solar flux would mean that the solar array surface area would remain about the same, but the longer daylight hours would reduce the battery mass requirement by about 20 percent.

#### 4.1.4 Summary

Table 4.5 shows the total mass of the EPS with MGA for all three cases for which the Compass Team completed a MEL. The solar array option is not included because of the undesirable array size. For a 21-day mission, the mass of the fuel cell system (case 3) is over 2.5 times larger than that of RPS (case 1), so RPS is the best power option from a mass standpoint. Section 4.1.5 shows detailed breakdowns of the EPS components along with mass growth for cases 1 to 3. Future work should include examining the modifications to the power system required for operation in the lunar environment.

#### 4.1.5 Master Equipment List

Table 4.6 to Table 4.8 show the EPS MELs for cases 1 to 3.

TABLE 4.5.—TOTAL EPS MASSES WITH GROWTH

Parameter	Case 1	Case 2	Case 3
Mass, kg	970.3	1,868.0	2,691.7
Notes	Includes RPS	Includes all fuel cell hardware	Includes all fuel cell hardware

TABLE 4.6.—CASE 1 EPS MEL

Radioisotope Power System	QTY	Unit Mass	Basic Mass	Growth	Growth	Total Mass
Case 1 DAPS CD 2019-172		(kg)	(kg)	(%)	(kg)	(kg)
<b>DAPS</b>			<b>987</b>	<b>26%</b>	<b>255</b>	<b>1243</b>
<b>Unpressurized Rover</b>			<b>580</b>	<b>20%</b>	<b>117</b>	<b>697</b>
<b>Electrical Power Subsystem</b>			<b>352.7</b>	<b>21%</b>	<b>73.3</b>	<b>426.0</b>
<b>Power Generation</b>			<b>268.2</b>	<b>20%</b>	<b>53.6</b>	<b>321.8</b>
GPHS Mass	3	28.8	86.4	20%	17.3	103.7
Primary Heat Transport	3	11.9	35.6	20%	7.1	42.7
Heat Source Assembly	3	5.8	17.5	20%	3.5	21.0
Stirling Convertor	6	11.1	66.6	20%	13.3	79.9
Controller Mass	3	20.7	62.1	20%	12.4	74.6
<b>Power Management &amp; Distribution</b>			<b>84.5</b>	<b>23%</b>	<b>19.6</b>	<b>104.2</b>
Misc. Mass	3	21.7	65.1	20%	13.0	78.2
Harness	1	3.9	3.9	50%	2.0	5.9
120 V PMAD	1	15.5	15.5	30%	4.7	20.2
<b>Pressurized Rover</b>			<b>406</b>	<b>34%</b>	<b>138</b>	<b>544</b>
<b>Electrical Power Subsystem</b>			<b>406.2</b>	<b>34%</b>	<b>138.1</b>	<b>544.3</b>
<b>Power Management &amp; Distribution</b>			<b>120.3</b>	<b>43%</b>	<b>52.3</b>	<b>172.6</b>
120 V PMAD	1	39.1	39.1	30%	11.7	50.8
Harness	1	81.2	81.2	50%	40.6	121.8
<b>Energy Storage</b>			<b>285.9</b>	<b>30%</b>	<b>85.8</b>	<b>371.7</b>
Lithium-Ion Battery	1	285.9	285.9	30%	85.8	371.7

TABLE 4.7.—CASE 2 EPS MEL

Fuel Cells - 6 Days w/ Lander Reprocessing	QTY	Unit Mass	Basic Mass	Growth	Growth	Total Mass
Case 2 DAPS CD 2019-172		(kg)	(kg)	(%)	(kg)	(kg)
<b>DAPS</b>			<b>1945</b>	<b>15%</b>	<b>296</b>	<b>2242</b>
<b>Unpressurized Rover</b>			<b>1154</b>	<b>17%</b>	<b>197</b>	<b>1351</b>
<b>Electrical Power Subsystem</b>			<b>300.5</b>	<b>30%</b>	<b>91.5</b>	<b>392.0</b>
<b>Power Management &amp; Distribution</b>			<b>33.1</b>	<b>34%</b>	<b>11.3</b>	<b>44.4</b>
Harness	1	6.6	6.6	50%	3.3	9.9
120 V PMAD	1	26.5	26.5	30%	8.0	34.5
<b>Energy Storage</b>			<b>267.4</b>	<b>30%</b>	<b>80.2</b>	<b>347.6</b>
Fuel Cell Stack	2	68.5	137.0	30%	41.1	178.1
Fuel Cell Ancillary	2	65.2	130.4	30%	39.1	169.5
<b>Pressurized Rover</b>			<b>34</b>	<b>33%</b>	<b>11</b>	<b>46</b>
<b>Electrical Power Subsystem</b>			<b>33.1</b>	<b>34%</b>	<b>11.3</b>	<b>44.4</b>
<b>Power Management &amp; Distribution</b>			<b>33.1</b>	<b>34%</b>	<b>11.3</b>	<b>44.4</b>
120 V PMAD	1	26.5	26.5	30%	8.0	34.5
Harness	1	6.6	6.6	50%	3.3	9.9



TABLE 4.8.—CASE 3 EPS MEL

Fuel Cells - 21 Days w/o Reprocessing	QTY	Unit Mass	Basic Mass	Growth	Growth	Total Mass
Case 3 DAPS CD 2019-172		(kg)	(kg)	(%)	(kg)	(kg)
<b>DAPS</b>			<b>2708</b>	<b>13%</b>	<b>346</b>	<b>3054</b>
<b>Unpressurized Rover</b>			<b>2674</b>	<b>13%</b>	<b>335</b>	<b>3008</b>
<b>Electrical Power Subsystem</b>			<b>330.5</b>	<b>30%</b>	<b>100.5</b>	<b>431.0</b>
<b>Power Management &amp; Distribution</b>			<b>33.1</b>	<b>34%</b>	<b>11.3</b>	<b>44.4</b>
Harness	1	6.6	6.6	50%	3.3	9.9
120 V PMAD	1	26.5	26.5	30%	8.0	34.5
<b>Energy Storage</b>			<b>297.4</b>	<b>30%</b>	<b>89.2</b>	<b>386.6</b>
Fuel Cell Stack	2	68.5	137.0	30%	41.1	178.1
Fuel Cell Ancillaries	2	65.2	130.4	30%	39.1	169.5
Fuel Cell Electrolyzer	1	30.0	30.0	30%	9.0	39.0
<b>Pressurized Rover</b>			<b>34</b>	<b>33%</b>	<b>11</b>	<b>46</b>
<b>Electrical Power Subsystem</b>			<b>33.1</b>	<b>34%</b>	<b>11.3</b>	<b>44.4</b>
<b>Power Management &amp; Distribution</b>			<b>33.1</b>	<b>34%</b>	<b>11.3</b>	<b>44.4</b>
120 V PMAD	1	26.5	26.5	30%	8.0	34.5
Harness	1	6.6	6.6	50%	3.3	9.9

## 4.2 Thermal System

The rover is used to explore the Mars surface on an extended multiday mission. The baseline case considered a RPS utilizing Stirling engines as the thermal power conversion device. Waste heat from the power system is collected and rejected to the surroundings through a radiator system. The thermal system also addressed the thermal control for the electronic components utilized in the operation of the power system.

### 4.2.1 System Requirements

The thermal system is required to dissipate the waste heat from the electronics and the power conversion system, and to provide a heat rejection mechanism for excess electrical power that is shunted when not needed. The system is also required to adequately regulate the temperature of various components whose temperature must be controlled to ensure proper performance. It is required to be nominally single fault tolerant as applicable and perform well in both lunar and martian environments.

### 4.2.2 System Assumptions

The Compass Team assumed the worst-case thermal operating condition to size the thermal components. For this design, this corresponds to the SPR operating on Mars at approximately 35° N latitude. The team also assumed that the martian atmosphere would degrade MLI performance, that dust will degrade radiator performance, and that electrical resistance heaters are used as needed in the design.

### 4.2.3 System Design

The design approach for the thermal system utilizes the worst-case hot and cold environmental conditions to size various components of the system. Solar intensity and view angle as well as the view to warm bodies such as the sunlit Mars surface along with the internal heat generation are used to determine the worst-case hot and cold conditions. Operating on the Mars surface means that both radiation and convection are factors in the heat rejection to the surroundings. Also, since there is a rarified atmosphere on Mars the insulation performance and the type of insulation selected needs to consider the presence of this atmosphere. The worst-case warm conditions occur while sunlit when all internal components are operating generating maximum waste heat. Whereas the worst-case cold operating conditions occur during nighttime.

Table 4.9 lists the main thermal system components used in the system, along with an operational summary. Figure 4.9 illustrates the thermal system layout on the rover, which includes radiator panels with louvers, cold plates, heat pipes (for electronics cooling), a pumped loop cooling system (for isotope power system), aerogel insulation, heaters, temperature sensors, controllers, switches, and data acquisition.

TABLE 4.9.—THERMAL SYSTEM OPERATIONAL SPECIFICATIONS

Specifications	Value/description
Dimensions of UPR section	Length: 2.8 m, width: 2.4 m, height: 2.8 m
Waste heat	Isotope power system: 6.4 kW, electronics: 260 W
Operating temperature	Isotope system cold end: 345 K, electronics: 300 K
Insulation	Silica aerogel: 100 kg/m <sup>3</sup>
Environment	35° N latitude, warm: surface 247 K, sky 197.5 K Cold: surface 155 K, sky 139.7 K
Radiators	Three single-sided surface mount radiators: power system, electronics, and shunt
Cooling	Pump loop cooling system was used for the power system radiator
	Electronics radiator utilized variable conductance heat pipes in conjunction with a series of cold plates used to move heat from the electronics and components to the radiator
	Shunt radiator is electrically powered
Heating	Electric heaters are used as needed

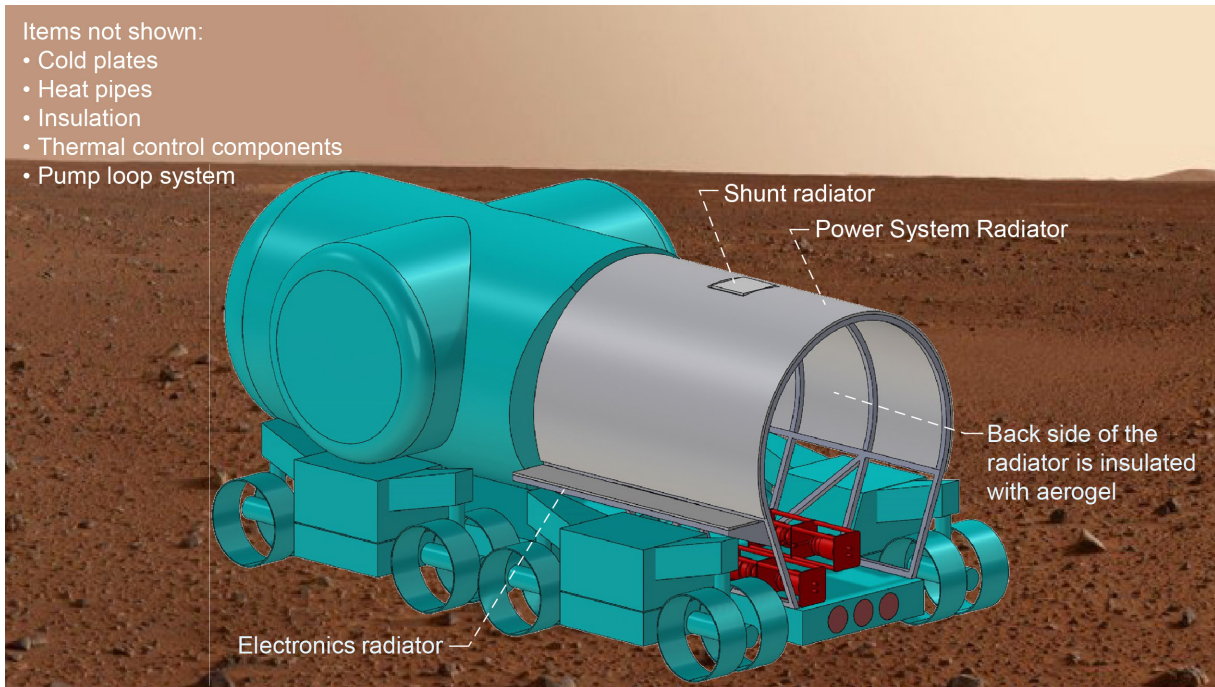


Figure 4.9.—Rover power system thermal components.

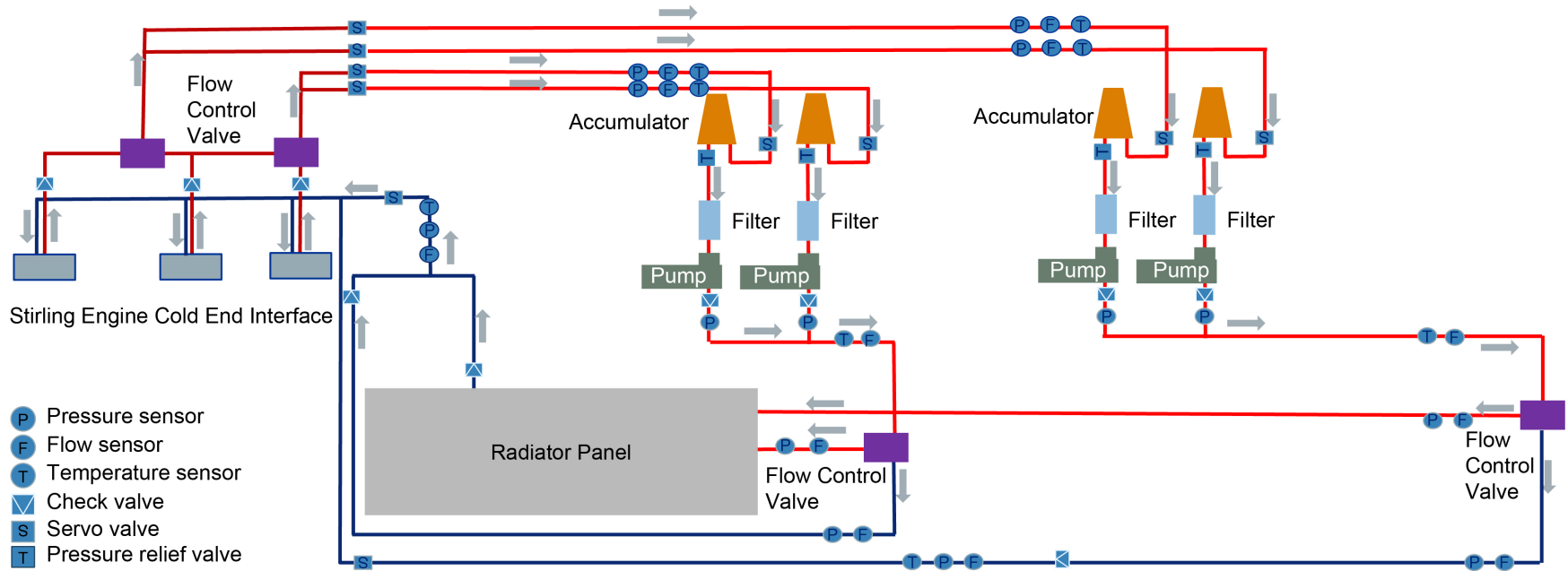
Electric heaters are incorporated onto the cold plates as well as on critical components as needed. These heaters are used to maintain the temperature of these components above their minimum operating temperature throughout the mission. Waste heat from the internal components as well as electric heaters are used to provide heat to the spacecraft electronic components if needed. The flexible strip and plate heaters are used to provide heat to the electronic and mechanical components within the spacecraft. Flat plate heaters are used on each of the cold plates to provide heat to the mounted electronics and or packaging if necessary.

Thermal control within the electronics enclosure is accomplished using a network of thermocouples whose output is used to control the power to the various heaters, and a data acquisition and control computer is used to operate the thermal system. During normal operation, it is estimated that the waste heat from the electronics components will be sufficient to maintain the temperature of the spacecraft components within their desired operating temperature range. Therefore, the heater power will be minimal during normal operations. Heater power will vary with the mission operation from 0.0 to 96 W during low-power operation at nighttime.

Aerogel foam insulation is used to insulate beneath the radiator and around the electronics boxes to minimize heat loss to the surroundings and maintain the internal component temperatures within the required range of 260 to 320 K as well as to insulate the back of the radiator to minimize the heat leak into the electronics and power system components. This is particularly needed on the back of the shunt radiator due to its high temperature of operation and correspondingly high heat flux. No insulation is used on the back of the electronics radiator since it only has a view to the surface. The heat transfer to the surface will help in the radiator's ability to reject heat to the surroundings since the surface temperature is cooler than the radiator operating temperature.

There are three separate radiator systems utilized on the rover, and each is sized to reject heat for their specific application. The three radiator systems are a main radiator for the isotope power system, an electronics radiator, and a shunt radiator. The main radiator was sized to remove the waste heat from the isotope power system during worst-case hot operational conditions that occur while sunlit on the Mars surface under full power operation. It is constructed in a semicylindrical shape on top of the UPR section, has an area of 11.6 m<sup>2</sup>, and is operated as a single segment with an average temperature of 345 K. Louvers were not used on the radiator since the RPS will be operating continuously. A pump loop cooling system was baselined as the means of moving heat from the Stirling engines to the radiator. This system circulates a coolant that collects heat from the cold end of the Stirling engines cold plates and transports that heat to a radiator that rejects the waste heat to the environment. Figure 4.10 shows this configuration and the corresponding components.

A single fixed radiator is utilized to provide cooling for the electronic components of the isotope power system. It is located along the base of the power system radiator, has a total surface area of 1.04 m<sup>2</sup>, and is designed to dissipate the estimated 260-W electronics heat load. A heat pipe system was used to move the heat from the electronics to this radiator and is designed to keep them operating at temperatures up to 330 K during the worst-case hot operational conditions, which occur while sunlit on the Mars surface under full-power operation. The radiator is coated to reflect most of the incoming visible solar radiation, which reduces the total heat load on the radiator.



Note: not all components are shown in the diagram  
Both loops feed the same radiator panel.

Figure 4.10.—Isotope pump loop cooling system operational diagram.

During shadow, nighttime, or if the electronics system thermal output decreases, heaters will be used to maintain the internal temperature of the electronics enclosure. Like the isotope power system radiator, louvers are not used on the radiator since the RPS will be operating continuously. The radiator orientation was chosen to provide the best operating conditions for the heat pipe system by locating the condenser section above the evaporator section thereby returning the fluid in the direction of the gravity field. Two heat pipes are run from each cold plate to the radiator. The heat pipes share the load from each electronics box. Each heat pipe can move the total heat generated from its corresponding electronics box to the radiator, thus providing a redundant heat transfer path for each heat source.

The electronics are mounted to the cold plates where the heat generated is collected. Variable conductance heat pipes move the heat from the cold plates to the radiator. For this design, there are 16 heat pipes that are 0.6 cm in radius, 2.0 m long, and transfer 33 W each.

There are eight aluminum cold plates used to interface the heat pipes to the loads. These plates are 0.1 by 0.1 m and are 5 mm thick. They are used to provide a good thermal connection between the heat source and the heat pipe evaporator section.

Since the isotope heat source produces a constant heat output, the Stirling engines need to continually remove the heat produced to maintain the isotope temperature within the desired range and prevent overheating. However, under conditions where the electrical load requirements are low (or off), the Stirling engines need to send electrical power to a load to continue to operate. Under these circumstances, a shunt radiator is used to reject any excess power that is being produced by the isotope power system. This resistive radiator allows the RPS to operate within its design output power limits when the load demands are too low. The radiator uses electrical resistance to generate heat from the output power of the Stirling engines. The back of the radiator panel is insulated to minimize the heat flux from the radiator to the electronics enclosure. A conceptual design for the shunt radiator is shown in Figure 4.11.

The shunt radiator is located at the top of the power system radiator and is oriented horizontally so that it has a full view to the sky, which avoids any view it might have of other components on the rover. Also, the radiator is positioned so that it would not have a view to either the power system or electronics radiators. This is done to avoid putting an additional heat load onto those radiators. The radiator is designed to operate at 800 K. This high operating temperature allows the size of the radiator to be 0.15 m<sup>2</sup> while still being capable of rejecting the full 3-kW output of the isotope power system.

#### 4.2.4 Analytical Methods

The analytical methods used to design and analyze the thermal control system are shown in the following sections. These methods include a mix of analytical and empirical data from various sources, including the Viking and Phoenix landers.

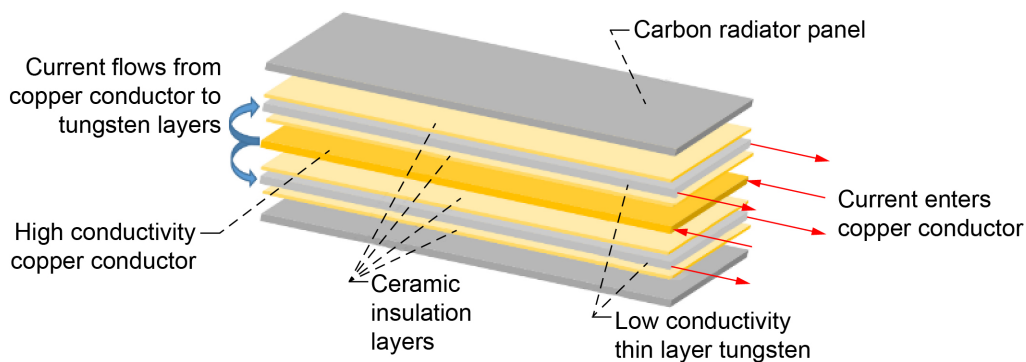


Figure 4.11.—Resistive shunt radiator.

#### 4.2.4.1 Mars Environment

The operational environment is a critical aspect to the thermal system design. To determine the operating conditions on the Mars surface, data from previous northern hemisphere missions were used. Two missions, where temperature data was available, that operated in the northern hemisphere were the Viking II and Phoenix landers. Figure 4.12 shows the landing sites for these two missions. Viking II operated for 1,281 martian days at a latitude of 48° N, and the Phoenix lander operated for 157 martian days, from late spring to late summer, at 68° N latitude (Ref. 13). The pressurized rover mission was designated to operate at approximately 35° N latitude on Mars. Since the Viking II data was closer in latitude to the operation of the rover, environmental data from this mission was used to determine the operating conditions for the radiator.

From a thermal perspective, the environment on Mars is unique. The atmosphere on Mars near the surface is rarefied, similar to the air density on Earth at 30 km (~100,000 ft). Unlike on the surface of Earth, this low-density atmosphere limits convection heat removal. That makes radiation the dominant heat transfer mechanism within the Mars surface environment. However, to accurately access a thermal system, convection still must be considered as the convective heat transfer contribution is not negligible. The atmosphere influences the selection of components for the thermal system. For example, in vacuum, MLI is ideal and provides excellent insulating properties by blocking radiation heat transfer. But on Mars, the atmosphere greatly reduces the effectiveness of MLI so other types of insulation, such as aerogels, are utilized. The secondary atmospheric effect of dust transport onto a radiator panel degrades its emissivity over time. This degradation mechanism must be considered in the design process or mitigated.

Accurately characterizing the Mars surface environment critically influences the design and sizing of the thermal system. Since the Mars atmosphere is mainly CO<sub>2</sub>, as given in Table 4.10, the atmospheric properties can be approximated by those for CO<sub>2</sub> at the low Mars surface pressure.

The dynamic viscosity ( $\mu$ ) of the atmosphere can be determined as a function of the surface atmospheric temperature ( $T_{sur}$ ) in Kelvin from Equations (1) and (2).

$$\mu = \frac{1.00697 \times 10^{-6} \sqrt{T_{sur}}}{e^a} \quad [\text{Pa} \cdot \text{s}] \quad (1)$$

Where:

$$a = a^0 + a^1 \ln \frac{T_{sur}}{251.096} + a^2 \left( \ln \frac{T_{sur}}{251.096} \right)^2 + a^3 \left( \ln \frac{T_{sur}}{251.096} \right)^3 + a^4 \left( \ln \frac{T_{sur}}{251.096} \right)^4 \quad (2)$$

Table 4.11 gives the coefficients  $a_0$  through  $a_4$ .

TABLE 4.10.—MARS ATMOSPHERIC COMPOSITION

Carbon dioxide (CO <sub>2</sub> ), percent by volume.....	95.32
Nitrogen (N <sub>2</sub> ), percent by volume.....	2.70
Argon (Ar), percent by volume.....	1.6
Oxygen (O <sub>2</sub> ), percent by volume.....	0.13
Carbon monoxide (CO), percent by volume.....	0.08
Trace gases: water (H <sub>2</sub> O), nitrogen oxide (NO), neon (Ne), hydrogen-deuterium-oxygen (HDO), krypton (Kr), xenon (Xe), percent by volume.....	0.17

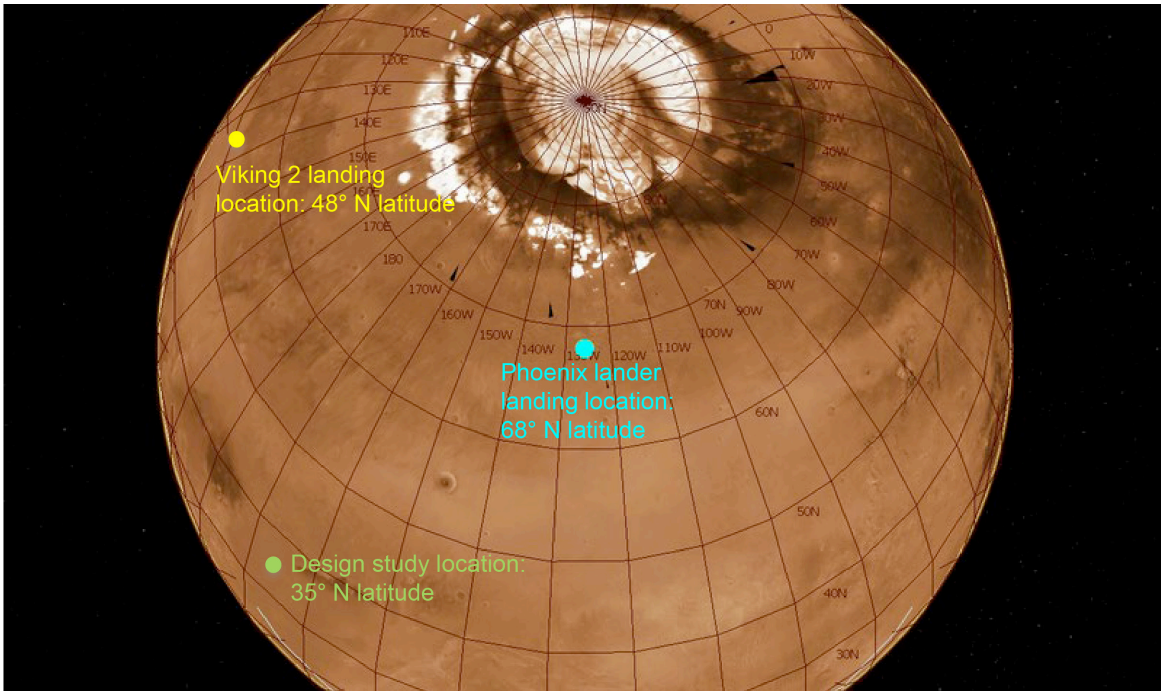


Figure 4.12.—Northern latitude environment data points and selected mission location.

TABLE 4.11.—VISCOSITY  
CALCULATION COEFFICIENTS

$a_0$ .....	0.235156
$a_1$ .....	-0.491266
$a_2$ .....	0.05211155
$a_3$ .....	0.05347906
$a_4$ .....	-0.01537102

The thermal conductivity ( $k$ ) of the atmosphere can also be estimated as a function of the atmospheric temperature in Kelvin in Equations (3) to (5).

$$k = \frac{0.119421\sqrt{T_{sur}}(1+b)}{cT_{sur}} \quad [\text{W/m} \cdot \text{K}] \quad (3)$$

Where:

$$b = b_0 + \frac{251.096b_1}{T_{sur}} + \frac{251.096^2b_2}{T_{sur}^2} + \frac{251.096^3b_3}{T_{sur}^3} + \frac{251.096^6b_6}{T_{sur}^6} + \frac{251.096^7b_7}{T_{sur}^7} \quad (4)$$

$$c = \sqrt{0.4 \left[ 1 + e^{-183.5/T_{sur}} \left( \frac{c_1T_{sur}}{100} + c_2 + \frac{100c_3}{T_{sur}} + \frac{100^2c_4}{T_{sur}^2} + \frac{100^3c_5}{T_{sur}^3} \right) \right]} \quad (5)$$

Table 4.12 gives the  $b$  and  $c$  coefficients for the thermal conductivity calculation.

TABLE 4.12.—THERMAL  
CONDUCTIVITY CALCULATION  
COEFFICIENTS

$b_0$ .....	0.4226159
$b_1$ .....	0.6280115
$b_2$ .....	-0.5387661
$b_3$ .....	0.6735941
$b_6$ .....	-0.4362677
$b_7$ .....	0.2255388
$c_1$ .....	0.02387869
$c_2$ .....	4.350794
$c_3$ .....	-10.33404
$c_4$ .....	7.98159
$c_5$ .....	-1.940558

The specific heat ( $c_p$ ) of the Mars atmosphere as a function of temperature can also be approximated with the specific heat of CO<sub>2</sub>. For CO<sub>2</sub>, the specific heat is linear over the temperature range seen within the Mars environment as given by Equation (6).

$$C_p = 0.001T_{sur} + 0.5177 \quad (6)$$

The atmospheric density at the surface can be determined from the ideal gas equation using the atmospheric temperature and pressure. This is given in Equation (7). For Mars, the gas constant for CO<sub>2</sub> ( $R_{CO_2}$ ), 188.9 J/kg·K, can be used to approximate the gas constant for the atmosphere. The pressure ( $P$ ) as well as the temperature on the surface varies throughout the year as shown in the Viking II lander data given in Figure 4.13 and Figure 4.14. The density ( $\rho$ ) can then be calculated from the ideal gas equation based on the atmospheric temperature and pressure (Eq. (7)).

$$\rho = \frac{P}{R_{CO_2}T_{sur}} \quad (7)$$

Using the data from Figure 4.13, Figure 4.14, and Equation (7), the variation in atmospheric density near the surface can be calculated as shown in Figure 4.15. The atmosphere density varies widely throughout the year ranging between 0.016 and 0.034 kg/m<sup>3</sup> with the daily variations from 0.02 to 0.025 kg/m<sup>3</sup>.

The effective sky temperature ( $T_{sky}$ ) is another required environmental property to accurately determine the radiative heat transfer to the surroundings. The sky temperature is difficult to calculate since it is dependent on several local factors, such as dust opacity, water vapor content, wind speed, etc., that can be highly variable for a given location and time of day/year. To estimate the effective sky temperature based on the surface temperature, a liner curve fit of the relationship between the worst-case surface and sky temperature was made and is given by Equation (8).

$$T_{sky} = 74.841 + 0.4185T_{sur} \quad [K] \quad (8)$$

Figure 4.14 shows that the temperature reaches a peak of 250 K (-23 °C) during the summertime. From this time on, the temperatures gradually decrease through the winter and reach a minimum of approximately 155 K (-118 °C). From this point, temperatures begin to increase again. This data set represents both the summer maximum and winter minimum temperatures. From this data, a worst-case warm and cold environmental temperature was established for both the surface and sky temperatures Table 4.13.



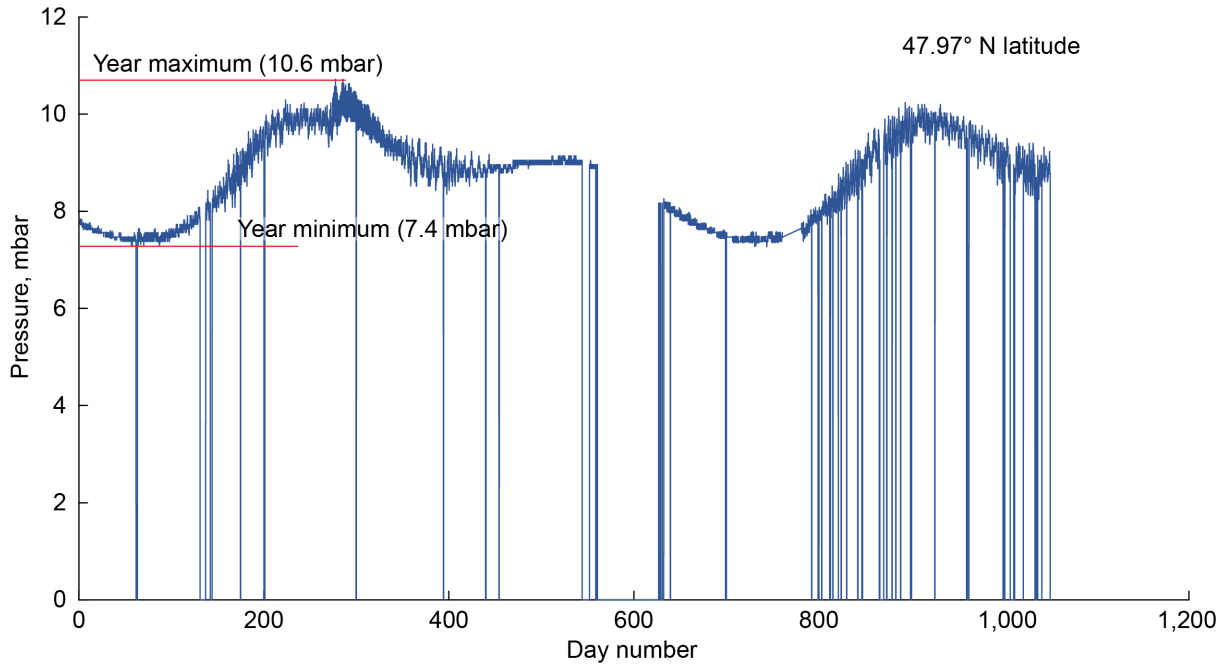


Figure 4.13.—Viking II lander surface pressure.

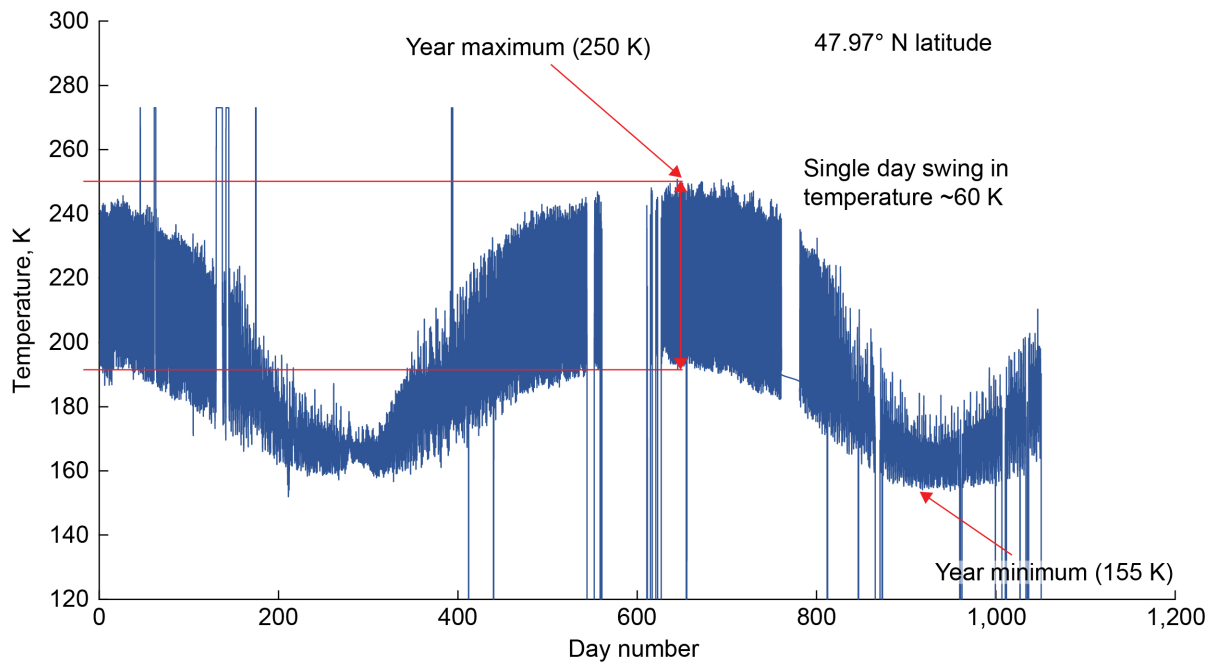


Figure 4.14.—Viking II lander surface temperature.

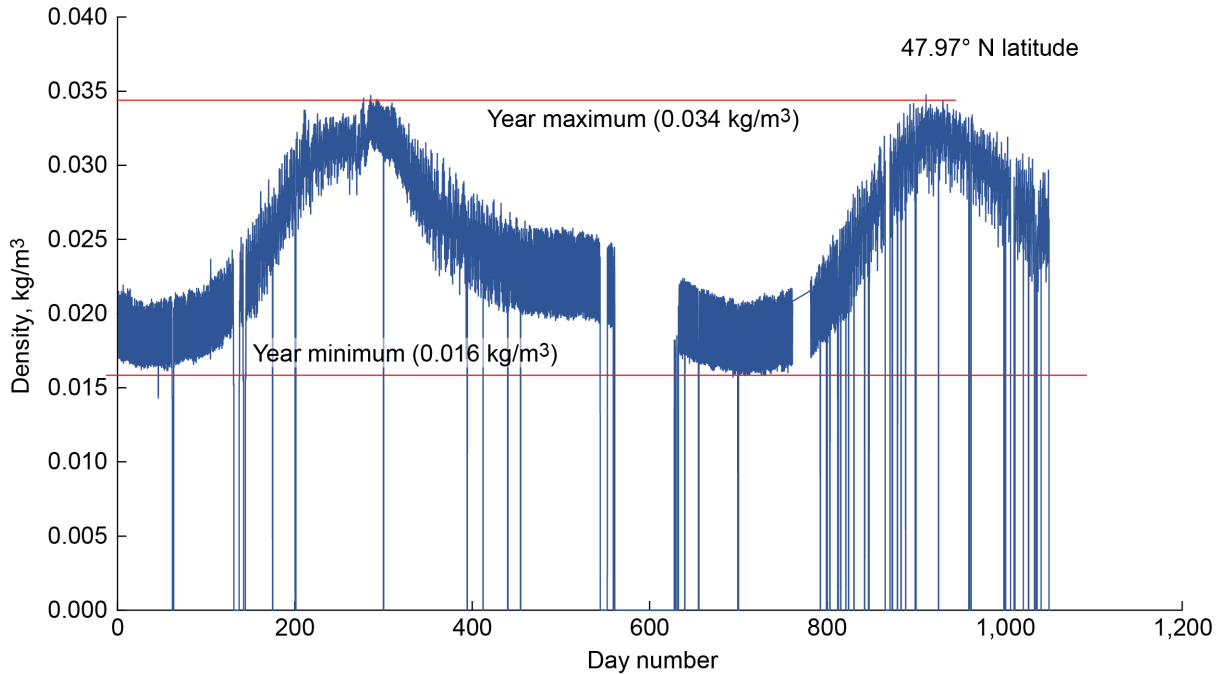


Figure 4.15.—Surface density based on Viking II data.

TABLE 4.13.—WORST-CASE ENVIRONMENTAL TEMPERATURES

Worst-case environment	Surface, K (°C)	Sky, K (°C)
Warm	247 (–26)	179.5 (–93.5)
Cold	155 (–118)	139.7 (–133.3)

#### 4.2.4.2 Radiator and Coolant System

The radiator sizing was based on an energy balance analysis of the area needed to reject the identified heat load to the surroundings. From the area, a series of scaling equations were used to determine the mass of the radiator. The radiator was sized to remove the waste heat from the isotope power system during worst-case hot operational conditions that occur while sunlit on the Mars surface under full power operation. There are three separate radiator systems utilized on the rover. Each of these are sized to reject heat for their specific application. These radiator systems include a main radiator for the isotope power system, an electronics radiator, and a shunt radiator. Figure 4.16 illustrates the radiators and their operating environment.

The sizing of the system is based on the heat load that has to be rejected and the heat transfer from the radiator to the surroundings. The heat transfer from the radiator is through both radiation and convection. Even though the atmosphere is rarefied, convection still plays a role in the heat removal from the radiator and therefore, must be accurately modeled to correctly size the radiator.

The heat transfer from the radiator to the surroundings through convection ( $Q_c$ ) is given by Equation (9). It is based on the radiator temperature ( $T_r$ ) and area ( $A_r$ ) as well as the local bulk atmosphere temperature ( $T_{atm}$ ).

$$Q_c = A_r h (T_r - T_{atm}) \quad (9)$$

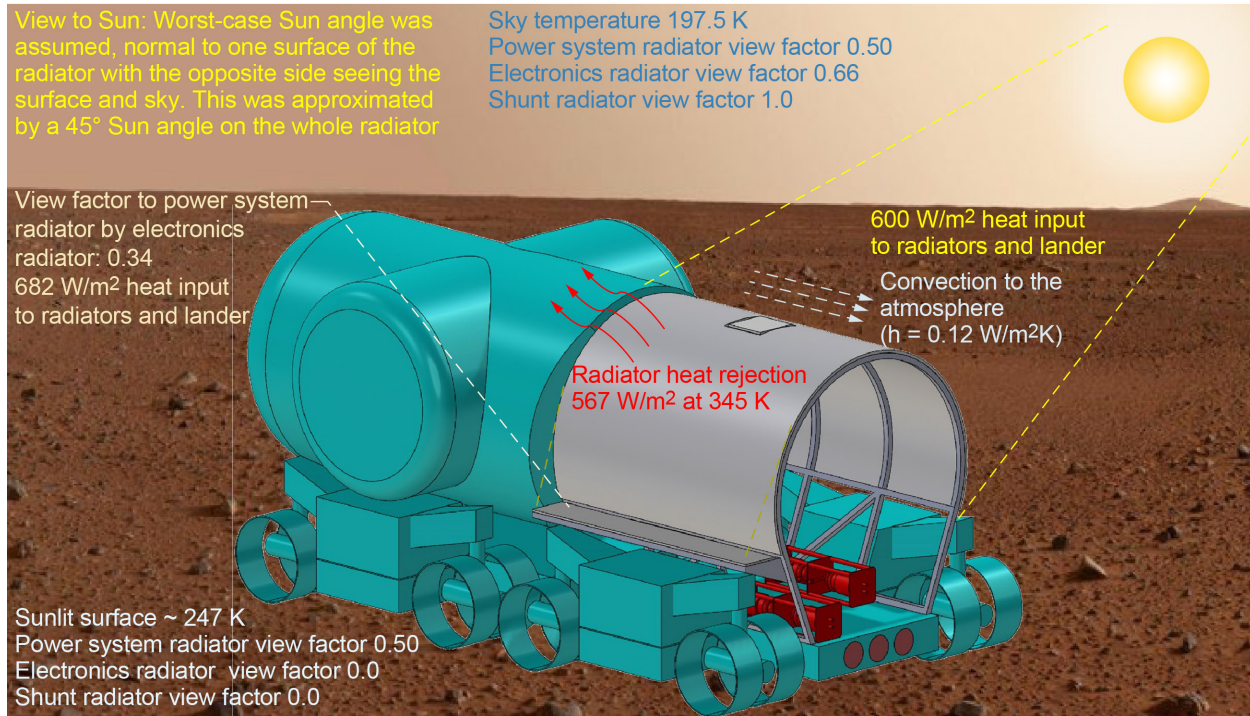


Figure 4.16.—Radiator energy balance and environment.

The convective coefficient ( $h$ ) is given by Equation (10), which is based on the characteristic length of the radiator ( $L$ ).

$$h = \frac{Nu k}{L} \quad (10)$$

The expression for the Nusselt number ( $Nu$ ) will depend on whether the wind speed results in natural or forced convection from the radiator surface. These cases are given by Equation (11) for natural convection and Equations (12) and (13) for laminar or turbulent flow forced convection, respectively. The transition between laminar to turbulent flow occurs at a Reynolds number ( $Re$ ) of approximately  $5 \times 10^5$ .

$$Nu = \frac{0.67 Ra^{1/4}}{\left[ 1 + \left( \frac{0.492}{Pr} \right)^{9/16} \right]^{4/9}} \quad (\text{natural convection}) \quad (11)$$

$$Nu = \frac{0.3387 Re^{1/2} Pr^{1/3}}{\left[ 1 + \left( \frac{0.0468}{Pr} \right)^{2/3} \right]^{1/4}} \quad (\text{laminar flow}) \quad (12)$$

$$Nu = 0.0296 Re^{4/5} Pr^{1/3} \quad (\text{turbulent flow}) \quad (13)$$

The Nusselt number (Ref. 14) equations are based on the Prandtl number ( $Pr$ ) (Ref. 15), Reynolds number ( $Re$ ) (Ref. 16), and the Rayleigh number ( $Ra$ ) (Ref. 17) given by Equations (14) to (16), respectively.

$$\text{Pr} = \frac{C_p \mu}{k} \quad (14)$$

$$\text{Re} = \frac{\rho V L}{\mu} \quad (15)$$

$$\text{Ra} = \frac{g(T_r - T_a)L^3 \rho^2 C_p}{T_f \mu} \quad (16)$$

Where the film temperature ( $T_f$ ) is assumed to be the average of the radiator temperature and the atmosphere temperature.

$$T_f = \frac{T_r + T_{atm}}{2} \quad (17)$$

Radiation heat transfer ( $Q_r$ ) is the next and main means of heat transfer from the radiator. On the surface of Mars, the radiator has a view to both the surface ( $F_{sur}$ ) and the sky ( $F_{sky}$ ). These two views compose the total view of the radiator to the surroundings as given by Equation (18).

$$1 = F_{sur} + F_{sky} \quad (18)$$

The total radiative heat transfer from the radiator to the surface and sky is dependent on the emissivity of the radiator ( $\epsilon$ ) as given by Equation (19).

$$Q_r = A_r \epsilon \sigma \left[ F_{sky} (T_r^4 - T_{sky}^4) + F_{sur} (T_r^4 - T_{sur}^4) \right] \quad (19)$$

Where the Stefan-Boltzmann constant ( $\sigma$ ) is

$$\sigma = 5.670367 \times 10^{-8} \quad [\text{W}/\text{m}^2\text{K}^4] \quad (20)$$

Based on Equations (9) and (19), the total heat rejection capability of the radiator ( $Q$ ) to the surroundings is given by Equation (21).

$$Q = Q_c + Q_r \quad (21)$$

An estimate of the mass of the radiator panel ( $m_r$ ) can be made based on its required area. The radiator structure can be separated into the following components with a scaling coefficient for each component to linearly scale the mass based on the required radiator area: panels ( $C_p$ ), coating ( $C_c$ ), tubing ( $C_t$ ), header ( $C_h$ ), adhesives ( $C_a$ ), stingers ( $C_s$ ), and attachment ( $C_{at}$ ). These coefficients were derived from satellite and spacecraft radiator mass data and are listed in Table 4.14. The total radiator mass is given by Equation (22).

$$m_r = C_p A_r + C_c A_r + C_t A_r + C_h A_r + C_a A_r + C_s A_r + C_{at} A_r \quad (22)$$

TABLE 4.14.—RADIATOR MASS—  
SCALING COEFFICIENTS

$C_p$ .....	3.3
$C_c$ .....	0.42
$C_t$ .....	1.31
$C_h$ .....	0.23
$C_a$ .....	0.29
$C_s$ .....	1.50
$C_{at}$ .....	0.75

TABLE 4.15.—COOLING FLUIDS FOR PEM THERMAL SYSTEM  
[References 18 to 20.]

Fluid	Thermal conductivity, W/m-K	Specific heat, kJ/kg-K	Viscosity, MPa-s	Density, kg/m <sup>3</sup>	Freezing point, °C	Boiling point, °C
Water	0.58	4.3	0.18	1,000	0	100
50-50 water-ethylene glycol	0.402	3.9	0.37	1,082	-37	107
50-50 water-propylene glycol	0.357	3.6	0.94	1,041	-45	106
CFC 11	0.05	1.0	0.16	1,485	-111	24
Dynalene HC-30	0.519	3.1	0.67	1,275	-40	112
Therminol® 59 <sup>a</sup>	0.11	2.1	0.75	978	-45	289
Galden HT200	0.065	0.96	0.77	1,790	-85	200
Syltherm™ XLT <sup>b</sup>	0.08	2.0	0.34	852	-111	260
Fluorinert FC-72	0.057	1.1	0.12	1,680	-90	56

<sup>a</sup>Eastman Chemical Company.

<sup>b</sup>ChemPoint.

#### 4.2.4.3 Isotope Power System Coolant System

The radiator is constructed in a semicylindrical shape on top of the UPR section and is operated as a single segment. This provides a good view to the sky and the surrounding Mars surface. The Compass Team assumed a 0.5 view factor to the sky and a 0.5 view factor to the Mars surface. A worst-case Sun angle onto the radiator was assumed. The team assumed that the solar flux was normal to one side of the radiator. However, due to the dual-sided operation of the radiator, the opposite side only had a view to deep space and the surface. This situation was approximated by a 45° Sun angle to the total radiator area. Louvers were not used on the radiator since the RPS will be operating continuously. A pump loop cooling system was baselined as the means of moving heat from the Stirling engines to the radiator. Based on the relatively low operating temperature of the cold end of the Stirling engine, which operates at approximately 345 K, several different cooling fluids can be used with the thermal control system. Table 4.15 shows several potential fluids and their properties. (Ref. 18).

Using the analysis described previously, the radiator was sized to meet the input thermal heat rejection requirements. Table 4.16 shows these inputs as well as the radiator sizing results.

#### 4.2.4.4 Electronics Coolant System

A single fixed radiator was utilized to provide cooling for the electronic components of the isotope power system. The radiator was located along the base of the power system radiator. A heat pipe system was used to move the heat from the electronics to the radiator.

TABLE 4.16.—ISOTOPE POWER SYSTEM RADIATOR SIZING INPUTS AND SIZING

Radiator solar absorptivity.....	0.14
Radiator emissivity.....	0.84
Maximum radiator Sun angle.....	45°
View factor to lunar surface.....	0.5
View factor to deep space.....	0.5
Radiator operating temperature (daytime), K.....	345 (average over surface)
Radiator operating temperature (nighttime), K.....	314 (average over surface)
Waste heat, W.....	6,400
Radiator heat rejection, W.....	6,580
Solar heat input, W.....	409
Convective heat rejection, W.....	227
Area, m <sup>2</sup> .....	11.6

The radiator sizing was based on the energy balance analysis given previously to determine the area needed to reject the specified heat load of 260 W to the surroundings. From the determined radiator area, the radiator mass is determined by Equation (22). The radiator was oriented horizontally facing the zenith. Therefore, it has no view of the Mars surface. However, it would have a view to the power system radiator and a potential view to the Sun.

The electronics are operated at a temperature up to 330 K. The radiator was sized to remove the waste heat from the isotope power system electronics during worst-case hot operational conditions that occur while sunlit on the Mars surface under full-power operation. During shadow or nighttime, and if the electronics system thermal output decreases, heaters will be used to maintain the internal temperature of the electronics enclosure. Louvers were not used on the radiator since the RPS will be operating continuously and the electronics will provide sufficient waste heat during operation. Table 4.17 shows the inputs to the radiator sizing as well as the radiator sizing results.

The radiator orientation was chosen to provide the best operating conditions for the heat pipe system by locating the condenser section above the evaporator section thereby returning the fluid in the direction of the gravity field. Two heat pipes are run from each cold plate to the radiator. The heat pipes share the load from each electronics box. Each heat pipe is capable of moving the total heat generated from its corresponding electronics box to the radiator. This provides a redundant heat transfer path for each heat source. Figure 4.17 illustrates the arrangement of the heat pipe coolant system.

Heat pipes in general operate by boiling a liquid fluid when the heat pipe is subjected to heat at a design operating temperature. The fluid vapor then moves to the opposite end of the heat pipe (radiator) where the heat is rejected, and the fluid condenses back to a liquid. A wick structure in the absence of gravity is used to help move the fluid back to the heating section through capillary forces. Once back to the heat input section, the fluid will boil again repeating the process.

Variable conductance heat pipes operate in a similar fashion but use a varying volume and a noncondensable gas to adjust the amount of heat that the heat pipe is capable of moving while maintaining a fixed operating temperature.

At high heat loads, the temperature dependent saturation pressure of the working fluid increases. This increase in pressure compresses the noncondensable gas into a reservoir at the end of the heat pipe to provide a larger active condenser area. Increasing the active condenser area thus enables more heat to be moved to the radiator by the heat pipe. As the heat load decreases, the pressure decreases, and the noncondensable gas fills up a greater volume of the heat pipe reducing the condenser area thereby reducing the heat flow. A variable conductance heat pipe is a passive device that adjusts automatically to varying heat load inputs maintaining a constant operating temperature.

TABLE 4.17.—POWER SYSTEM ELECTRONICS  
RADIATOR SIZING INPUTS AND SIZING

Variable	Value
Radiator solar absorptivity .....	0.14
Radiator emissivity .....	0.84
Maximum radiator Sun angle.....	90° (normal to radiator)
View factor to Mars surface.....	0
View factor to sky.....	0.66
View factor to power radiator .....	0.34
Radiator operating temperature.....	300 to 330 K
Power dissipation and radiator area .....	260 W waste heat
.....	20.4 W convection
.....	73.4 W solar heat input (worst case)
.....	313 W radiative heat load
.....	1.04 m <sup>2</sup> (horizontal fixed)

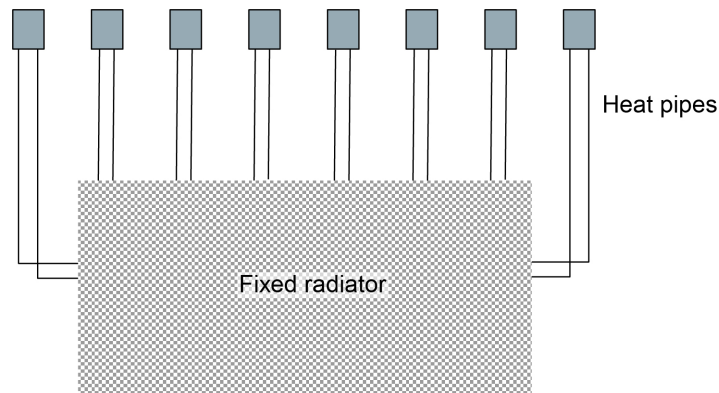


Figure 4.17.—Electronics system cooling system layout.

The working fluid for the heat pipe is chosen based on the desired operating temperature of the heat pipe and the heat removal requirement. To size the heat pipe and select the best working fluid, a factor termed the Merit number is utilized. The Merit number ( $N$ ) is based on the properties of the working fluid as given by Equation (23). These properties include the latent heat of vaporization ( $H_v$ ), the density ( $\rho_{wf}$ ), surface tension ( $\sigma_{wf}$ ), and the dynamic viscosity ( $\mu_{wf}$ ).

$$N = \frac{H_v \rho_{wf} \sigma_{wf}}{\mu_{wf}} \quad (23)$$

This number is plotted for various fluids in Figure 4.18. The higher  $N$  is, the greater the performance of the heat pipe. From this figure, it can be seen for the desired operating temperature of 300 K that water provides the best choice.

Using  $N$ , the heat pipe thermal power ( $P_{hp}$ ) transfer capacity can be calculated as given by Equation (24), which is based on the heat pipe wick cross-sectional area ( $A_w$ ), the wick material permeability ( $K_w$ ), the wick pore radius ( $r_{wp}$ ), and the heat pipe length ( $L_{hp}$ ).

$$P_{hp} = \frac{2NA_w K_w}{r_{wp} L_{hp}} \quad (24)$$

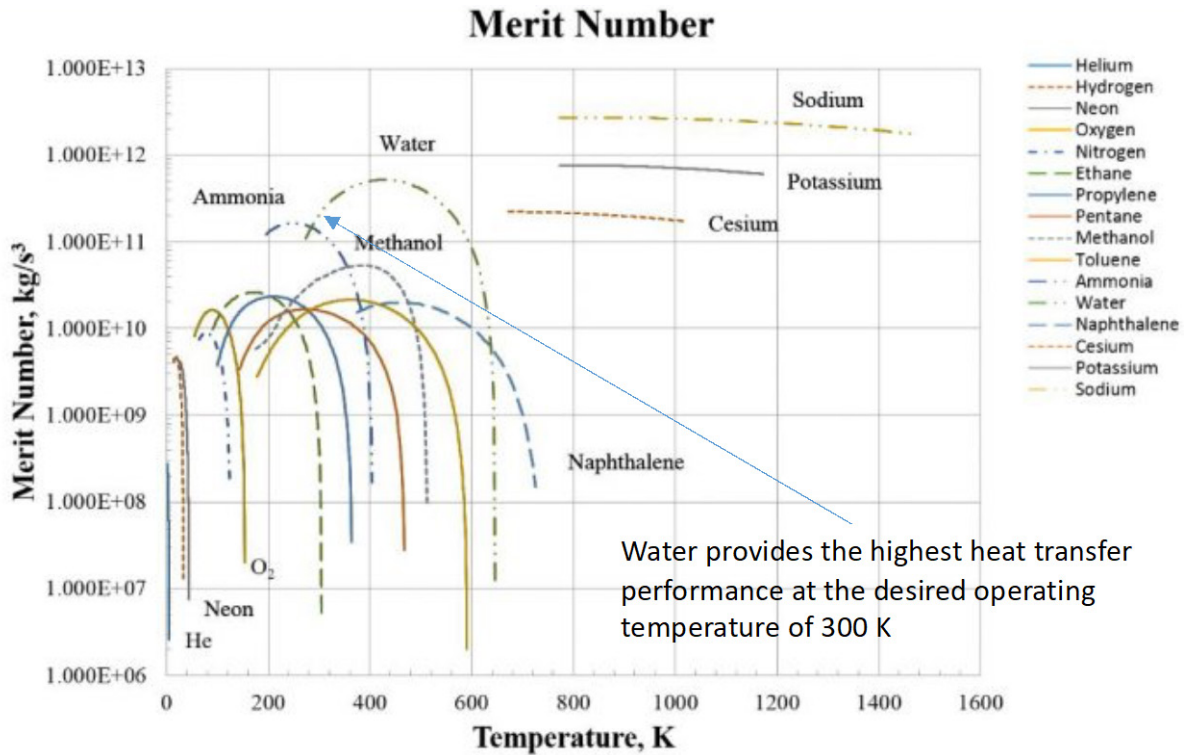


Figure 4.18.—Heat pipe merit number comparison for various working fluids (Ref. 21).

TABLE 4.18.—HEAT PIPE SIZING SPECIFICATIONS FOR EACH LOAD TYPE IN PROPULSION SECTION

Heat pipe radius, cm .....	0.6
Heat pipe length, m.....	2.0
Heat transfer capability, W per heat pipe.....	33
Heat pipe mass, kg (kg/m) per heat pipe.....	0.36 (0.18)
Number of heat pipes.....	16

Using Equation (6), the heat pipes were sized for the heat produced by each of the loads. Table 4.18 gives the required heat pipe size and specific mass.

#### 4.2.4.5 Insulation

Aerogel foam insulation is used to insulate beneath the radiator and around the electronics boxes to minimize heat loss to the surroundings while maintaining the internal component temperatures to between 260 to 320 K, and to also insulate the back side of the radiator, minimizing the heat leak into the electronics and power system components. Aerogel is lightweight, open-cell insulation with a very low thermal conductivity of approximately 0.016 W/m·K. The cells within the aerogel constrain the natural convection of the atmospheric gas within the insulation. This enables thermal conductivity to approach that of the atmospheric gas. Aerogel sheets comprise silica gel and are available in several different densities.

The heat loss through the insulation is calculated by determining the enclosure surface temperature ( $T_{es}$ ) and then calculating the heat flow through the insulation ( $Q_e$ ) based on this temperature. The electronics will operate near the internal operating temperature of the enclosure. Heat will be removed from the enclosure through the electronics radiator to maintain a constant operating temperature.



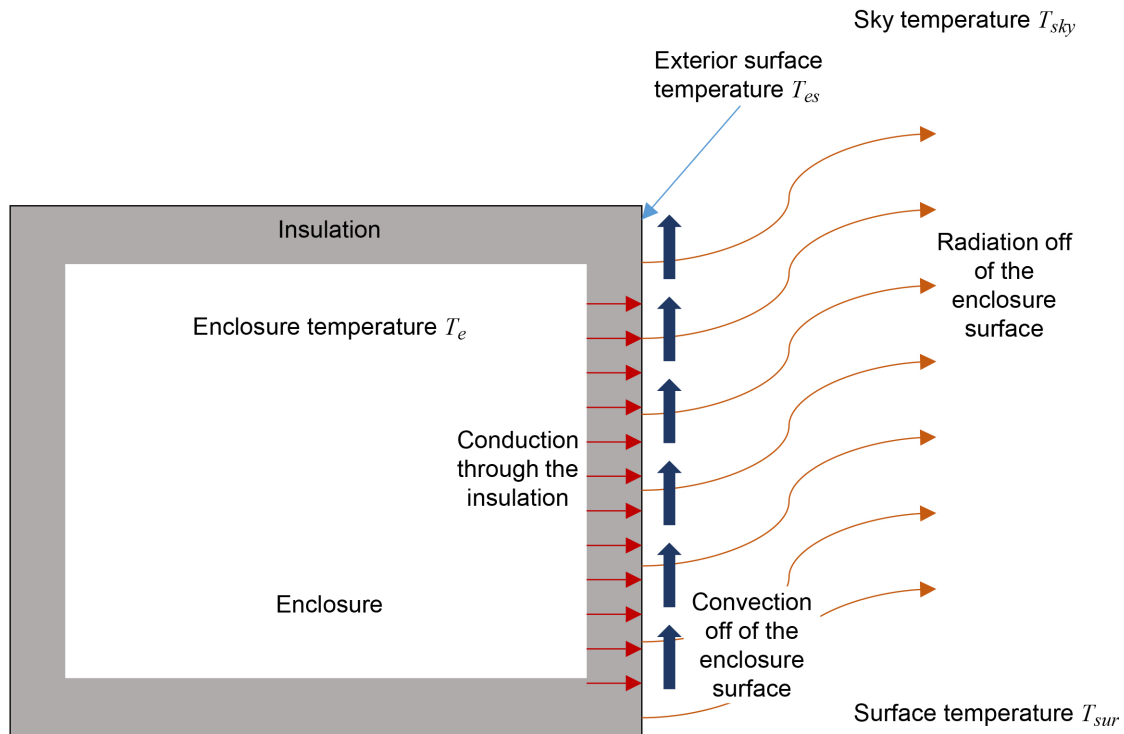


Figure 4.19.—Heat transfer from enclosure to surroundings.

The  $Q_e$  is dependent on the convective ( $Q_{ec}$ ) and radiative heat transfer ( $Q_{er}$ ) from the enclosure to the surroundings as given by Equation (25).

$$Q_e = Q_{ec} + Q_{er} \quad (25)$$

The heat flow through the insulation is given by Equation (26) and is based on the temperature difference between the enclosure interior ( $T_{ei}$ ) and the exterior surface ( $T_{es}$ ), the enclosure area ( $A_e$ ), and the thermal conductivity ( $k_i$ ) of the insulation and its thickness ( $t_i$ ).

$$Q_e = \frac{A_e k_i (T_{ei} - T_{es})}{t_i} \quad (26)$$

The  $Q_{ec}$  and  $Q_{er}$  from the enclosure to the surroundings are given by Equations (27) and (28), respectively. Equations (26) to (28) are solved iteratively to determine the enclosure surface temperature for a given internal enclosure temperature. Once this is determined, the heat loss through the insulation can be calculated from Equation (25). The heat loss through the insulation is then compared to the total waste heat generated within the enclosure. If they differ, the internal temperature is adjusted, and the iterative process is repeated until the waste heat equals the heat loss. This process is illustrated in Figure 4.20.

$$Q_{ec} = A_e h (T_{es} - T_{sur}) \quad (27)$$

The convective coefficient is determined from Equation (10) where the characteristic length is the length of the enclosure.

$$Q_{er} = A_e \epsilon \sigma \left[ F_{esky} (T_{es}^4 - T_{sky}^4) + F_{esur} (T_{es}^4 - T_{sur}^4) \right] \quad (28)$$

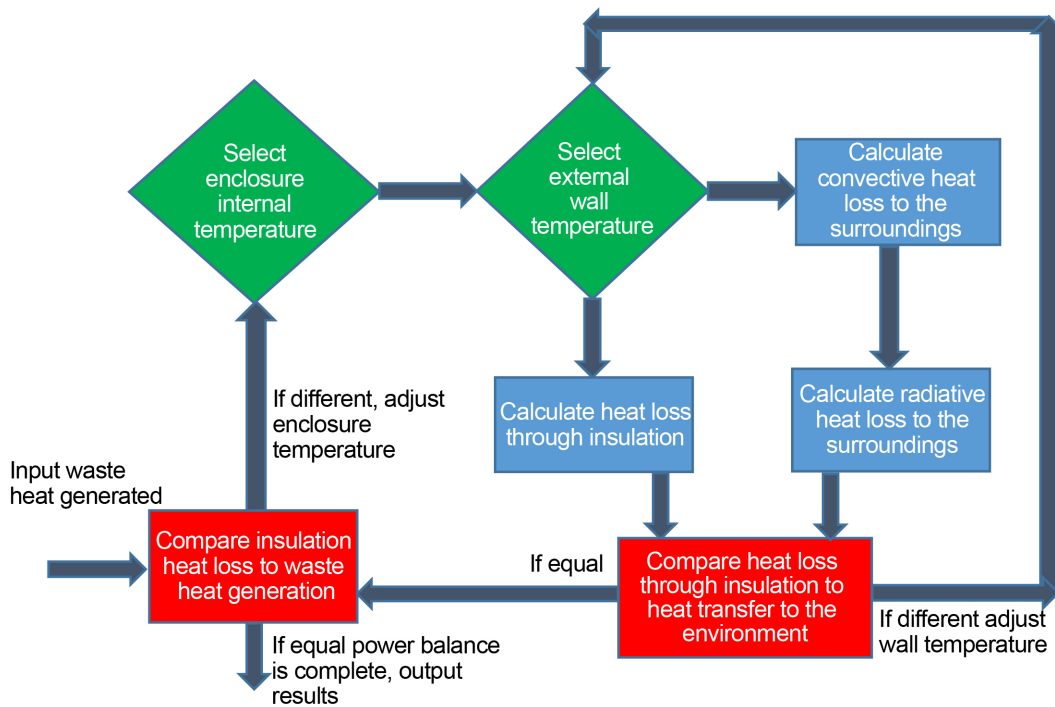


Figure 4.20.—Iterative process for calculating enclosure internal temperature.

TABLE 4.19.—INSULATION CHARACTERISTICS AND DESIGN RESULTS

Insulation thickness, cm.....	0.2
Insulation thermal conductivity, W/m·K.....	0.016
Insulation density (includes backing material), kg/m <sup>3</sup> .....	100
Heat leak through radiator insulation, W (W/m <sup>2</sup> ) .....	360 (31)
Enclosure temperature, K.....	300
Convective coefficient W/m <sup>2</sup> K.....	0.89
Heat loss through insulation, W.....	105.7
Total insulation mass, kg .....	23.8

The sky and surface temperatures are the same as those for the radiator, but the surface ( $F_{esur}$ ) and sky ( $F_{esky}$ ) view factors may be different for the enclosure than the radiator depending on its mounting location on the power platform.

Table 4.19 gives the insulation specifications and heat loss from the enclosure.

#### 4.2.5 System Lunar Operation

An analysis was performed on the rover to see if the thermal control design was applicable to the lunar environment. The environment near the lunar pole is different from the Mars environment; however, there are some similarities. The initial difference is that the Moon does not have an atmosphere. This primarily affects the insulation choice. MLI is preferred, but metalized aerogel has also been shown to be an effective insulation in vacuum conditions. The other main difference is the solar intensity, which increases from approximately 600 W/m<sup>2</sup> on Mars to 1,360 W/m<sup>2</sup> on the lunar surface. The surrounding temperature on the lunar surface near the pole is colder than on Mars but comparable. The colder surface temperature is a benefit to the radiator in that it provides a lower temperature sink for the rejection of heat. The operation of the rover within the lunar polar environment is summarized in Figure 4.21.

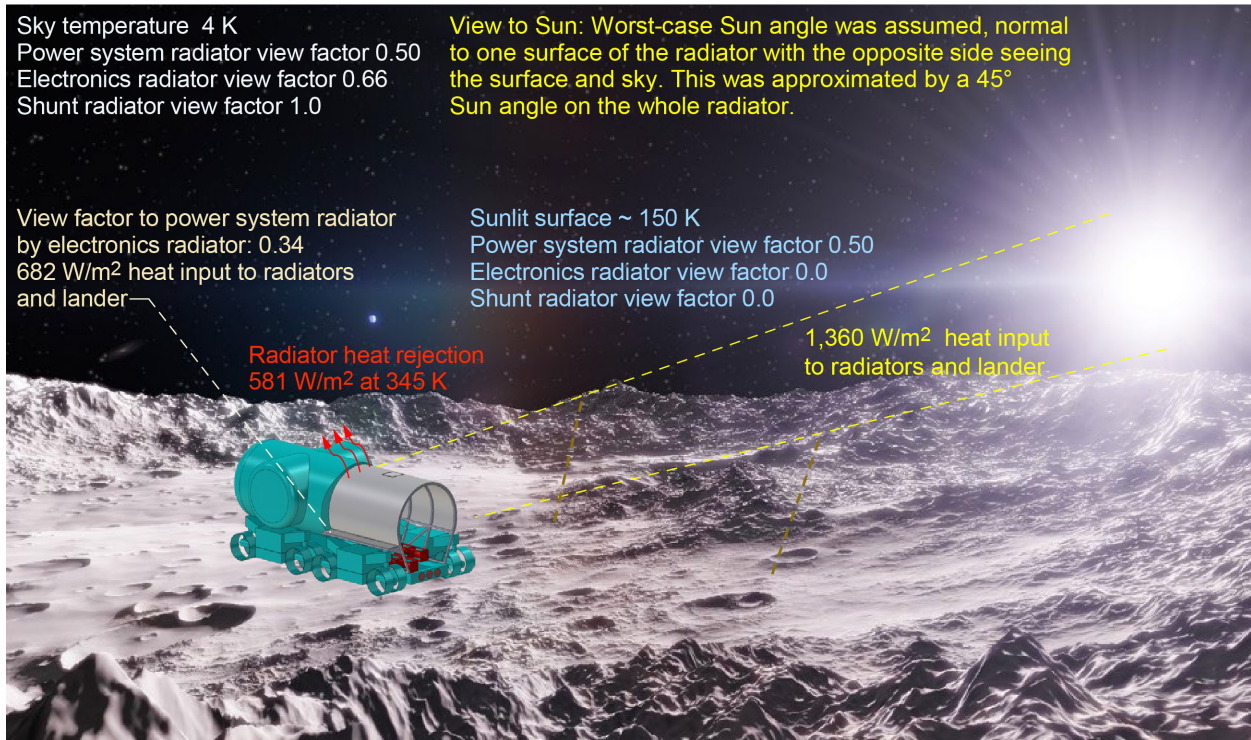


Figure 4.21.—Lunar polar operational environment for rover.

TABLE 4.20.—ROVER RADIATOR SIZING COMPARISON BETWEEN OPERATION ON MARS AND LUNAR SURFACE

Case	Description	Heat load	Radiator size, m <sup>2</sup>	Thermal system mass (before growth), kg
1	Isotope power system: radiator operating temperature 345 K on Mars	Stirling engine and electronics: 6,580 W	11.6	188.5
2	Fuel cell power system: radiator operating temperature 300 K on Mars	Fuel cell: 2,400 W	9.6	169.1
3	Isotope power system: radiator operating temperature 345 K on Moon	Stirling engine and electronics: 6,580 W	11.0	180.9

A similar thermal analysis to that described previously was performed using the lunar environmental conditions. Table 4.20 provides the radiator sizing results compared to those for operation on Mars. The required radiator area for the same power level is just slightly lower for the Moon than that for operation on Mars. In addition, the Compass Team ran a case for the operation on Mars with a fuel cell system that operated at a power level of 2,400 W versus 6,400 W for the isotope system. However, the fuel cell system operated at a lower rejection temperature of 300 K versus the 345 K for the isotope system. Therefore, the decrease in radiator size for the fuel cell system over that of the isotope system was not as great as the reduction in heat load would indicate. The 62.5 percent reduction in rejected heat translated into a reduction in radiator size of only 17 percent due to the decrease in rejection temperature.

#### 4.2.6 Master Equipment List

Table 4.21 to Table 4.23 show the thermal system MEL for the three cases designed by the Compass Team. No MEL is shown for the lunar case. Note that the Passive Thermal Control section includes some active components. This is a side effect of the MEL setup and should be interpreted as such.

TABLE 4.21.—CASE 1 THERMAL SYSTEM MEL

Radioisotope Power System	QTY	Unit Mass	Basic Mass	Growth	Growth	Total Mass
Case 1 DAPS CD 2019-172		(kg)	(kg)	(%)	(kg)	(kg)
<b>DAPS</b>			<b>987</b>	<b>26%</b>	<b>255</b>	<b>1243</b>
<b>Unpressurized Rover</b>			<b>580</b>	<b>20%</b>	<b>117</b>	<b>697</b>
<b>Thermal Control (Non-Propellant)</b>			<b>188.5</b>	<b>18%</b>	<b>33.9</b>	<b>222.4</b>
<b>Active Thermal Control</b>			<b>13.3</b>	<b>18%</b>	<b>2.4</b>	<b>15.7</b>
Heaters	25	0.2	5.0	18%	0.9	5.9
Thermal Control	6	0.2	1.2	18%	0.2	1.4
Thermocouples	8	0.0	0.1	18%	0.0	0.1
Data Acquisition	6	0.3	1.5	18%	0.3	1.8
Switches	25	0.1	2.5	18%	0.5	3.0
Servo Valves	6	0.5	3.0	18%	0.5	3.5
<b>Passive Thermal Control</b>			<b>71.0</b>	<b>18%</b>	<b>12.8</b>	<b>83.8</b>
Radiator Insulation	1	23.8	23.8	18%	4.3	28.0
Flow Diverter Valve	2	1.5	3.0	18%	0.5	3.5
Check Valve	7	0.3	2.1	18%	0.4	2.5
Coolant Pump	2	6.8	13.5	18%	2.4	15.9
Vent Valve	2	0.1	0.2	18%	0.0	0.2
Filter	2	0.4	0.8	18%	0.1	0.9
Accumulator	2	4.0	8.0	18%	1.4	9.4
Heat Exchanger	1	6.8	6.8	18%	1.2	8.0
Temperature Sensor	4	0.1	0.4	18%	0.1	0.5
Pressure Sensor	7	0.1	0.7	18%	0.1	0.8
Flow Sensor	6	0.6	3.6	18%	0.6	4.2
Coolant Lines	1	3.3	3.3	18%	0.6	3.9
Coolant	1	4.9	4.9	18%	0.9	5.8
<b>Semi-Passive Thermal Control</b>			<b>104.2</b>	<b>18%</b>	<b>18.8</b>	<b>123.0</b>
Power System Radiator	1	93.7	93.7	18%	16.9	110.5
Electronics Radiator	1	7.4	7.4	18%	1.3	8.7
Electronics Heatt Pipes	8	0.3	2.0	18%	0.4	2.4
Electronics Cold Plates	8	0.1	1.1	18%	0.2	1.3

TABLE 4.22.—CASE 2 THERMAL SYSTEM MEL

Fuel Cells - 6 Days w/ Lander Reprocessing	QTY	Unit Mass	Basic Mass	Growth	Growth	Total Mass
Case 2 DAPS CD 2019-172		(kg)	(kg)	(%)	(kg)	(kg)
<b>DAPS</b>			<b>1945</b>	<b>15%</b>	<b>296</b>	<b>2242</b>
<b>Unpressurized Rover</b>			<b>1154</b>	<b>17%</b>	<b>197</b>	<b>1351</b>
<b>Thermal Control (Non-Propellant)</b>			<b>169.1</b>	<b>18%</b>	<b>30.4</b>	<b>199.5</b>
<b>Active Thermal Control</b>			<b>13.3</b>	<b>18%</b>	<b>2.4</b>	<b>15.7</b>
Heaters	25	0.2	5.0	18%	0.9	5.9
Thermal Control	6	0.2	1.2	18%	0.2	1.4
Thermocouples	8	0.0	0.1	18%	0.0	0.1
Data Acquisition	6	0.3	1.5	18%	0.3	1.8
Switches	25	0.1	2.5	18%	0.5	3.0
Servo Valves	6	0.5	3.0	18%	0.5	3.5
<b>Passive Thermal Control</b>			<b>70.1</b>	<b>18%</b>	<b>12.6</b>	<b>82.8</b>
Radiator Insulation	1	23.8	23.8	18%	4.3	28.0
Flow Diverter Valve	2	1.5	3.0	18%	0.5	3.5
Check Valve	7	0.3	2.1	18%	0.4	2.5
Coolant Pump	2	6.8	13.5	18%	2.4	15.9
Vent Valve	2	0.1	0.2	18%	0.0	0.2
Filter	2	0.4	0.8	18%	0.1	0.9
Accumulator	2	4.0	8.0	18%	1.4	9.4
Heat Exchanger	1	6.8	6.8	18%	1.2	8.0
Temperature Sensor	4	0.1	0.4	18%	0.1	0.5
Pressure Sensor	7	0.1	0.7	18%	0.1	0.8
Flow Sensor	6	0.6	3.6	18%	0.6	4.2
Coolant Lines	1	3.3	3.3	18%	0.6	3.9
Coolant	1	4.0	4.0	18%	0.7	4.8
<b>Semi-Passive Thermal Control</b>			<b>85.7</b>	<b>18%</b>	<b>15.4</b>	<b>101.1</b>
Power System Radiator	1	75.1	75.1	18%	13.5	88.6
Electronics Radiator	1	7.4	7.4	18%	1.3	8.7
Electronics Heatt Pipes	8	0.3	2.0	18%	0.4	2.4
Electronics Cold Plates	8	0.1	1.1	18%	0.2	1.3

TABLE 4.23.—CASE 3 THERMAL SYSTEM MEL

Fuel Cells - 21 Days w/o Reprocessing	QTY	Unit Mass	Basic Mass	Growth	Growth	Total Mass
Case 3 DAPS CD 2019-172		(kg)	(kg)	(%)	(kg)	(kg)
<b>DAPS</b>			<b>2708</b>	<b>13%</b>	<b>346</b>	<b>3054</b>
<b>Unpressurized Rover</b>			<b>2674</b>	<b>13%</b>	<b>335</b>	<b>3008</b>
<b>Thermal Control (Non-Propellant)</b>			<b>169.1</b>	<b>18%</b>	<b>30.4</b>	<b>199.5</b>
<b>Active Thermal Control</b>			<b>13.3</b>	<b>18%</b>	<b>2.4</b>	<b>15.7</b>
Heaters	25	0.2	5.0	18%	0.9	5.9
Thermal Control	6	0.2	1.2	18%	0.2	1.4
Thermocouples	8	0.0	0.1	18%	0.0	0.1
Data Acquisition	6	0.3	1.5	18%	0.3	1.8
Switches	25	0.1	2.5	18%	0.5	3.0
Servo Valves	6	0.5	3.0	18%	0.5	3.5
<b>Passive Thermal Control</b>			<b>70.1</b>	<b>18%</b>	<b>12.6</b>	<b>82.8</b>
Radiator Insulation	1	23.8	23.8	18%	4.3	28.0
Flow Diverter Valve	2	1.5	3.0	18%	0.5	3.5
Check Valve	7	0.3	2.1	18%	0.4	2.5
Coolant Pump	2	6.8	13.5	18%	2.4	15.9
Vent Valve	2	0.1	0.2	18%	0.0	0.2
Filter	2	0.4	0.8	18%	0.1	0.9
Accumulator	2	4.0	8.0	18%	1.4	9.4
Heat Exchanger	1	6.8	6.8	18%	1.2	8.0
Temperature Sensor	4	0.1	0.4	18%	0.1	0.5
Pressure Sensor	7	0.1	0.7	18%	0.1	0.8
Flow Sensor	6	0.6	3.6	18%	0.6	4.2
Coolant Lines	1	3.3	3.3	18%	0.6	3.9
Coolant	1	4.0	4.0	18%	0.7	4.8
<b>Semi-Passive Thermal Control</b>			<b>85.7</b>	<b>18%</b>	<b>15.4</b>	<b>101.1</b>
Power System Radiator	1	75.1	75.1	18%	13.5	88.6
Electronics Radiator	1	7.4	7.4	18%	1.3	8.7
Electronics Heatt Pipes	8	0.3	2.0	18%	0.4	2.4
Electronics Cold Plates	8	0.1	1.1	18%	0.2	1.3

### 4.3 Fuel Cell Reactant Storage

For two of the three designs developed under this study, a hydrogen- and oxygen-based fuel cell was selected for electrical power generation. Therefore, tanks capable of storing adequate reactants at high pressure and a feed system to adequately regulate the pressure and meter the flow of those reactants to the fuel cells is required for both cases 2 and 3. Case 2, however, also requires fuel cell reactant and water storage tanks on the lander because water is recycled back into reactants via electrolysis for additional missions in that design case.

#### 4.3.1 System Requirements

The fuel cell reactant storage system is required to provide high-pressure storage at a nominal 300 K and regulated flow control for all fuel cell reactants to the fuel cell system. The storage system is required to be capable of refueling all reactants for all cases and unloading water byproduct (case 2 only). The systems are required to be human rated.

### 4.3.2 System Assumptions

The fuel cell reactant storage system is assumed to consist of COTS or near COTS components as applicable to reduce cost and risk. The high-pressure gas storage tanks are assumed to be T-1000 composite overwrapped pressure vessel (COPV) spherical tanks based on the European Aeronautic Defence and Space Company (EADS) 300-L pressure tanks (Ref. 22). Both the water and electrolyzer system buffer tanks are assumed to be low-pressure metallic tanks. To meet human-rating requirements, there are redundant valves and compressor systems with the compressors located on the lander.

### 4.3.3 System Trades

Various geometric and pressure trades were conducted as part of this study. Once the mass of the fuel cell reactants for each case was determined, various potential tank configurations were developed. Due to the volume of the gas tanks, and the limited space on the rover, the storage pressure was increased as much as is practical. Cylindrical tanks did not package as well on the rover as two spherical tanks did for either case, and the spherical tanks had an overall lower mass. Therefore, the high-pressure spherical tank approach was considered the better option for these designs.

To reduce tank size, the pressure in the reactant’s storage tanks was increased to 68.9 MPa (10.0 ksi) for both cases 2 and 3. For case 2, it is assumed that the lander would store an entire charge of hydrogen and oxygen to refill the rover, thus the tanks would be approximately the same size. The water tank is then sized to hold an entire charge of reactants converted into water plus ~5 percent ullage, while the buffer tanks are selected to be of nominal size.

### 4.3.4 Fuel Cell Reactant Storage Design

There are three designs as part of this study. Case 1 utilizes a RPS and batteries, therefore no fuel cells or reactants are present. Cases 2 and 3, however, do have fuel cells and their associated reactants on the rover, and case 2 has an electrolysis system for recycling the water back into reactants on the lander. Table 4.24 shows a listing of the various tank diameters and mean operating pressures (MOP) for both cases 2 and 3.

TABLE 4.24.—FUEL CELL REACTANT SYSTEM TANK DIAMETERS

Tank	Case 2 (6 days)		Case 3 (21 days)	
	Diameter	MOP	Diameter	MOP
Rover				
Hydrogen	100 cm (39 in.)	68.9 MPa (10.0 ksi)	172 cm (68 in.)	68.9 MPa (10.0 ksi)
Oxygen	85 cm (34 in.)	68.9 MPa (10.0 ksi)	132 cm (52 in.)	68.9 MPa (10.0 ksi)
Water	80 cm (32 in.)	138 kPa (20.0 psi)	120 cm (47 in.)	138 kPa (20.0 psi)
Buffer	-----	-----	30 cm (12 in.)	689 kPa (100 psi)
Lander				
Hydrogen	100 cm (39 in.)	68.9 MPa (10.0 ksi)	-----	-----
Oxygen	85 cm (34 in.)	68.9 MPa (10.0 ksi)	-----	-----
Water	80 cm (32 in.)	138 kPa (20.0 psi)	-----	-----
Buffer	30 cm (12 in.)	689 kPa (20.0 psi)	-----	-----

The tank and flow control system on the cases 2 and 3 rovers are both regulated systems with positive isolation for launch and pressure relief protection. Regulated reactants flow into the fuel cell, and the resulting water is pumped to a storage tank. Case 2, however, also includes hardware for both refueling the reactants and transferring the water back to the lander for recycling.

#### **4.3.4.1 Case 2 Rover and Lander Fuel Cell Reactant Storage**

For the case 2 design variant, the rover had adequate reactants for the fuel cell onboard to provide the rover's power needs for 6 days. The subsequent water created by the rover is transferred into a tank on the rover during operation. Once the rover returns to the lander, the water is transferred to a storage tank on the lander. High-pressure oxygen and hydrogen gas waiting on the lander is then transferred to the rover to power another mission. While the rover is out on a mission, the water transferred by the rover to the lander is run through the electrolyzer, and the resulting oxygen and hydrogen gas is compressed and used to refill the high-pressure storage tanks.

On the lander, a coupling system is used to transfer both gases to the rover and the liquid water from the rover. All three lines have purge vents to prevent trapped volumes between the coupling and the isolation valves. The water line also includes a gas line from the oxygen system for line purge if required. Water is pumped as needed to the electrolyzer, and the resulting gases flow into small buffer tanks. Once adequate gas is collected and power is available, the compressors pull the gases from their respective buffer tanks and compress them into their high-pressure storage tanks to await transfer to the rover. During the transfer, a large portion of the gas simply flows via pressure difference to the rover. The remainder is compressed and transferred over to the rover via the compressors by setting three-way valves so that the gas flows through the compressors and then out to the coupling.

The high-pressure tanks initially launch with a full charge of gas; therefore, normally closed pyrotechnic valves are used for positive isolation, and a redundant pressure relief system is placed on both gas tanks to prevent any tank overpressure. Figure 4.22 is a preliminary piping and instrumentation diagram (P&ID) of the lander reactant storage and processing system.

On the rover, there are also two high-pressure tanks and a single water storage tank. Similar to the lander, the rover has high-pressure hydrogen and oxygen tanks with redundant pressure relief and positive isolation for launch and transport. Once the system is activated, the gases flow through redundant pressure regulator strings to the fuel cell. The water byproduct is then pumped to a storage tank. Both gases and the water can be transferred to the lander via a coupling system with redundant isolation valves. Figure 4.23 shows a preliminary P&ID of the rover reactant storage system.

#### **4.3.4.2 Case 3 Rover Fuel Cell Reactant Storage**

For this variant, all the hydrogen and oxygen required by the fuel cells for a 21-day mission is placed on the rover, with no processing or refueling on the lander. The basic system is similar to the rover system in case 2, but without the coupling and transfer systems. There is one hydrogen and one oxygen tank onboard. They are 172 cm (68 in.) and 132 cm (52 in.) in diameter, respectively, and have a MOP of 68.9 MPa (10.0 ksi). The feed system includes redundant pressure relief systems, redundant regulators, and water storage system for the fuel cell byproduct. Figure 4.24 shows a preliminary P&ID of the rover reactant storage system for case 3.



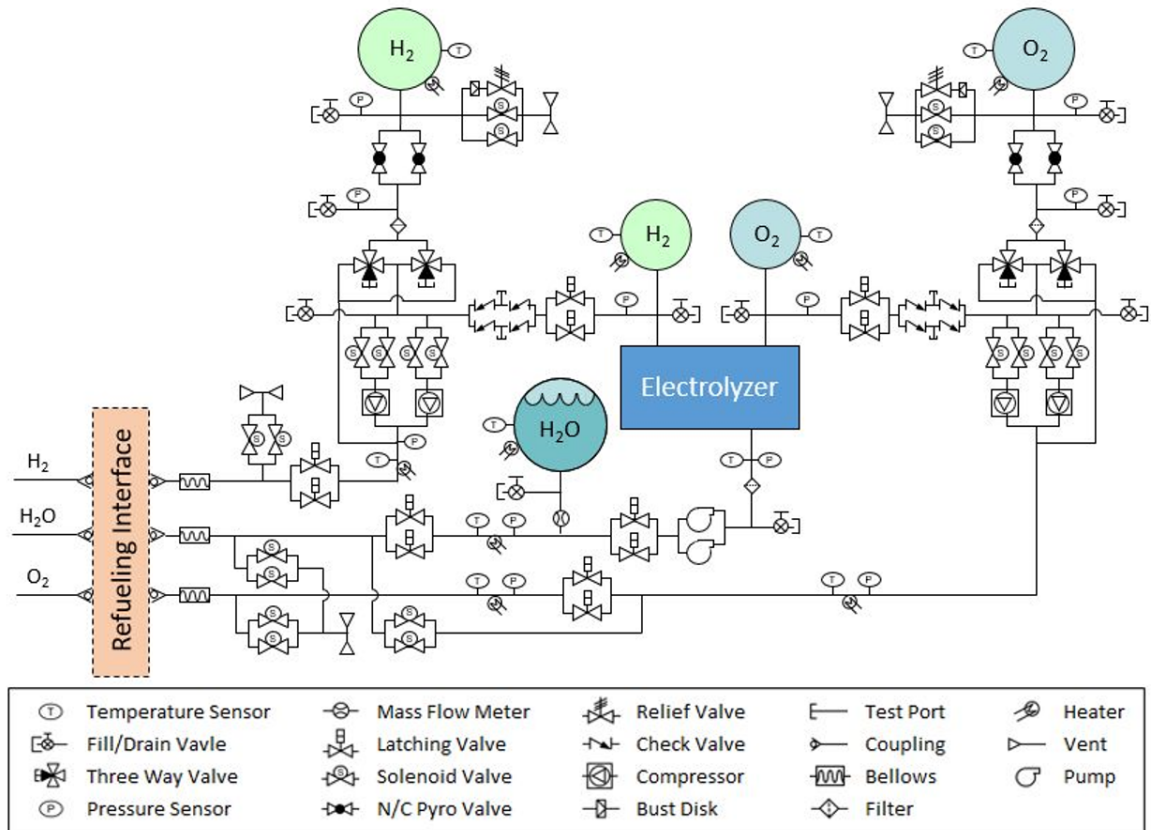


Figure 4.22.—Lander-side fuel cell reactants preliminary P&ID for case 2.

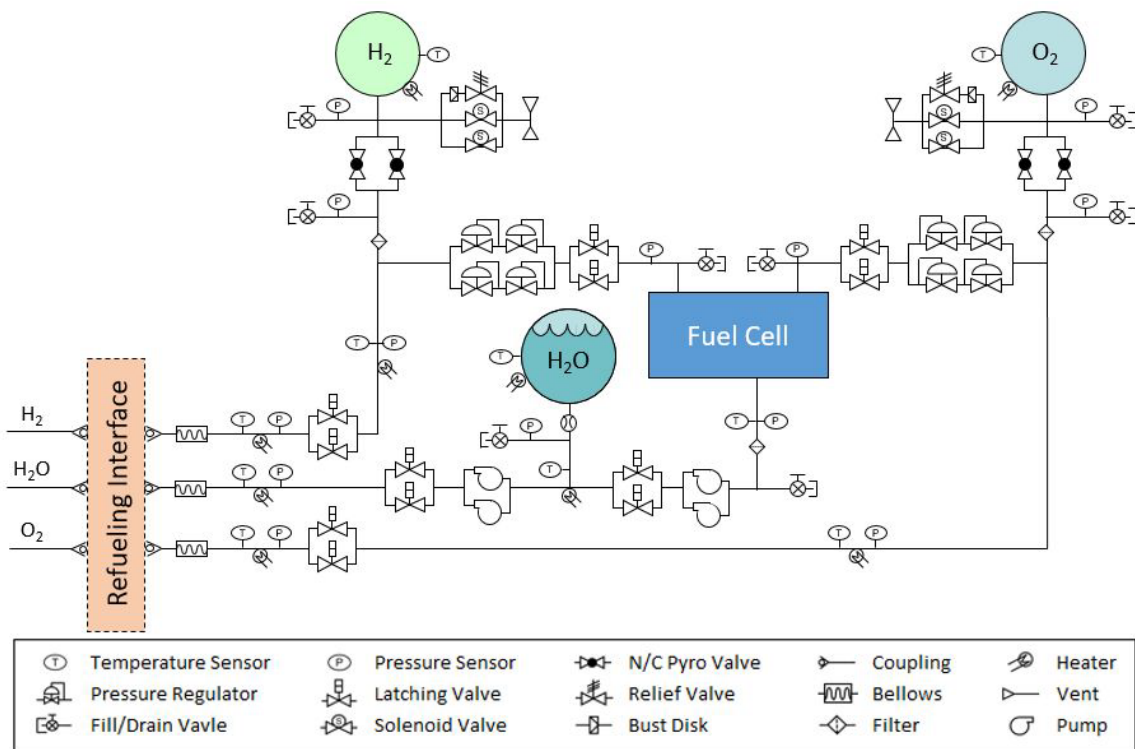


Figure 4.23.—Rover-side fuel cell reactants preliminary P&ID for case 2.

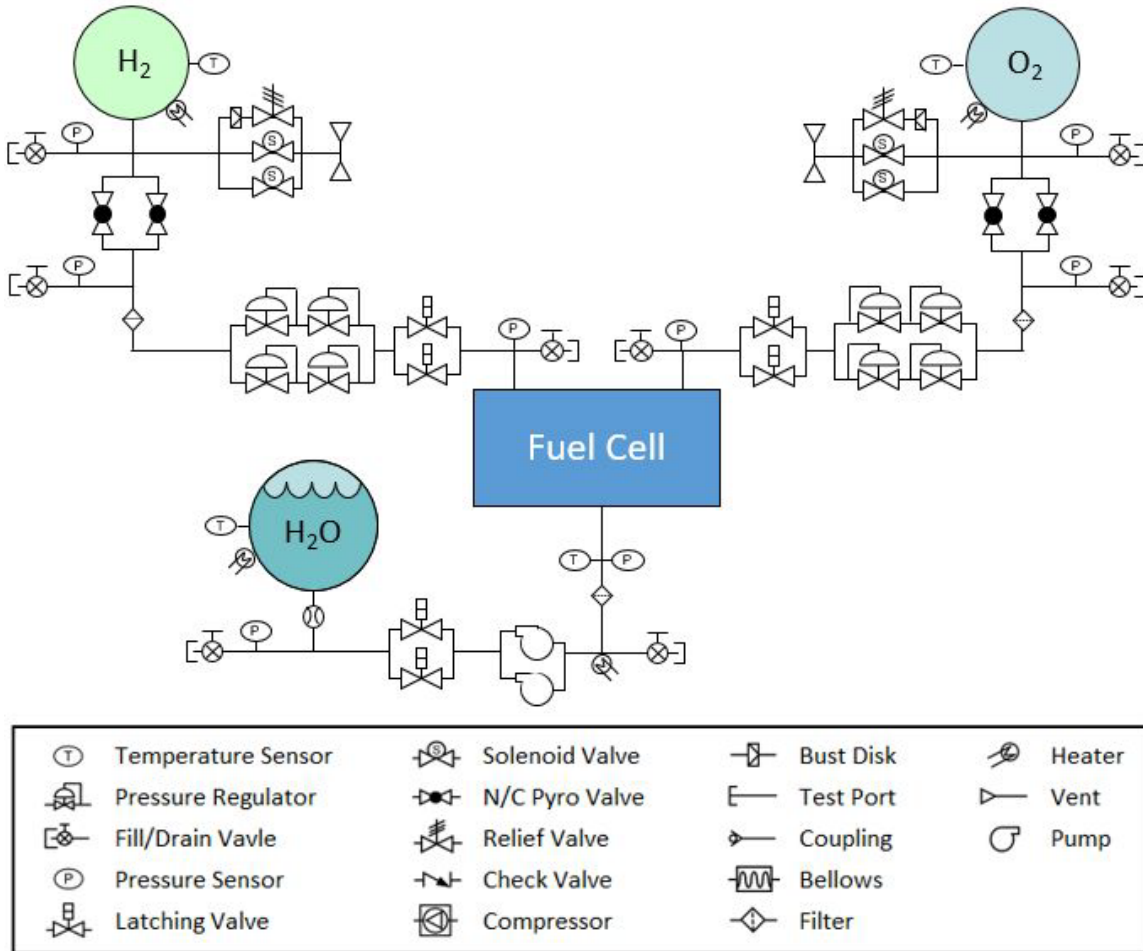


Figure 4.24.—Rover fuel cell reactants preliminary P&ID for case 3.

### 4.3.5 Fuel Cell Reactants Storage Analytical Methods

The methods used to design the fuel cell reactants storage system involve using a mix of published values, empirical data, and analytical tools. Published values for COTS components and empirical data are used wherever possible, with analytical tools being employed as necessary. Empirical data is used to aid in the mass and size estimation of similar components when published values are not available. Numerous analytical tools are used in this analysis, including National Institute of Standards and Technology (NIST) data, fluid, and gas property codes, as well as custom tools developed from basic physical relationships and conservation equations with empirical-based inclusions for real-life hardware requirements (mounting bosses, flanges, etc.).

### 4.3.6 Fuel Cell Reactants Storage Risk Inputs

There are three primary risks identified for the fuel cell reactants storage system. First, this design utilizes components for high-pressure reactant storage that operate at a MOP slightly higher than most aerospace COPV tanks and flow control components. Although similar to COTS components, they do have unique operational requirements and their development may pose a cost and schedule risk. Second, the fuel cell byproduct (water) is dense and can be stored at a low pressure, but there is a risk of it freezing during nighttime. Since water expands when it freezes, it can damage and even burst lines, valves, and other components, if allowed to do so. Third, there is a risk of both contamination and

potential sealing issues while establishing fluid connections, especially in the dusty lunar environment. This design assumes a commodity coupling system based on the dust-tolerant automated umbilical system currently being developed at Kennedy Space Center to help ensure minimal operational impact due to lunar dust incursion. Analytical modeling, ground testing, and proper design can minimize these risks.

#### 4.3.7 Fuel Cell Reactant Storage Recommendations

For the reactant tanks to be of a manageable size and still contain the required reactants, the tank MOP is required to be rather high. This high pressure may affect the loading schedule and compressor discharge temperature (especially near the end of the transfer). Although this is a level of detail beyond this study, it is recommended that it be considered in future designs as it may affect rover recharging operations.

#### 4.3.8 Fuel Cell Reactant Storage System MEL

The following tables show a listing of the fuel cell reactant storage system components and their masses. Table 4.25 shows the MEL for the case 2 rover fuel cell reactant storage system, and Table 4.26 shows the lander specific hardware for this case. Table 4.27 shows the MEL for case 3.

TABLE 4.25.—CASE 2 FUEL CELL REACTANT STORAGE SYSTEM MEL

6 Day w/ Fuel Cells	QTY	Unit Mass	Basic Mass	Growth	Growth	Total Mass
Case 2 DAPS CD 2019-172						
		(kg)	(kg)	(%)	(kg)	(kg)
<b>DAPS</b>			<b>1945</b>	<b>15%</b>	<b>296</b>	<b>2242</b>
<b>Unpressurized Rover</b>			<b>1154</b>	<b>17%</b>	<b>197</b>	<b>1351</b>
<b>Fuel Cell Reactant Hardware</b>			<b>355.0</b>	<b>15%</b>	<b>53.3</b>	<b>408.3</b>
<b>Primary Chemical System Hardware</b>			<b>355.0</b>	<b>15%</b>	<b>53.3</b>	<b>408.3</b>
<i>Main Engine Hardware</i>			355.0	15%	53.3	408.3
Hydrogen Feed System	1	48.0	48.0	15%	7.2	55.2
Oxygen Feed System	1	45.0	45.0	15%	6.8	51.8
Hydrogen Tank	1	170.0	170.0	15%	25.5	195.5
Oxygen Tank	1	80.0	80.0	15%	12.0	92.0
Water Tank and Feed System	1	12.0	12.0	15%	1.8	13.8
<b>Fuel Cell Reactants (Chemical)</b>			<b>220.6</b>	<b>0%</b>	<b>0.0</b>	<b>220.6</b>
<b>Reactants</b>			<b>220.6</b>	<b>0%</b>	<b>0.0</b>	<b>220.6</b>
<i>Fuel</i>			24.6	0%	0.0	24.6
Fuel Usable	1	23.0	23.0	0%	0.0	23.0
Fuel Margin	1	1.2	1.2	0%	0.0	1.2
Fuel Residuals (Unused)	1	0.5	0.5	0%	0.0	0.5
<i>Oxidizer</i>			196.0	0%	0.0	196.0
Oxidizer Usable	1	183.0	183.0	0%	0.0	183.0
Oxidizer Margin	1	9.2	9.2	0%	0.0	9.2
Oxidizer Residuals (Unused)	1	3.8	3.8	0%	0.0	3.8

TABLE 4.26.—CASE 2 ADDITIONAL LANDER HARDWARE MEL

6 Day w/ Fuel Cells	QTY	Unit Mass	Basic Mass	Growth	Growth	Total Mass
Case 2 DAPS CD 2019-172						
		(kg)	(kg)	(%)	(kg)	(kg)
<b>DAPS</b>			<b>1945</b>	<b>15%</b>	<b>296</b>	<b>2242</b>
<b>Additional Lander Hardware</b>			<b>757</b>	<b>12%</b>	<b>87</b>	<b>845</b>
<b>Fuel Cell Reactant Hardware</b>			<b>471.2</b>	<b>15%</b>	<b>71.9</b>	<b>543.1</b>
<b>Primary Chemical System Hardware</b>			<b>471.2</b>	<b>15%</b>	<b>71.9</b>	<b>543.1</b>
<i>Fuel Cell Hardware</i>			471.2	15%	71.9	543.1
Fuel Cell Reactant Feed System - H2	1	91.0	91.0	15%	13.7	104.7
Fuel Cell Reactant Feed System - O2	1	88.0	88.0	15%	13.2	101.2
Reactants Transfer Probe	1	25.0	25.0	20%	5.0	30.0
Hydrogen Tank	1	170.0	170.0	15%	25.5	195.5
Oxygen Tank	1	80.0	80.0	15%	12.0	92.0
Water Tank and Feed System	1	12.2	12.2	15%	1.8	14.0
Buffer Tanks	2	2.5	5.0	15%	0.8	5.8
<b>Fuel Cell Reactants (Chemical)</b>			<b>220.6</b>	<b>0%</b>	<b>0.0</b>	<b>220.6</b>
<b>Reactants</b>			<b>220.6</b>	<b>0%</b>	<b>0.0</b>	<b>220.6</b>
<i>Fuel</i>			24.6	0%	0.0	24.6
Fuel Usable	1	23.0	23.0	0%	0.0	23.0
Fuel Margin	1	1.2	1.2	0%	0.0	1.2
Fuel Residuals (Unused)	1	0.5	0.5	0%	0.0	0.5
<i>Oxidizer</i>			196.0	0%	0.0	196.0
Oxidizer Usable	1	183.0	183.0	0%	0.0	183.0
Oxidizer Margin	1	9.2	9.2	0%	0.0	9.2
Oxidizer Residuals (Unused)	1	3.8	3.8	0%	0.0	3.8

TABLE 4.27.—CASE 3 FUEL CELL REACTANT STORAGE SYSTEM MEL

Description	QTY	Unit Mass	Basic Mass	Growth	Growth	Total Mass
Case 3 DAPS CD 2019-172						
		(kg)	(kg)	(%)	(kg)	(kg)
<b>DAPS</b>			<b>2708</b>	<b>13%</b>	<b>346</b>	<b>3054</b>
<b>Unpressurized Rover</b>			<b>2674</b>	<b>13%</b>	<b>335</b>	<b>3008</b>
<b>Fuel Cell Reactant Hardware</b>			<b>1179.4</b>	<b>15%</b>	<b>176.9</b>	<b>1356.4</b>
<b>Primary Chemical System Hardware</b>			<b>1179.4</b>	<b>15%</b>	<b>176.9</b>	<b>1356.4</b>
<i>Main Engine Hardware</i>			1179.4	15%	176.9	1356.4
Hydrogen Feed System	1	66.0	66.0	15%	9.9	75.9
Oxygen Feed System	1	58.0	58.0	15%	8.7	66.7
Hydrogen Tank	1	707.1	707.1	15%	106.1	813.2
Oxygen Tank	1	319.3	319.3	15%	47.9	367.2
Water Tank and Feed System	1	24.0	24.0	15%	3.6	27.6
Buffer Tanks	2	2.5	5.0	15%	0.8	5.8
<b>Fuel Cell Reactants (Chemical)</b>			<b>859.9</b>	<b>0%</b>	<b>0.0</b>	<b>859.9</b>
<b>Propellant</b>			<b>859.9</b>	<b>0%</b>	<b>0.0</b>	<b>859.9</b>
<i>Fuel</i>			96.3	0%	0.0	96.3
Fuel Usable	1	89.9	89.9	0%	0.0	89.9
Fuel Margin	1	4.5	4.5	0%	0.0	4.5
Fuel Residuals (Unused)	1	1.9	1.9	0%	0.0	1.9
<i>Oxidizer</i>			763.6	0%	0.0	763.6
Oxidizer Usable	1	713.0	713.0	0%	0.0	713.0
Oxidizer Margin	1	35.7	35.7	0%	0.0	35.7
Oxidizer Residuals (Unused)	1	15.0	15.0	0%	0.0	15.0

## **4.4 Structures and Mechanisms**

The lunar-Mars rover structures must contain the necessary hardware for electrical power and thermal control. The structural components must be able to withstand applied mechanical and thermal loads. In addition, the structures must provide minimum mass and deflections, sufficient stiffness, and vibration damping. The operational loads include approximately 5.5 g axial acceleration and a 2.0 g lateral acceleration from the launch vehicle. The launch vehicle, such as NASA's SLS (Ref. 23) also needs the payload cantilevered fundamental mode frequency to have a minimum of 8 Hz lateral and 15 Hz axial. The Ariane 5 launch vehicle is similar with a minimum first bending frequency of 7.5 Hz (Ref. 24).

### **4.4.1 System Requirements**

The bus is to support the mounted hardware bearing launch and operational mechanical and thermal loads without failure. The structures must not degrade for the extent of the mission in the Earth, lunar, martian, and deep space environments.

### **4.4.2 System Assumptions**

The bus provides the backbone for the mounted hardware. The primary material for the bus is aluminum. The aluminum alloy is 7075-T651 as described in the Metallic Materials Properties Development and Standardization (MMPDS-11) (Ref. 25). The material is at a TRL 6, as presented by Mankins (Ref. 26). Components are of shells and tubular members. Joining of components is by threaded fasteners, riveting, or welding.

### **4.4.3 System Trades**

Three study cases were covered. Cases 2 and 3 utilized a fuel cell, whereas case 1 used a RPS. No trades were considered for the main structural system for this study. Minor secondary structural changes were made to accommodate tanks for the fuel cell of cases 2 and 3. The overall system was relatively simple, and the design was quite restricted with the need to integrate with existing designs.

### **4.4.4 Analytical Methods**

Analytical methods utilize spreadsheets for populating the MEL and to conduct preliminary stress analysis. Finite element analysis (FEA) was applied for this study using a simplified general model based on the study's CAD model.

### **4.4.5 Risk Inputs**

A potential risk for the structural system may be excessive g loads or impact from operational loads or a foreign object, which may cause too much deformation, vibrations, or fracture of sections of the support structure. Consequences include lower performance from mounted hardware to loss of mission.

The likelihood is a medium ranking of three. Consequences may be relatively high with a ranking of four for cost, schedule, and performance. Safety may also be at ranking of four.

For risk mitigation, the structure is to be designed to NASA standards to withstand expected g loads, a given impact, and to have sufficient stiffness and damping to minimize issues with vibrations. Trajectories and lunar operations are to be planned to minimize the probability of impact with foreign objects and to minimize excessive loads.

### **4.4.6 System Design**

The material of the structural components is aluminum 7075-T651. Per the MMPDS-11 (Ref. 25), the ultimate strength is 531 MPa (77 ksi), and the yield strength is 469 MPa (68 ksi). Applying safety

factors of 1.4 on the ultimate strength and 1.25 on the yield strength and selecting the lower value, as per NASA Standard 5001b (Ref. 27), results in an allowable stress of 375 MPa (54 ksi) at room temperature. The Young's modulus is 723 GPa ( $10.5 \times 10^6$  psi), and the density is  $2.80 \text{ g/cm}^3$  ( $0.101 \text{ lb/in}^3$ ).

Figure 4.25 illustrates the CAD model of the radiators and their support structure. A preliminary stress calculation was performed on the radiator support arch. The masses supported by the arch include the power system radiator with 93.7 kg (206 lb) of mass, the electronics radiator at 7.4 kg (16 lb) of mass, and a shunt radiator at 1.18 kg (2.6 lb) of mass for a total supported mass of 102 kg (224 lb).

The load is assumed to be equally distributed among the eight vertical members. The maximum launch acceleration of 5.5 g is applied. The resulting stress in each vertical member is 2.5 MPa (360 psi) providing a positive margin of 149.

In addition, the Compass Team conducted a quick FEA. The radiators were modeled with linear plate elements, and the support structure was modeled with linear beam elements. Rigid RBE2 elements were used to connect the plate elements of the radiators to the beam elements of the support structure. Constraints were applied to the base with fixed translations and rotations. A Young's modulus of 34 GPa ( $5.0 \times 10^6$  psi) was assumed for the radiators. Radiator densities were calculated from the solid model volume and provided component mass. Figure 4.26 illustrates the meshed model.

The first analysis determined the modal frequencies of the structure. The first modal frequency is at 6.5 Hz, and the second modal frequency is at 22.9 Hz. Figure 4.27 and Figure 4.28 illustrate the first and second modes, respectively.

In addition to determining the first two modal frequencies, the structure was loaded with the anticipated launch acceleration. The stresses in the support structure were determined. Figure 4.29 shows the stress contour (in psi) for the support structure under a 5.5-g acceleration. The resulting peak stress is 30.3 MPa (4.4 ksi) providing a positive margin of 11.3 relative to the allowable stress of 375 MPa (54 ksi).

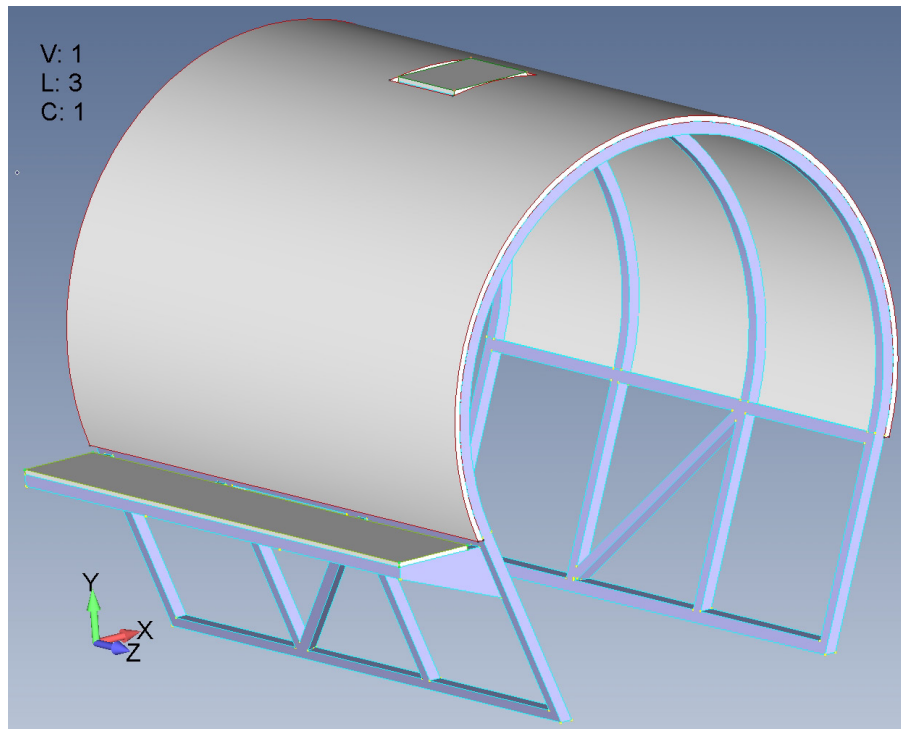


Figure 4.25.—Radiators and radiator support structure.

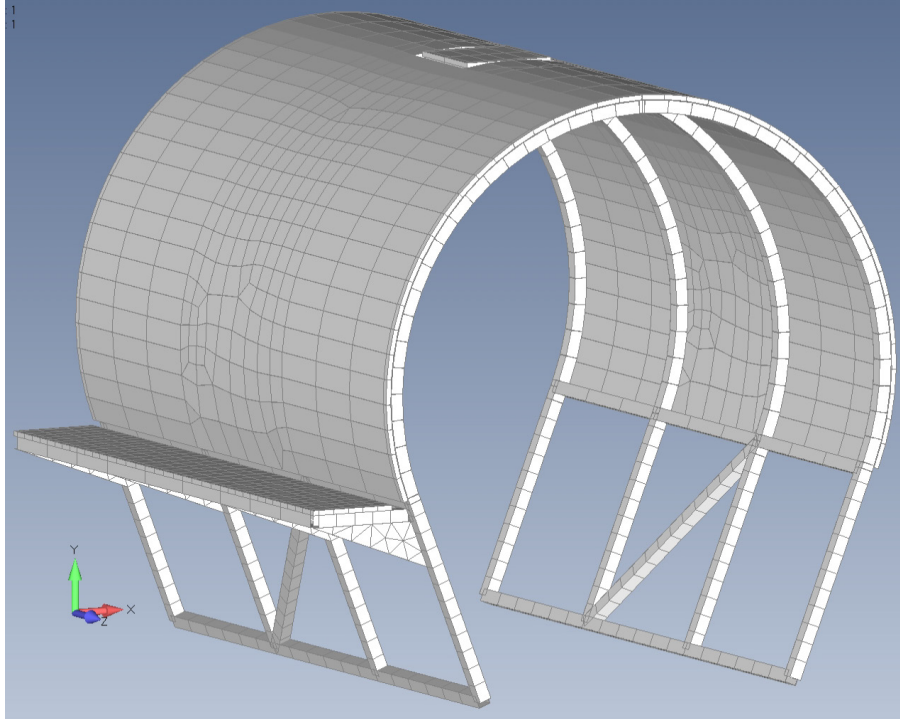


Figure 4.26.—FEA-meshed model of radiators and radiator support structure.

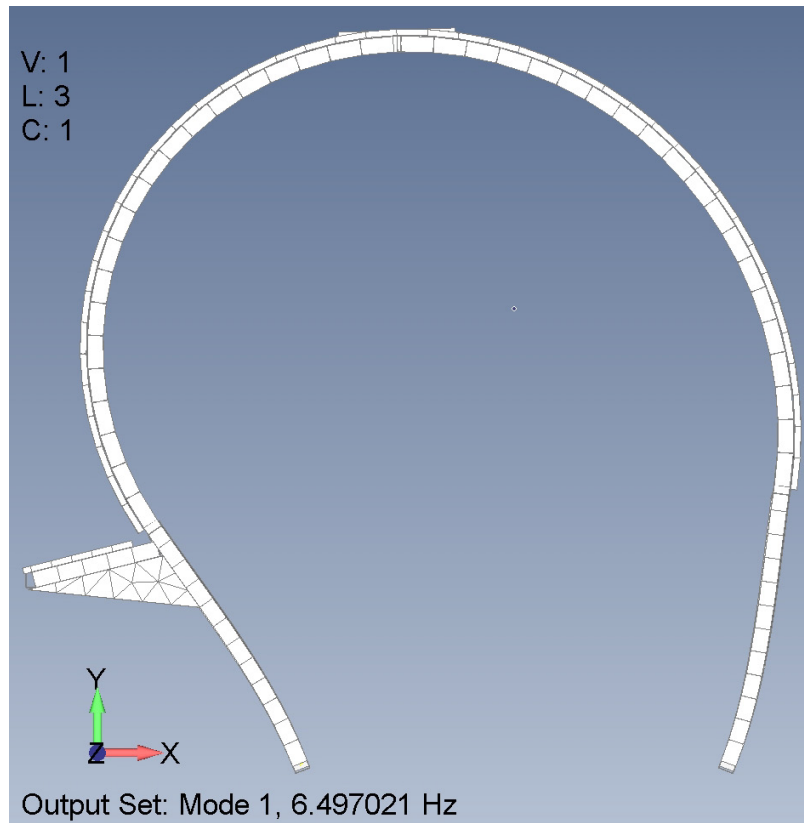


Figure 4.27.—First modal frequency at 6.5 Hz.

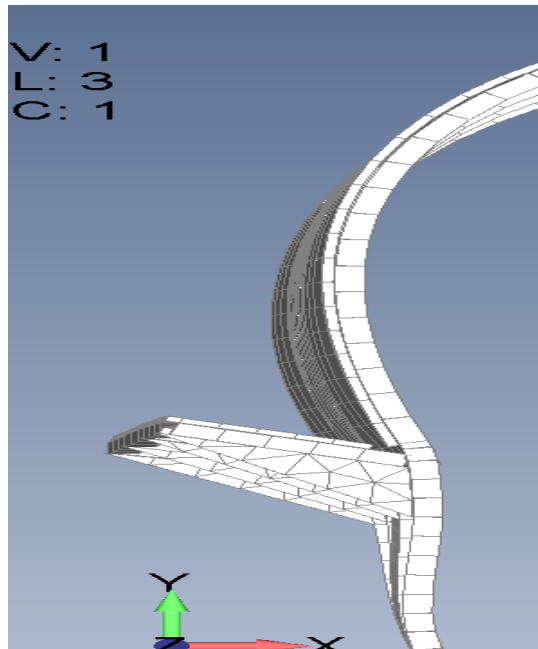


Figure 4.28.—Second modal frequency at 22.9 Hz.

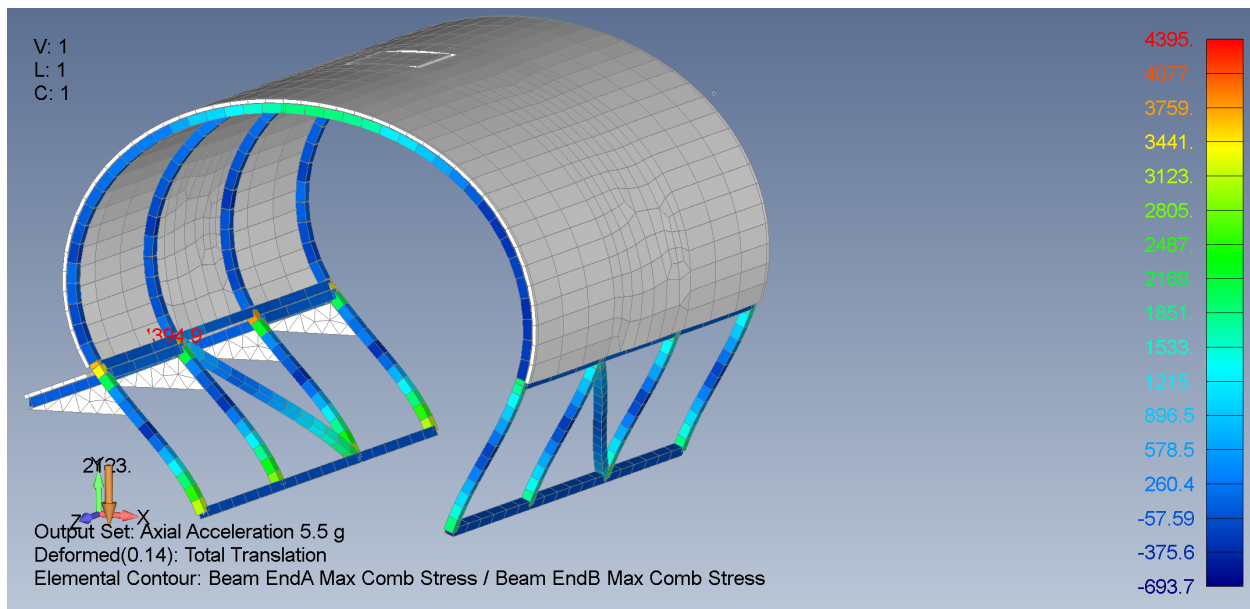


Figure 4.29.—Stress contours for radiator support structure under 5.5-g vertical acceleration stress is in psi. Resulting peak stress is 30.3 MPa (4.4 ksi).

During the launch phase, it is anticipated that the structure may be placed under a lateral acceleration of 2.0 g. Figure 4.30 shows the stress contour (in psi) for the radiator support structure under the 2.0-g acceleration in the x-direction, or normal to the axis of the radiator cylinder. The maximum stress is 46.8 MPa (6.8 ksi). The resulting margin is positive at 6.9.

The radiator assembly was loaded in the z-direction or along the axis of the radiator cylinder. Figure 4.31 illustrates the stress contour in the radiator support structure. The maximum stress is 8.1 MPa (1.2 ksi). The resulting margin is 44 relative to the allowable stress of 375 MPa (54 ksi).



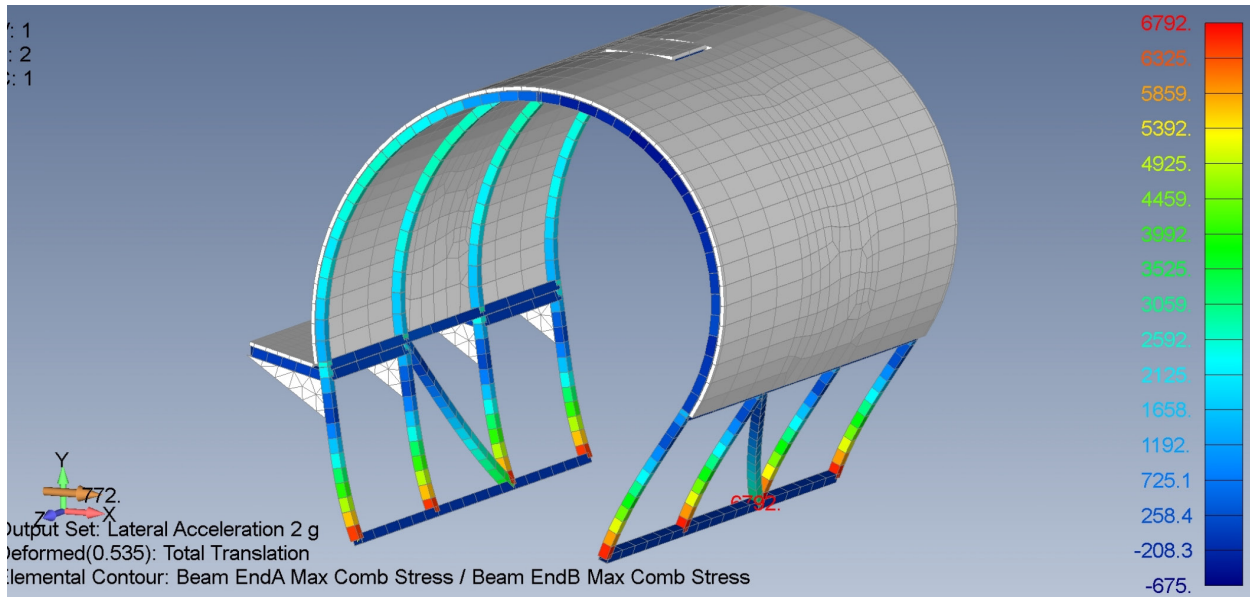


Figure 4.30.—Stress contours for radiator support structure under 2.0-g lateral acceleration in the x-direction. Stress is in psi. Maximum stress is 46.8 MPa (6.8 ksi).

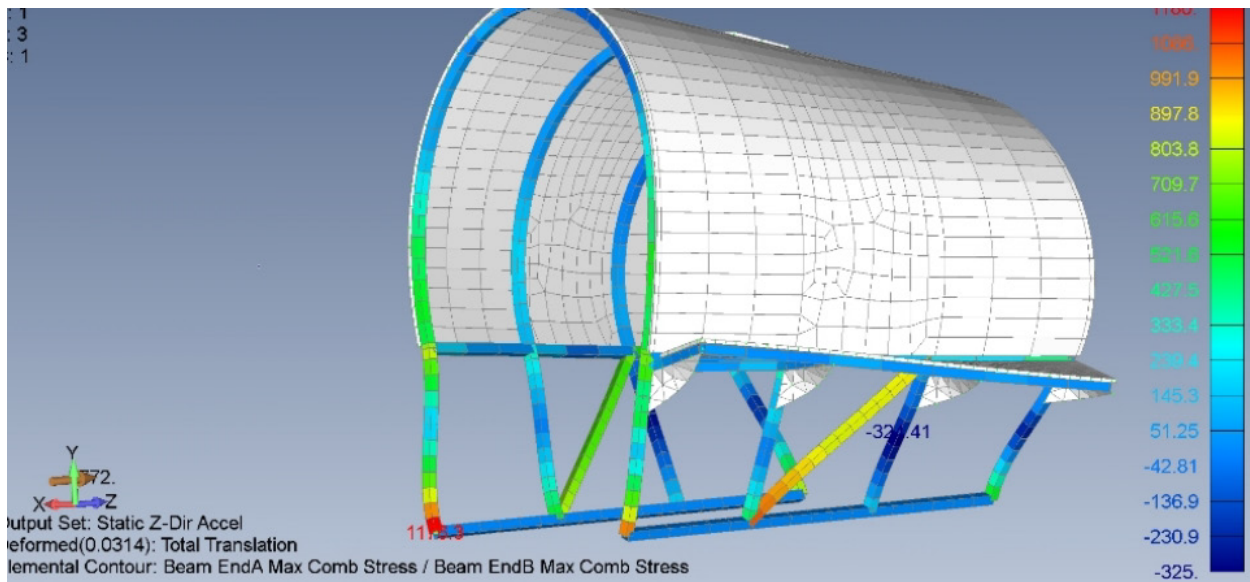


Figure 4.31.—Stress contour for radiator support under 2.0-g lateral acceleration in z-direction. Stress is in psi. Maximum stress is 8.1 MPa (1.2 ksi).

Installation hardware mass is estimated by taking 4 percent of the installed hardware mass. The installation hardware represents fasteners, small brackets, and other hardware used to attach main system components to the bus. Heineman (Ref. 28) has shown that past spacecraft have shown that the 4 percent is a good approximation for the mass.

#### 4.4.7 Recommendation(s)

Higher fidelity structural analysis would provide more details in the structural response of the radiator support assembly. Different operational loads may be evaluated. That would provide information for optimizing the structure for high stiffness and strength along with a low mass. Greater use of advanced

materials and architectures may further enhance the structure’s performance. The application of carbon-fiber-reinforced polymer matrix composites and orthogrid or isogrid panels would be worth investigating.

#### 4.4.8 Master Equipment List

The structural MELs for all three cases are shown in Table 4.28 to Table 4.30, respectively.

TABLE 4.28.—CASE 1 STRUCTURAL MEL

Radioisotope Power System	QTY	Unit Mass	Basic Mass	Growth	Growth	Total Mass
Case 1 DAPS CD 2019-172		(kg)	(kg)	(%)	(kg)	(kg)
<b>DAPS</b>			<b>987</b>	<b>26%</b>	<b>255</b>	<b>1243</b>
<b>Unpressurized Rover</b>			<b>580</b>	<b>20%</b>	<b>117</b>	<b>697</b>
<b>Structures and Mechanisms</b>			<b>38.9</b>	<b>25%</b>	<b>9.7</b>	<b>48.7</b>
<b>Structures</b>			<b>38.9</b>	<b>25%</b>	<b>9.7</b>	<b>48.7</b>
<i>Primary Structures</i>			38.9	25%	9.7	48.7
Radiator Frame	1	33.0	33.0	25%	8.3	41.3
Shunt Radiator Mount	1	1.2	1.2	25%	0.3	1.5
Electronics Radiator Mount	1	4.7	4.7	25%	1.2	5.9
<b>GPHS Launch and Transit Box</b>			<b>1</b>	<b>18%</b>	<b>0</b>	<b>1</b>
<b>Structures and Mechanisms</b>			<b>1.0</b>	<b>18%</b>	<b>0.2</b>	<b>1.2</b>
<b>Mechanisms</b>			<b>1.0</b>	<b>18%</b>	<b>0.2</b>	<b>1.2</b>
<i>Installations</i>			1.0	18%	0.2	1.2
Electrical Power Installation	1	1.0	1.0	18%	0.2	1.2

TABLE 4.29.—CASE 2 STRUCTURAL MEL

Fuel Cells - 6 Days w/ Lander Reprocessing	QTY	Unit Mass	Basic Mass	Growth	Growth	Total Mass
Case 2 DAPS CD 2019-172		(kg)	(kg)	(%)	(kg)	(kg)
<b>DAPS</b>			<b>1945</b>	<b>15%</b>	<b>296</b>	<b>2242</b>
<b>Unpressurized Rover</b>			<b>1154</b>	<b>17%</b>	<b>197</b>	<b>1351</b>
<b>Structures and Mechanisms</b>			<b>108.5</b>	<b>21%</b>	<b>22.2</b>	<b>130.7</b>
<b>Structures</b>			<b>53.4</b>	<b>23%</b>	<b>12.3</b>	<b>65.8</b>
<i>Primary Structures</i>			38.9	25%	9.7	48.7
Radiator Frame	1	33.0	33.0	25%	8.3	41.3
Shunt Radiator Mount	1	1.2	1.2	25%	0.3	1.5
Electronics Radiator Mount	1	4.7	4.7	25%	1.2	5.9
<i>Secondary Structures</i>			14.5	18%	2.6	17.1
LH2 Tank Mount	1	4.0	4.0	18%	0.7	4.7
LOX Tank Mount	1	10.0	10.0	18%	1.8	11.8
Misc# 06.1.11.a.b.c	1	0.5	0.5	18%	0.1	0.6
<b>Mechanisms</b>			<b>55.0</b>	<b>18%</b>	<b>9.9</b>	<b>65.0</b>
<i>Installations</i>			55.0	18%	9.9	65.0
Electrical Power Installation	1	34.1	34.1	18%	6.1	40.2
Thermal Control Installation	1	6.8	6.8	18%	1.2	8.0
Chemical Propulsion Installation	1	14.2	14.2	18%	2.6	16.8
<b>Pressurized Rover</b>			<b>34</b>	<b>33%</b>	<b>11</b>	<b>46</b>
<b>Structures and Mechanisms</b>			<b>1.3</b>	<b>18%</b>	<b>0.2</b>	<b>1.6</b>
<b>Mechanisms</b>			<b>1.3</b>	<b>18%</b>	<b>0.2</b>	<b>1.6</b>
<i>Installations</i>			1.3	18%	0.2	1.6
Electrical Power installation	1	1.3	1.3	18%	0.2	1.6
<b>Additional Lander Hardware</b>			<b>757</b>	<b>12%</b>	<b>87</b>	<b>845</b>
<b>Structures and Mechanisms</b>			<b>35.6</b>	<b>18%</b>	<b>6.4</b>	<b>42.0</b>
<b>Mechanisms</b>			<b>35.6</b>	<b>18%</b>	<b>6.4</b>	<b>42.0</b>
<i>Installations</i>			35.6	18%	6.4	42.0
Electrical Power Installation	1	16.7	16.7	18%	3.0	19.7
Chemical Propulsion Installation	1	18.8	18.8	18%	3.4	22.2

TABLE 4.30.—CASE 3 STRUCTURAL MEL

Fuel Cells - 21 Days w/o Reprocessing	QTY	Unit Mass	Basic Mass	Growth	Growth	Total Mass
Case 3 DAPS CD 2019-172		(kg)	(kg)	(%)	(kg)	(kg)
<b>DAPS</b>			<b>2708</b>	<b>13%</b>	<b>346</b>	<b>3054</b>
<b>Unpressurized Rover</b>			<b>2674</b>	<b>13%</b>	<b>335</b>	<b>3008</b>
<b>Structures and Mechanisms</b>			<b>134.7</b>	<b>20%</b>	<b>27.0</b>	<b>161.7</b>
<b>Structures</b>			<b>79.7</b>	<b>21%</b>	<b>17.1</b>	<b>96.7</b>
<i>Primary Structures</i>			38.9	25%	9.7	48.7
Radiator Frame	1	33.0	33.0	25%	8.3	41.3
Shunt Radiator Mount	1	1.2	1.2	25%	0.3	1.5
Electronics Radiator Mount	1	4.7	4.7	25%	1.2	5.9
<i>Secondary Structures</i>			40.7	18%	7.3	48.0
LH2 Tank Mount	1	28.0	28.0	18%	5.0	33.0
LOX Tank Mount	1	12.0	12.0	18%	2.2	14.2
Water Tank Mount	1	0.7	0.7	18%	0.1	0.8
<b>Mechanisms</b>			<b>55.0</b>	<b>18%</b>	<b>9.9</b>	<b>65.0</b>
<i>Installations</i>			55.0	18%	9.9	65.0
Electrical Power Installation	1	34.1	34.1	18%	6.1	40.2
Thermal Control Installation	1	6.8	6.8	18%	1.2	8.0
Chemical Propulsion Installation	1	14.2	14.2	18%	2.6	16.8
<b>Pressurized Rover</b>			<b>34</b>	<b>33%</b>	<b>11</b>	<b>46</b>
<b>Structures and Mechanisms</b>			<b>1.3</b>	<b>18%</b>	<b>0.2</b>	<b>1.6</b>
<b>Mechanisms</b>			<b>1.3</b>	<b>18%</b>	<b>0.2</b>	<b>1.6</b>
<i>Installations</i>			1.3	18%	0.2	1.6
Electrical Power installation	1	1.3	1.3	18%	0.2	1.6

## 5.0 Cost

### 5.1 Ground Rules and Assumptions

There are several ground rules and assumptions that apply to the cost estimates. First, the scope of the estimate includes the design development test and evaluation (DDT&E) and flight hardware costs for the assemblies associated with providing a power system to a crewed rover on the martian surface. However, technology maturation costs are not included. The team created a RPS case and two separate fuel cell cases.

Next, integration of the assemblies with the rovers or lander and the associated system-level tests are not included in the cost. Integration costs were included at the assembly level only.

Due to the crewed nature of the mission, it is assumed that three prototypes at the assembly level are provided for each assembly for use in testing. Industry-average default rates are used, and the operating specification platform is set to 2.5 to account for human-rated nature of the mission.

The GPHS blocks are assumed to be government furnished equipment (GFE), and the cost for the 48 blocks used in the system are not included. All costs are presented in fiscal year 2020 million dollars (FY20\$M), and no management reserves or contractor fees are included with the estimates. Due to the lack of definition for the rest of the rover(s) and lander, all costs should be considered rough order of magnitude.

### 5.2 Estimating Methodology

The Compass Team estimated the power systems using TruePlanning<sup>®</sup> by PRICE Systems, LLC, a commercial tool for developing parametric estimates for NASA and Department of Defense hardware developments. The exception is the fuel cells, which were estimated outside of TruePlanning<sup>®</sup>. The fuel cells were estimated using human-rated PEM fuel cell data from the Gemini program. Escalation was applied, along with a year of technology reduction of 2 percent per year. These costs were cross-checked

with a cost estimating relationship developed externally for Shuttle-Orbiter (Shuttle used a different type of fuel cell, which of course was also human rated).

### 5.3 Cost Estimates

Table 5.1 to Table 5.3 show cost estimates for all three design cases. Table 5.4 shows a summary of all three cases.

TABLE 5.1.—CASE 1 (RPS) COST, CONSTANT FY20\$M

RPS Case 1	Description	Cost in FY20\$M		
		DDT&E	FHW	Total
UPR	Electrical power assembly	209.9	47.8	257.8
	EPS assembly integration	2.8	2.1	4.8
	DRPS	150.7	40.9	191.7
	Harness	0.7	0.1	0.7
	120-V PMAD	55.8	4.8	60.6
	Thermal control assembly	40.4	12.1	52.5
	Structures assembly	7.0	0.9	8.0
SPR	Electrical power assembly	29.4	3.0	32.4
	EPS assembly integration	0.7	0.3	0.9
	120-V PMAD	6.1	0.2	6.3
	Harness	5.8	0.4	6.3
	Li-ion battery	16.8	2.0	18.8
Total	-----	286.8	63.8	350.7

\*GPHS blocks are assumed to be GFE, and no cost has been included for them in this estimate.

TABLE 5.2.—CASE 2 (FUEL CELLS) COST, CONSTANT FY20\$M

Fuel cells case 2	Description	Cost in FY20\$M		
		DDT&E	FHW	Total
UPR	Electrical power assembly	251.3	31.7	282.9
	EPS assembly integration	16.7	11.6	28.3
	Fuel cell	146.9	7.9	154.7
	Hydrogen feed system	5.0	1.3	6.3
	Oxygen feed system	4.8	1.2	6.0
	Hydrogen tank	4.5	0.7	5.2
	Oxygen tank	2.6	0.4	2.9
	Water tank and feed system	0.6	0.1	0.7
	Harness	0.8	0.1	0.9
	120-V PMAD	69.4	8.4	77.9
	Thermal control assembly	39.1	11.9	50.9
	Structures assembly	10.9	1.6	12.5
SPR	Electrical power assembly	6.0	0.3	6.3
Additional lander HW	Electrical power assembly	32.7	7.0	39.7
	Structures assembly	3.0	0.5	3.6
Total	-----	343.0	53.0	395.9

TABLE 5.3.—CASE 3 (FUEL CELLS) COST, CONSTANT FY20\$M

Fuel cells case 3	Description	Cost in FY20\$M		
		DDT&E	FHW	Total
UPR	Electrical Power Assembly	273.2	35.8	309.0
	EPS Assembly Integration	17.4	11.8	29.2
	Fuel Cell (Stack and Ancillary)	146.9	7.9	154.7
	Fuel Cell Electrolyzer	5.0	0.5	5.6
	Hydrogen Feed System	6.4	1.7	8.2
	Oxygen Feed System	5.8	1.5	7.4
	Hydrogen Tank	13.0	2.4	15.4
	Oxygen Tank	7.2	1.2	8.4
	Water Tank and Feed System	1.1	0.1	1.2
	Buffer Tanks	0.3	0.0	0.3
	Harness	0.8	0.1	0.9
	120-V PMAD	69.4	8.4	77.9
	Thermal Control Assembly	39.1	11.9	50.9
	Structures Assembly	12.7	2.0	14.6
SPR	Electrical Power Assembly	6.0	0.3	6.3
Total	-----	331.0	49.9	380.9

TABLE 5.4.—SUMMARIZED COST COMPARISON

Description	Cost in FY20\$M		
	RPS case 1	Fuel cells case 2	Fuel cells case 3
Electrical power total	290.2	322.3	308.7
Thermal control total	52.5	50.9	50.9
Structures total	8.0	16.1	14.6
Total	350.7	389.3	374.3



## Appendix A.—Acronyms and Abbreviations

$\Delta V$	delta-velocity, change in velocity	FEA	finite element analysis
AES	Advanced Exploration Systems	FHW	flight hardware
AIAA	American Institute for Aeronautics and Astronautics	FOM	figure of merit
ALARA	as low as reasonably achievable	FY20\$M	fiscal year 2020 million dollars
ALIP	annular linear induction electromagnetic pumps	GCR	galactic cosmic ray
AMPS	AES Modular Power System	GFE	government furnished equipment
ASRG	Advanced Stirling Radioisotope Generator	GH <sub>2</sub>	gaseous hydrogen
BOL	beginning of life	GO <sub>2</sub>	gaseous oxygen
BSGM	bus switchgear module	GPHS	general-purpose heat source
C&DH	command and data handling	GPHS-RTG	general-purpose heat source radioisotope thermoelectric generator
CAD	computer-aided design	GRC	Glenn Research Center
CD	Compass Document	HW	hardware
CFE	customer-furnished equipment	JSC	Johnson Space Center
CLV	Commercial Launch Vehicle	LSGM	load switchgear module
COPV	composite overwrapped pressure vessel	MEL	master equipment list
COTS	commercial off-the-shelf	MGA	mass growth allowance
CBE	current best estimate	Misc.	miscellaneous
DAPS	Destination Agnostic Pressurized System	MLI	multilayer insulation
DDT&E	design development test and evaluation	MMPDS	Metallic Materials Properties Development and Standardization
DOD	depth of discharge	MMRTG	multi-mission radioisotope thermoelectric generator
DOE	Department of Energy	MOP	mean operating pressure
DRPS	Dynamic Radioisotope Power Systems	MSL	Mars Science Laboratory
EADS	European Aeronautic Defence and Space Company	NIST	National Institute of Standards and Technology
ECLSS	Environmental Control and Life Support System	NRC	Nuclear Regulatory Commission
EP	electric power	NTE	not to exceed
EPS	electrical power system	ORNL	Oak Ridge National Laboratory
EVA	extravehicular activity	P&ID	pipng and instrumentation diagram
		PDU	power distribution unit
		PEL	power equipment list

PEM	proton-exchange membrane	SLS	Space Launch System
PI	principal investigator	SOC	state of charge
PMAD	power management and distribution	SPE	solar particle event
POC	point of contact	SPR	small pressurized rover
PuO <sub>2</sub>	plutonium oxide	sr	steradians
Qty	quantity	TRL	technology readiness level
RAD	Radiation Assessment Detector	UPR	unpressurized rover
RPS	radioisotope power system	w/	with
S/C	spacecraft	w/o	without



## Appendix B.—Study Participants

Table B.1 gives design trade information.

TABLE B.1.—POWER SYSTEM DESIGN TRADES FOR A PRESSURIZED LUNAR/MARS ROVER

Subsystem	Name	Center	Email
Design customer POC/PI	June Zakrasjek	GRC	June.F.Zakrasjek@nasa.gov
Compass Team			
Compass Team lead	Steve Oleson	GRC	Steven.R.Oleson@nasa.gov
System integration, MEL	Jim Fittje	GRC	James.E.Fittje@nasa.gov
Report integration and technical editing	Lee Jackson	GRC	Lee.A.Jackson@nasa.gov
Computer-aided design (CAD), configuration	Tom Packard	GRC	Thomas.W.Packard@nasa.gov
Thermal, environmental	Tony Colozza	GRC	Anthony.J.Colozza@nasa.gov
Structures and mechanisms	John Gyekenyesi	GRC	John.Z.Gyekenyesi@nasa.gov
Reactant storage systems	Jim Fittje	GRC	James.E.Fittje@nasa.gov
Cost	Tom Parkey	GRC	Thomas.J.Parkey@nasa.gov
Cost	Betsy Turnbull	GRC	Betsy.Turnbull@nasa.gov
Power	Paul Schmitz	GRC	Paul.C.Schmitz@nasa.gov
Power	Brandon Klefman	GRC	Brandon.T.Klefman@nasa.gov
Power	Lucia Tian	GRC	Lucia.Tian@nasa.gov
Power	Steven Korn	GRC	Steven.M.Korn@nasa.gov
Power	Max Chaiken	GRC	Max.F.Chaiken@nasa.gov
Radiation mitigation	Mike Smith	ORNL	SmithMB@ornl.gov
Rover point of departure	Taylor Phillips-Hungerford	JSC	Taylor.Phillips-Hungerford@nasa.gov
Mars integration advisor	Michelle Rucker	JSC	Michelle.A.Rucker@nasa.gov
Mars integration advisor	Bret Drake	JSC	Bret.G.Drake@nasa.gov
Mars integration advisor	Jeff George	JSC	Jeffrey.A.George@nasa.gov



## Appendix C.—Radiation Contributions to Total Mission Dose

Table C.1 and Table C.2 give dose predictions. Figure C.1 and Figure C.2 give radiation implications, while Figure C.3 gives a radiation analysis.

TABLE C.1.—TOTAL INTEGRATED DOSE PREDICTIONS FROM RPS AND SPACE RADIATION

Integrated dose scenarios	Dose during transit duration, <sup>a</sup> rem	Dose during surface duration, <sup>b</sup> rem	Total mission dose, rem	NASA dose limits, rem
Lunar RPS dose unshielded	NA	1.33	1.33	30 day:25
Lunar space radiation dose	1.70	2.76	4.46	
Lunar total combined doses	-----	-----	5.79	1 year:50
Martian RPS dose unshielded	NA	1.33	1.33	Career:100 to 400
Martian space radiation dose	124.10	1.92	126.02	
Martian total combined doses	-----	-----	127.35	

<sup>a</sup>Transit durations assume 10 days for lunar and 730 days for martian missions.

<sup>b</sup>Surface durations assume 30 days for both lunar and martian missions.

TABLE C.2.—DOSE RATE PREDICTIONS FROM RPS AND SPACE RADIATION

Dose rate scenarios	Highest calculated mean dose rates in SPR, <sup>a</sup> rem/h	Highest calculated mean dose rates above RPS, <sup>a</sup> rem/h	Radiation area, rem/h	High-radiation area, rem/h
Lunar unshielded [shielded]	0.0089 [0.0057]	0.1389 [0.1141]	≥0.0050	≥0.1000
Martian unshielded [shielded]	0.0078 [0.0046]	0.1378 [0.1130]		

<sup>a</sup>Dose rates include ~0.0038 rem/h for lunar and ~0.0027 rem/h for martian scenarios.

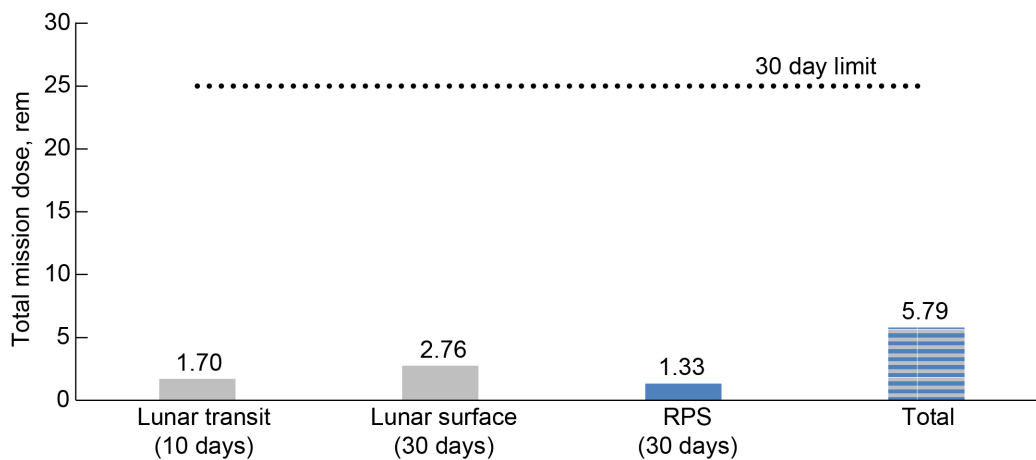


Figure C.1.—Radiation implications for lunar mission.

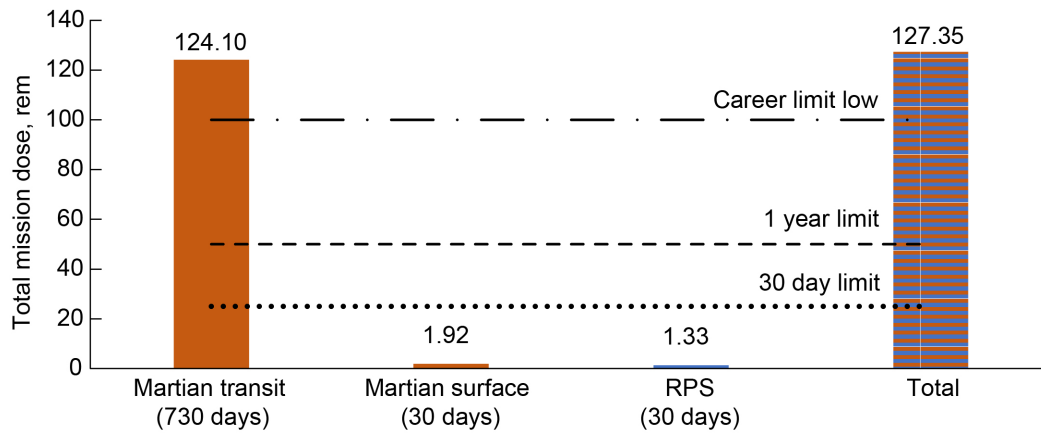


Figure C.2.—Radiation implications for martian mission.

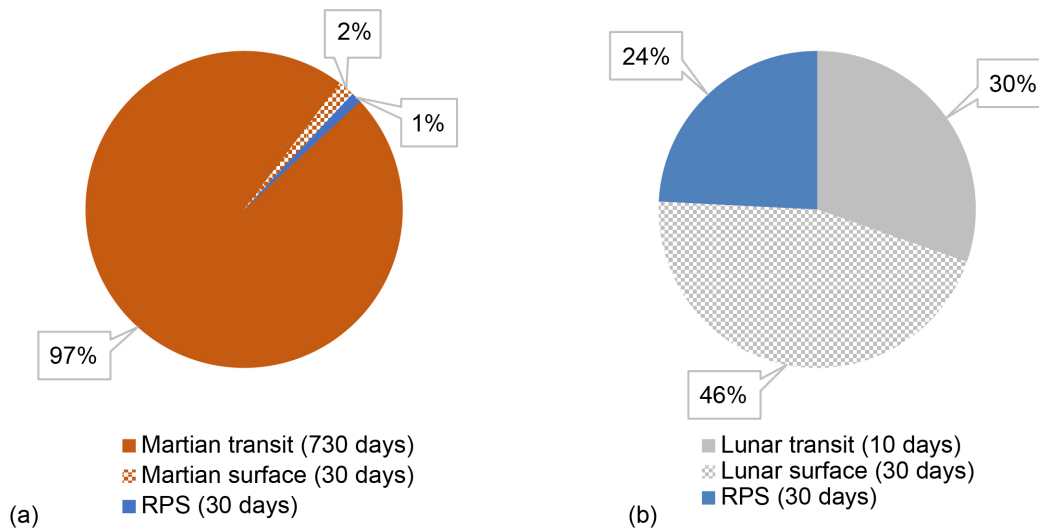


Figure C.3.—Martian and lunar mission segments used for radiation analysis.

## References

1. Matlack, G.M.; and Metz, C.F.: Radiation Characteristics of Plutonium-238. LA-3696, 1967.
2. Rinehart, Gary H.: Design Characteristics and Fabrication of Radioisotope Heat Sources for Space Missions. *Prog. Nucl. Energy*, vol. 39, nos. 3–4, 2001, pp. 305–319.
3. Taherzadeh, Mojtaba: Neutron Radiation Characteristics of Plutonium Dioxide Fuel. NASA CR-127045, 1972. <https://ntrs.nasa.gov>
4. Guo, Jingnan, et al.: Variations of Dose Rate Observed by MSL/RAD in Transit to Mars. *Astron. Astrophys.*, vol. 577, no. A58, 2015.
5. Hassler, Donald M., et al.: Mars' Surface Radiation Environment Measured With the Mars Science Laboratory's Curiosity Rover. *Science*, vol. 343, no. 6169, 2014.
6. United States Nuclear Regulatory Commission: NRC Regulations 20.1003 Definitions. NRD, 10 CFR, 2021. <https://www.nrc.gov/reading-rm/doc-collections/cfr/part020/part020-1003.html> Accessed Aug. 11, 2020.
7. National Aeronautics and Space Administration: NASA Space Flight Human-System Standard. NASA-STD-3001, Vol. 1, Rev. A, 2014.
8. Bennet, Gary L., et al.: Mission of Daring: The General-Purpose Heat Source Radioisotope Thermoelectric Generator. AIAA 2006-4096, 2006.
9. Lee, Young; and Bairstow, Brian: Radioisotope Power Systems Reference Book for Mission Designers and Planners. NASA JPL Publication 15-6, 2015.
10. Rearden, B.T.; and Jessee, M.A., eds.: SCALE Code System. ORNL/TM-2005/39, Version 6.2.3, 2018. [https://www.ornl.gov/sites/default/files/SCALE\\_6.2.3.pdf](https://www.ornl.gov/sites/default/files/SCALE_6.2.3.pdf) Accessed Aug. 11, 2020.
11. American Institute of Aeronautics and Astronautics: Standard—Mass Properties Control for Space Systems. ANSI/AIAA S-120A-2015(2019), 2019.
12. Litaker, Harry L.; and Howard, Robert L.: Habitability Lessons Learned From Field Testing of a Small Pressurized Rover. AIAA 2020-4261, 2020.
13. National Aeronautics and Space Administration: Viking Mission to Mars. 2020. <https://nssdc.gsfc.nasa.gov/planetary/viking.html> Accessed Oct. 30, 2020.
14. Elsevier B.V.: ScienceDirect: Nusselt Number. 2020. <https://www.sciencedirect.com/topics/chemical-engineering/nusselt-number> Accessed Oct. 21, 2020.
15. Elsevier B.V.: ScienceDirect: Prandtl Number. 2020. <https://www.sciencedirect.com/topics/chemistry/prandtl-number> Accessed Oct. 21, 2020.
16. Elsevier B.V.: ScienceDirect: Reynolds Number. 2020. <https://www.sciencedirect.com/topics/engineering/reynolds-number#> Accessed Oct. 21, 2020.
17. Elsevier B.V.: ScienceDirect: Rayleigh Number. 2020. <https://www.sciencedirect.com/topics/engineering/rayleigh-number> Accessed Oct. 21, 2020.
18. Laird Thermal Systems, Inc.: Common Coolant Types and Their Uses in Liquid Cooling Systems. <https://www.lairdthermal.com/thermal-technical-library/application-notes/common-coolant-types-and-their-uses-liquid-cooling-systems> Accessed Nov. 5, 2020.
19. Dow Corning Corporation: Table 01 - Properties of SYLTHERM XLT. 1997. <https://detector-cooling.web.cern.ch/data/TABLE01.HTM> Accessed Nov. 5, 2020.
20. Eastman Chemical Company: Therminol 59: Heat Transfer Fluid. 2019. [https://www.therminol.com/sites/therminol/files/documents/TF-9029\\_Therminol\\_59\\_Product\\_Bulletin.pdf](https://www.therminol.com/sites/therminol/files/documents/TF-9029_Therminol_59_Product_Bulletin.pdf) Accessed Nov. 5, 2020.

21. Zohuri, Bahman; Lam, Stephen; and Forsberg, Charles: Heat-Pipe Heat Exchangers for Salt-Cooled Fission and Fusion Reactors to Avoid Salt Freezing and Control Tritium: A Review. Nucl. Technol., vol. 206, no. 11, 2019, pp. 1642–1658.
22. Benedic, Fabien; Leard, Jean-Philippe; and Lefloch, Christian: Helium High Pressure Tanks at EADS Space Transportation: New Technology With Thermoplastic Liner. European Aeronautic Defence and Space Company (EADS), Jalles, France, 2005.
23. National Aeronautics and Space Administration: Space Launch System (SLS): Mission Planner's Guide. ESD 30000, Rev. A, 2018. <https://ntrs.nasa.gov>
24. Arianespace: Ariane 5 User's Manual. Issue 5, Rev. 1, 2011.
25. SAE International: Metallic Materials Properties Development and Standardization (MMPDS) Handbook - 11, B-983, 2016.
26. Mankins, John C.: Technology Readiness Levels. NASA White Paper, 1995.
27. National Aeronautics and Space Administration: Structural Design and Test Factors of Safety for Spaceflight Hardware. NASA-STD-5001, Rev. B, 2016.
28. Heineman, Jr., William: Design Mass Properties II: Mass Estimating and Forecasting for Aerospace Vehicles Based on Historical Data. NASA JSC-26098, 1994.



